Tesis doctoral para optar al título de Doctor por la Universidad de Sevilla y al título de Doctor Internacional

(Doctoral thesis for the degree of Doctor of Philosophy and International Doctorate)

GASIFICACIÓN DE RESIDUOS URBANOS EN LECHO FLUIDIZADO: DISTRIBUCIÓN DE COMPUESTOS INORGÁNICOS Y TRAZA

(GASIFICATION OF URBAN WASTES IN FLUIDIZED BED: DISTRIBUTION OF INORGANICS AND TRACE ELEMENTS)

Vanessa Ferreira de Almeida

Director de Tesis (Thesis director): Alberto Gómez Barea

Departamento de Ingeniería Química y Ambiental

Escuela Superior de Ingeniería (Universidad de Sevilla)

Febrero 2023

To my parents, Claudia and Juramir

Abstract

Processing waste in fluidized bed (FB) by gasification is an interesting alternative over other thermochemical options and types of equipment. However, it still presents several drawbacks compared to processing other standardized fuels, like coal or clean biomass. The challenges are associated with the intrinsic nature of waste fuels, especially their heterogeneity in size and composition, and with the higher content in contaminants precursors (N, S and Cl) and trace elements, such as heavy metals.

This thesis aims to study the gasification of waste-derived fuels in a fluidized bed, emphasizing the main aspects that make the thermal conversion of these solid wastes different from other cleaner fuels, such as standardised biomass. In particular, this thesis focuses on the distribution of inorganic and trace elements during the gasification of urban wastes in fluidized bed (FB).

In order to achieve this objective, experimental tests and thermodynamic models have been conducted, and extensive comparison with experimental experiences collected and published by researchers during the last decades. The results provide an understanding of the content in inorganics and trace elements in different types of waste fuels, some key issues during sampling and measuring contaminants, and establish rational prediction of the distribution of the main and trace elements during thermal conversion.

More specifically, the main achievements of this thesis work are summarized as follows:

- An extensive review of the literature regarding the content of inorganics and trace elements in waste fuels and their distribution during thermal conversion in the different product phases.
- Detailed experimental tests identifying the most suitable materials, sampling methods and measurement technics for gasification tests at lab-scale aiming at measuring inorganics and trace elements.
- Experimental results on the distribution of inorganics and trace elements during gasification of continuous tests in a bench-scale fluidized bed gasifier processing Refuse-Derived Fuel (RDF) and thermal conversion of various waste fuels in muffle furnace and batchwise-operated lab-scale fluidized bed reactor under different operating conditions.

Additional works on thermodynamic models to predict the distribution of the main compounds during the gasification of waste fuels and an environmental analysis to preliminarily assess the advantages

of gasification of some fraction of wastes from municipal solid wastes compared to the option of landfilling are appended to this thesis.

Keywords: gasification; fluidized bed; waste fuels; municipal solid waste (MSW); Refuse-Derived Fuel (RDF); Dried Sewage Sludge (DSS); trace elements; heavy metals; thermal conversion.

Papers

Part of the work of this thesis was materialized into two papers already published in international journals, both with a focus on contaminants, presented as follows. The content of papers 1 and 2 are gathered in Chapters 2 and 4, respectively. They are the following:

PAPER 1. de Almeida, V.F., Gómez-Barea, A., Arroyo-Caire, J. and Pardo, I., 2020. On the Measurement of the Main Inorganic Contaminants Derived from Cl, S and N in Simulated Waste-Derived Syngas. *Waste and Biomass Valorization*, pp.1-16

PAPER 2. de Almeida, V. F., Gómez-Barea, A., Nilsson, S. and Tuomi, S., 2021. Distribution of Inorganics and Trace Elements during Waste Gasification in a Bench-Scale Fluidized Bed. *Energy & Fuels*, 35(19), pp.15802-15816.

Complementary conference papers were published along this thesis (papers 3 – 5), which are listed below. Paper 3 is a previous preliminary discussion of the content of paper 1, and papers 3 and 4 contain part of the results presented in Chapter 3. They are the following:

PAPER 3. de Almeida, V. F., Arroyo-Caire, J., Suárez-Almeida, M., Pardo, I., Nilsson, S., Haro, P., Gómez-Barea. On the measurement of main inorganic contaminants (HCl, H_2S and NH_3) in waste-derived syngas. *7th International Conference on Engineering for Waste and Biomass Valorization*, July 2018, Prague, Check Republic.

PAPER 4. de Almeida, V. F., Ronda, A., Arroyo-Caire, J., Suárez-Almeida, M., Pardo, I., Fuentes-Cano, D., Haro, P., Gómez-Barea, A. Heavy metals partitioning during thermal devolatilization of solid wastes in a fluidized bed reactor. *7th International Conference on Engineering for Waste and Biomass Valorization*, July 2018, Prague, Check Republic.

PAPER 5. de Almeida, V.F., Ronda, A., Pardo, I. and Gomez-Barea, A., Partitioning of contaminant and inorganic species during thermal devolatilization of dried sewage sludge. *Proceedings of 7th International Conference on Sustainable Solid Waste Management*, June 2019, Heraklion, Crete Island, Greece.

During the doctorate, the candidate has contributed to the discussion, edition and preparation of several works, along with other researchers. These works were related to the thematic of this thesis.

Papers 6 – 10 comprise these works, which are relevant to this thesis but not included in this document. They are the following:

PAPER 6. Nilsson, S., Gómez-Barea, A., Pardo-Arias, I., Suárez-Almeida, M. and de Almeida, V.F., 2019. Comparison of Six Different Biomass Residues in a Pilot-Scale Fluidized Bed Gasifier. *Energy & Fuels, 33*(11), pp.10978-10988.

PAPER 7. Ronda, A., Gómez-Barea, A., Haro, P., de Almeida, V.F. and Salinero, J., 2019. Elements partitioning during thermal conversion of sewage sludge. *Fuel Processing Technology, 186*, pp.156-166.

PAPER 8. Suárez-Almeida, M., de Almeida, V. F., Arroyo-Caire, J., Haro, P., Gómez-Barea, A. Techno-economic assessment for implementing gasification technologies to process MSW refuse in Spain. *7th International Conference on Engineering for Waste and Biomass Valorization*, July 2018, Prague, Check Republic.

PAPER 9. Ronda, A., de Almeida, V.F., Salinero, J., Haro, P., Fuentes-Cano, D., Nilsson, S. Gómez-Barea, A. Study of the potential ecological risk of heavy metals in the residue from thermal conversion of a sewage sludge. *26th European Biomass Conference & Exhibition*, May 2018, Copenhagen, Denmark.

PAPER 10. Haro, P., Arroyo-Caire, J., de Almeida, V.F., Salinero, J., Vidal-Barrero, F., Gómez-Barea, A. Waste gasification for power generation: Assessment of industrial and non-industrial alkaline residues as sorbents for acid gas removal. *26th European Biomass Conference & Exhibition*, May 2018, Copenhagen, Denmark.

Resumen de la tesis doctoral (Summary in Spanish)

1. Introducción

Durante los últimos años, la sociedad ha ido cambiando de una economía lineal a una circular. La creciente demanda de energía y la necesidad de procesos más sostenibles ha llevado a un mayor interés en el uso de residuos como materia prima para la producción de energía. La conversión térmica de residuos sólidos presenta la ventaja de generar energía mientras se procesa una fracción que de otro modo se depositaría en vertederos, siendo un proceso atractivo que responde a la necesidad aguda de procesos circulares y sostenibles. Sin embargo, esta alternativa aún presenta varios inconvenientes asociados con la naturaleza intrínseca de los combustibles residuales, es decir, heterogeneidad en tamaño y composición y contenido en precursores de contaminantes, en comparación con otros combustibles estandarizados, como el carbón o la biomasa limpia.

El propósito de este trabajo es estudiar la gasificación de combustibles derivados de residuos en lecho fluidizado y los principales puntos que diferencian la gasificación de residuos de un combustible limpio, como la biomasa, con el objetivo de contribuir a la aplicación del proceso a mayor escala. Como la emisión de contaminantes durante el procesamiento de residuos es uno de los mayores retos con respecto a la utilización de biomasas limpias, esta tesis se ha centrado principalmente en el comportamiento de los precursores de contaminantes durante la conversión térmica de estos combustibles residuales sólidos en el proceso de gasificación.

En los siguientes capítulos se revisará la literatura, incluyendo las principales técnicas para la medición de contaminantes, su contenido en el combustible y en las corrientes de producto. Luego, se presentarán los datos de experimentos propios tanto en escala de laboratorio como en "*bench scale*". En los anexos se presentarán los resultados de las simulaciones de modelización y, por último, se mostrará una evaluación ambiental de los procesos de gasificación en operación continúa utilizando combustible derivado de residuo. A continuación, se presenta un resumen de los capítulos de la presente tesis.

2. Resumen capitular

2.1. Capítulo 1: Introducción

En este capítulo, se explica el cambio por el cual la sociedad actual viene pasando, de una economía linear a una economía circular, en la cual los productos y residuos pueden ser reaprovechados, tanto para producir nuevos productos, como para la producción de energía. A continuación, se presenta una introducción a la gasificación de residuos sólidos, especificando las ventajas y los retos de su procesamiento con respecto a los combustibles estandarizados. Se pone de manifiesto el alto contenido en nitrógeno, cloro y azufre de estos combustibles, así como el contenido en elementos traza, y en particular los metales pesados. A continuación, se analizan los factores que influyen en la formación de contaminantes y su reparto en los productos de la gasificación – gaseoso o sólido. Por último, se presentan los objetivos y el contenido de la tesis.

2.2. Capítulo 2: Medición de los principales contaminantes inorgánicos en combustibles derivados de residuos

En este capítulo se ha estudiado la medición de los principales contaminantes inorgánicos en los combustibles derivados de residuos, constituyendo el artículo publicado anteriormente mencionado como Paper 1.

El propósito de este capítulo es revisar los métodos más comunes para la caracterización y medición de contaminantes de la literatura; revisar y discutir los datos encontrados en la literatura; y presentar los resultados de experimentos propios para la evaluación de los métodos de medición de contaminantes.

Los resultados del estudio presentado en este capítulo demuestran que puede haber incoherencias en los niveles de contaminantes presentes en el gas de síntesis en la literatura. Además, se han dado recomendaciones acerca de métodos de muestreo y medición. De manera complementaria, también se han analizado diferentes materiales de reactores y su desempeño a alta temperatura con gases conteniendo cloro y azufre.

2.3. Capítulo 3: Medición y distribución de elementos inorgánicos y traza durante la devolatilización de combustibles en un reactor de lecho fluidizado

En este capítulo se han presentado los resultados de los experimentos de devolatilización discontinua utilizando lodos de depuradora secos (DSS), combustible derivado de residuos (RDF) y pellets de biomasa proveniente de madera (pellets de madera comerciales).

Se ha hecho énfasis en el comportamiento (reparto y distribución bajo diversas condiciones de operación) de elementos traza durante la conversión térmica. Las mediciones y análisis realizados en este capítulo se centran tanto en la fase gaseosa, como en el residuo sólido de la conversión termoquímica. En la fase gaseosa, se centra el análisis en especies que contengan azufre, cloro y nitrógeno. En el residuo sólido, se analiza el contenido en elementos traza y su distribución tras la conversión termoquímica.

2.4. Capítulo 4: Resultados de ensayos de gasificación en continuo en lecho fluidizado utilizando combustible derivado de residuos (RDF)

En el capítulo cuatro se han presentado los resultados de los experimentos en continuo realizados en una planta de gasificación de lecho fluidizado (*bench scale*) en el centro de investigación VTT (Bioruukki Pilot Centre) en Finlandia. El contenido de este capítulo corresponde al artículo publicado anteriormente mencionado como Paper 2.

Se analiza el efecto de los principales parámetros del proceso (la temperatura, la relación de equivalencia (ER), el material del lecho (arena de silicio / dolomita) sobre los productos principales, así como los contaminantes menores derivados de azufre, cloro y nitrógeno. Se estudia la composición de las cenizas, tanto las de fondo ("*bottom ashes*"), como las que han quedado retenidas en el filtro, haciendo énfasis en el estudio del efecto de la filtración en caliente de la corriente de gas producto sobre los elementos traza.

2.5. Capítulo 5: Conclusiones

El último capítulo se hace un breve resumen de los objetivos y las conclusiones más significativas del presente trabajo, listando las contribuciones más relevantes obtenidas.

2.6. Anexo I: Estudio termodinámico del proceso de conversión termoquímica de la biomasa

Se presenta un estudio termodinámico encaminado a predecir la distribución de los elementos traza presentes en los combustibles residuales durante las condiciones de gasificación, empleando el software HSC Chemistry ®.

2.7. Anexo II: Análisis de Ciclo de Vida (LCA) y Evaluación Tecno-Económica (TEA) de la Gasificación de RDF en lecho fluidizado

Se presenta un Análisis de Ciclo de Vida Ambiental (E-LCA) del proceso de la gasificación de biomasa y se compara el impacto ambiental con la opción de depósito en vertedero controlado gasificación continua. Para este estudio se usan algunos de los resultados obtenidos de los resultados experimentales del cuarto capítulo, en especial la composición de las corrientes de salida (sólido y gas).

El análisis tecno-económico de la gasificación se lleva a cabo, considerando tres diferentes escenarios, de condiciones peores a mejores. El “peor escenario” representa una situación en que los costes son los más altos y los ingresos son lo más bajos o directamente inexistentes. El “mejor escenario” considera el opuesto de eso, los costes son los más bajos y los ingresos más altos. Los valores utilizados para los escenarios fueron obtenidos de la literatura.

3. Conclusiones

3.1. Resumen de los estudios y contribuciones realizadas

En este trabajo se ha evaluado el desempeño de la gasificación de residuos sólidos en lecho fluidizado enfocado a su contenido en elementos potencialmente nocivos. Para lograr este objetivo, se ha estudiado este proceso a través de la revisión de la literatura, ensayos en escala de laboratorio y "bench", además de procesos de modelización.

Primeramente, se ha realizado una exhaustiva revisión de la literatura sobre la gasificación de diferentes tipos de combustibles - sobre todo RDF y DSS. Simultáneamente, se han realizado varios experimentos para analizar los métodos de muestreo y medición de contaminantes tanto en procesos de gasificación. Además, se han realizado pruebas de devolatilización y gasificación continua utilizando RDF como combustibles, lo que dio como resultado datos experimentales que permitieron estudiar la partición de los precursores de contaminantes, así como otros parámetros clave. Además, se realizó un análisis termodinámico (utilizando el software HSC) para ayudar a comprender los resultados experimentales. Por último, se ha realizado un estudio comparativo del impacto ambiental de la gasificación RDF con respecto al depósito en vertedero controlado, utilizando los datos experimentales para la evaluación del impacto de la gasificación y una evaluación técnico-económica de la gasificación para investigar la viabilidad económica de la planta de gasificación.

3.2. Trabajos futuros

Los principales esfuerzos para continuar este trabajo deben centrarse en una mayor comprensión de los precursores de la formación de contaminantes durante la gasificación – los elementos inorgánicos y traza - presentes en los residuos sólidos. La forma química en que estos componentes están presentes en los combustibles, como también en los productos sólidos tras la conversión termoquímica, son aspectos claves. La comprensión de cómo la forma química en que los elementos inorgánicos y traza están presentes en los diferentes tipos de combustibles y como eso influye en el proceso de conversión termoquímica sería determinante para aportar datos claves para el diseño de sistemas de limpieza y tratamiento. La simulaciones termodinámicas actuales aun necesitan refinarse para el mejor entendimiento de las reacciones que ocurren. Así mismo es necesario ahondar en la composición y el potencial de lixiviación de los elementos presentes en las cenizas y su daño potencial al medio ambiente. Ello puede contribuir significativamente en el establecimiento de una economía circular,

por ejemplo, basada en una mayor reutilización de metales presentes en las cenizas en nuevos productos.

Durante esta tesis se realizaron experimentos preliminares utilizando un reactor de cuarzo, sin embargo, no fueron suficientes para trazar elementos y para ser incluidos aquí. Por lo tanto, sería necesario realizar pruebas adicionales en una instalación similar para aclarar ciertos aspectos que no se han podido escalecer durante la presente investigación.

Además, la investigación de diferentes tipos de residuos sólidos como combustibles, o diferentes RDF, contribuiría a una comprensión y parametrización más sólidas de la composición de residuos sólidos y gas de síntesis. También se alienta el trabajo de modelado utilizando los extensos datos experimentales proporcionados en este trabajo.

Por último, en términos de análisis de ciclo de vida (LCA) y análisis técnico-ambiental (TEA), la comparación de otras tecnologías novedosas de conversión termoquímica, como la pirólisis, la gasificación en diferentes tipos de reactores, usando datos empíricos (es decir, todos los experimentos en diferentes instalaciones usando el mismo combustible y medidas tipos) sería de interés para una comparación adecuada y fiable de estas tecnologías en términos de su potencial de mejora y futura implementación.

Content

Acknowledgements

I would like to thank everybody who has supported me during the development of this thesis, colleagues, family, and friends.

First and foremost, I would like to praise and thank God, the Almighty, who supported me in each step of my progress towards the successful completion of my research work, and who has granted countless blessings and knowledge so that I have been finally able to accomplish this thesis.

Especially, I would like to thank my director, Professor Alberto Gómez Barea, for his assistance and advice during the development of this thesis and for allowing me to work on this project. In addition, I also want to thank Dr Susanna Nilsson for her assistance in developing this thesis.

I would also like to thank Professor Fengqi You for receiving me at Peese Research Group and also Professor Jefferson Tester and Professor Johannes Lehmann for all the support and knowledge shared with me during my stay at Cornell. I want to also express my gratitude to Sanna Tuomi during my stay at VTT for all her support and guidance and to Dr Esa Kurkela for receiving me at his research group.

This thesis would not have been completed without the help of my co-authors and colleagues. Thank you, Javi and Isra, for sharing knowledge and working with me at the laboratory. Your contribution was essential for the experimental part developed at the University of Seville. Thanks, Maite, Diego and Rafa for your support and kindness in the laboratory. I am also grateful for my colleagues and friends from the Chemical Engineering Department of the University of Seville, all the time together at "*becaria*". Special thanks to Karla y Neto (Dr Gutiérrez) for sharing this PhD journey with me, which friendship and support were indispensable to keep me going. Also, thanks to Soko and Yanqiu for our time together at Cornell.

I want to thank all my colleagues and friends from IDENER. Maria Tripiana and Dr Alejandro del Real, thanks for believing in me, allowing me to work on research and continuously learn. Special thanks to Maria Tripiana for her friendship and being my mentor along these years. Special thanks Patri, Andrea, Fer, Ivan and Alex Hall, which friendship and support have kept me going since 2019. Also, thanks to Cris and Ciro for their support in this final stage.

To my family and friends: my deepest gratitude for giving me the strength to believe in myself and pursue my dreams, even if it was on the other side of the ocean. To my parents, Claudia and Juramir - to whom this thesis is dedicated - and whose love, support, friendship, values and encouragement enabled the development of this thesis. To my godmother, Chica, my aunts Ana, Zita, Dete, Elena and Biga, and to Amanda - who, together with my mother and grandmothers – are the inspirational women of my life. To my uncle Hélio and cousins Rafael, Gabriela and Ingrid, which friendship was so important to fuel my work. To the memory of my grandparents, João, Maria, Juliano and Noemia. To William, Kate and Amora, which company and love were indispensable to finishing this work. To Marina (now Dr Casanova), my dearest friend, whose support and friendship are invaluable to me and have supported my journey since 2015. To my beloved friends Bianca and Judy, who have shared their passion for Chemical Engineering with me since 2009. To Gonzalo, whose continuous encouragement, kindness and understanding in this last sprint made everything looks easier. I cannot imagine this thesis without you all. Thanks for everything.

Finally, I would like to acknowledge the financial support from the "Science without Borders" program, supported by CNPq, Brazil (Project 201591/2015-4), that enabled the development of this thesis. In addition, the financial support from the Spanish National Plan I+D+I (project NetuWas, CTM2016-78089-R) is also acknowledged. Complementary, I would like to thank the University of Seville for the financial support for my stay at the Robert Frederick Smith School of Chemical and Biomolecular Engineering, Cornell University (USA). I would also like to thank the funding from Horizon 2020's Research and Innovation Program under grant agreement number 731101 (Brisk II) for financially supporting my stay at the VTT Research Centre Ltd (Finland).

"Life is not easy for any of us. But what of that? We must have perseverance and, above all, confidence in ourselves. We must believe that we are gifted for something, and that this thing, at whatever cost, must be attained."

Marie Curie

Gasification of urban wastes in fluidized bed: distribution of inorganics and trace elements

Chapter 1

Introduction

1.1. Gasification of solid wastes

In recent years, society has changed from a linear to a circular economy. The escalating energy demand and the requirement for more sustainable processes have increased interest in using waste as feedstock for energy production.

The thermal conversion of solid wastes presents the advantage of generating energy while processing a fraction that would otherwise be landfilled (1–3), being an attractive process that responds to the acute need for circular and sustainable processes. However, this alternative still presents several drawbacks associated with the intrinsic nature of waste fuels - i.e., heterogeneity in size and composition and content in contaminants precursors - compared to other standardized fuels, such as coal or clean biomass (4).

Incineration is the most common process for the large-scale thermal valorisation of such fuels, while pyrolysis and gasification are still in development and, thus, are typically used at smaller plants (5). Nevertheless, gasification is of great interest since it produces a gas that can be used in boilers, engines, turbines, and fuel cells to generate electricity when efficiently cleaned.

Municipal Solid Waste (MSW) can be processed to generate Refuse Derived Fuel (RDF), or Solid Recovered Fuel (SRF), the latter being a standardized material from MSW, which can be easier processed to generate energy (6). Nevertheless, solid wastes, such as MSW, RDF, SRF and Dried Sewage Sludge (DSS) contain high amounts of species that potentially form pollutants during gasification: Cl, S, N and trace elements, i.e. heavy metals (HM) (4,7–9). Therefore, the thermochemical processes that use these fuels must be adapted with cleaning steps and close control of the pollutants generated.

1.2. Nitrogen, Chlorine, and Sulphur in waste-derived fuels

During the gasification of wastes, special attention is paid to the formation of some compounds derived from Cl, S and N in the gas phase, i.e., HCl, H_2S, NH_3, and HCN, as well as to some harmful HM. Furthermore, the content of pollutants precursors in these fuel types is much higher than in plant-based biomass, which is the most common fuel in gasification plants. Hence, the novelty of dealing with high amounts of Cl, S and N in the fuel may justify why several lab-scale plants are not appropriately prepared for quantifying such pollutants. Table 1.1 below shows the typical content of S, **N** and Cl for different types of fuels.

Table 1.1. *Content of S, **N** and Cl for different types of fuels according to literature. ND and NM stand for not detected and not measured, respectively* (4,10–19)

Fuel	Amount of S, N and Cl (% wt. daf)	Reference
Wood	<0.1 / **0.1 – 0.5** / 0.08 – 0.1	*R. Zevenhoven & P. Kilpinen (10 – 12)*
	0.03 / **0.4** / 0.02	*Paasen et al. (taken from the Phyllis2 database) (4)(15)*
	<0.03 / **<0.03** / <0.03	*Schweitzer et al. (19)*
Pinewood	ND / **ND** / ND	*Ryu et al. (16)*
Reed canary grass	0 / 1.3 / 0.6	*Ryu et al. (16)*
Bark	2 / **~ 0.5** / 0.02 – 0.4	*R. Zevenhoven & P. Kilpinen (10 – 12)*
Straw	~ 0.2 / **0.5 – 1** / 0.1 – 1.5	*R. Zevenhoven & P. Kilpinen (10 – 12)*
Dry Sewage sludge (DSS)	~ 0.2 / **1 – 5** / 0.03 – 1	*R. Zevenhoven & P. Kilpinen (10 – 12)*
	2 / **7** / 0.03	*A. Ronda et al. (14)*
	0.1 – 1.1 / **0.3 – 7.6** / 0.02 – 0.5	*Literature in A. Ronda et al. (14)*
	0.02 / **0.07** / 0.002	*Schweitzer et al. (19)*
Poultry litter	0.9 / **6. 5** / 0.7	*D. Pandey et al. (17)*
Cattle manure	0.01 / **0.03** / 0.008	*Schweitzer et al. (19)*
Pig manure	0.01 **0.03** / 0.005	*Schweitzer et al. (19)*
Municipal solid waste (MSW)	0.1 – 1 / **~ 1** / 0.05 – 0.25	*R. Zevenhoven & P. Kilpinen (10 – 12)*
	0.5 / **1.2** / 1.1	*Paasen et al. (taken from the Phyllis2 database) (4)(15)*
Refuse-derived fuel (RDF)	0.1 – 1 / **~ 1** / 0.3 – 0.8	*R. Zevenhoven & P. Kilpinen (10 – 12)*
	0.1 / **0.5** / 0.7	*V. F. de Almeida et al. (13)*
	0.4 / **1.1** / 0.4	*Paasen et al. (taken from the Phyllis2 database) (4)(15)*
	0.1 / **1.2** / 2.3	*Ryu et al. (16)*
Solid recovered fuel (SRF) – 80% plastic, 20% cellulose	0.03 / **0.1** / NM	*U. Arena & F. Di Gregorio (18)*

From Table 1.1 data, some highlights can be made, even though, due to the intrinsic heterogeneity of waste fuels, concentrations can vary substantially:

- DSS typically contains around 0.1 – 1.1% wt. dry and ash-free (daf) of S (up to 2.0% wt. daf) and 0.03 to 1% wt. daf of Cl (15)(13).

- RDF usually contains less S (0.1 – 0.4% wt. daf, up to 1% daf) and more Cl (0.3 – 0.8% wt. daf), up to 2.3% wt. daf. Nitrogen is also higher in DSS due to its protein content, up to 7.6% wt. daf, while about 0.5 – 1.2% wt. daf in RDF (4).
- For wood, S and Cl appear in trace amounts, from 0.03 – 1% for S and 0.02 – 0.08% wt. daf, while N varies from 0.03 to 0.5% wt. daf (4).

1.3. Trace elements and heavy metals in waste-derived fuels

Besides the major elements (elements that constitute more than 1 percent of the fuel by weight: carbon, hydrogen, oxygen, nitrogen, and sometimes chlorine and sulphur) the fuel contains minor elements (between 1.0 to 0.01 %w/w) like Ca, Cl, S, Mg, Na, K, Si, Al, Fe, P. The rest of elements in the fuel in concentrations less than 0.1% wt. is called trace elements. They typically include the EDD (European Dirty Dozen: As, Cd, Cr, Cu, Co, Hg, Mn, Ni, Pb, Sb and V (20)) as well as Zn and Sn. The major elements have a significant role in chemical balance, which affects the behaviour of pollutants during thermal conversion.

Due to the nature of waste-derived fuels, such as MSW, RDF, and Dried Sewage Sludge (DSS), their content in trace elements and heavy metals is much higher than the content in clean biomass, or coal. For instance, clean biomass usually contains a high amount of Mn, K, P, Cl, Ca, Mg and Na. In the other side, waste-fuels normally presents a substantial content in Cu, Pb, Mn, and even harmful metals, such as Hg, As, and Cd.

Table 1.2 below shows the typical concentrations of different elements for DSS, RDF and wood, gathering data from own dedicated tests (ODT) and the literature.

Table 1.2. *Comparative concentration of trace elements in different types of fuels in g/kg of dry fuel.*

Element	**DSS**	**DSS**	**DSS**	**DSS**	**RDF**	**RDF**	**RDF**	**Wood**	**Wood**
Description	*(840µm – 2mm)*	*(500 - 840µm)*	*(500µm – 2mm)*	*Literature range**	*Pellets*	*Pellets*	*NA*	*Pellets*	*NA*
Reference	*ODT*	*ODT*	*A. Ronda et al. (15)*	*A. Ronda et al. (15)*	*ODT*	*De Almeida et al. (14)*	*Zevenhoven & Kilpinen (21)*	*ODT*	*Zevenhoven & Kilpinen (21)*
Al	14.34	5.13	8.26	10.5 – 23.6	3.28	17.60	NM	2.00	NM
As	0.01	0.01	0.05	0.01 – 1.50	3.47	0.00	~ 0.01	0.33	0.00
Ba	NM	0.25	NM	NM	ND	1.15	NM	ND	NM
Be	NM	NM	0.00	ND	NM	NM	0.00	NM	NM
Ca	46.54	23.89	24.49	22.8 – 82.6	17.24	2.55	NM	1.90	NM
Cd	0.00	0.00	0.00	0.00 – 0.05	0.01	0.00	0.00 – 0.01	0.01	NM
Co	0.01	0.01	0.00	0.00 – 0.05	0.00	0.01	NM	0.03	0.00
Cr	0.14	0.08	0.07	0.00 – 0.50	0.04	0.06	0.05 – 0.25	0.03	0.00
Cu	0.73	0.40	0.21	0.11 – 1.22	0.17	0.04	< 1.00	0.19	0.00
Fe	21.52	11.50	17.86	6.80 –107.00	1.58	1.70	NM	0.23	NM
Hg	ND	0.01	NM	NM	ND	0.01	0 – 0.01	ND	0.00
In	NM	0.00	NM	NM	ND	NM	NM	ND	NM
K	4.96	7.72	4.51	2.38 – 9.70	2.90	0.42	NM	0.89	NM
Mg	7.55	3.74	5.63	3.13 – 6.72	1.33	1.15	NM	0.67	NM
Mn	0.20	0.19	0.21	0.03 – 1.93	0.01	0.05	~ 0.25	0.07	0.01 – 1.00
Na	2.25	6.95	3.05	0.01 – 3.00	2.33	7.45	NM	2.78	NM
Ni	0.17	0.13	0.11	0.02 – 1.52	0.25	0.01	0 – 0.10	0.25	0.00
P	30.06	23.94	27.42	0.23 – 21.00	ND	8.15	NM	ND	NM
Pb	0.09	0.07	0.05	0.09 – 0.264	0.00	0.04	0.10 – 0.50	ND	0.00 – 0.02
Sb	0.01	0.02	0.01	0.01	0.03	0.03	< 0.01	0.01	NM
Se	ND	0.00	<0.01	0.00 – 0.02	ND	NM	0.00 – 0.01	ND	0.00
Si	16.58	ND	0.46	1.00 – 71.10	9.49	2.05	NM	0.89	NM
Sn	0.06	1.06	0.28	0.00 – 0.09	0.08	0.01	~ 0.50	0.00	NM
Sr	ND	0.35	NM	NM	ND	0.04	NM	ND	NM
Te	ND	0.00	NM	NM	ND	NM	NM	ND	NM
Ti	1.29	1.16	1.09	0.01 – 1.500	1.67	0.21	NM	0.01	NM
V	0.02	0.02	0.06	0.00 – 0.03	0.00	0.01	NM	0.00	~ 0.00
Zn	1.17	1.18	0.30	0.10 – 2.33	0.24	0.22	0.30 – 0.80	0.16	0.01 – 0.15

NA: Not applicable / NM: Not measured / ND: Not detected / ODT: Own dedicated tests
Ronda et al. (15)*; Zevenhoven & Kilpinen* (21)*; de Almeida et al.* (14)

From Table 1.2, it is possible to observe that the content of trace elements is in the same range for the different types of fuels presented, in this case Dried Sewage Sludge (DSS), Refuse-Derived Fuel (RDF) and wood. Additionally, in this table it is evidenced that the content of trace elements is much higher in the waste fuels compared to clean biomass.

1.4. The release of inorganic elements during the gasification of waste-derived fuels

The chemical form in which these elements are bounded in the parent fuel – for instance, organic or inorganic compounds - greatly affects its partitioning between gas and solid phases. Therefore, when processing waste-derived fuels in thermochemical routes, it is important to understand how the elements in the fuel behave during their processing, i.e., if the element tends to stay in the solid phase or be released to the gas phase, as well as the way in which the combine one with each other. This knowledge should be estimated as a function of the physical (size, density) and chemical properties (elemental and proximate analysis) of the fuel and the operating conditions (temperature, pressure, and composition of the bulk gas environment). Furthermore, adapting the downstream processes to comply with the current normative for heavy metals is crucial for scaling up a process, such as fluidized-bed gasification to meaningful scales.

Complementary, nowadays, the need for some of valuable elements, such as the Critical Raw Materials (CRM) -includes Mg, Co, Ti, Li, V and P – suggest that the recuperation of these elements are also of great interest during the waste processing for energy (22).

During thermal conversion, organic compounds are more prone to be released to the gas phase, because their bound energies are weaker (23,24). Other parameters also influence the contaminants partitioning, i.e. temperature, oxygen ratio (or equivalence ratio, ER), fuel particles size, solids residence time, gasification agent and reactor design (8,9,25–28). Measurement of contaminants is an essential task, both for gas cleaning design, as well as for keeping contaminants under the environmental limits enforced by governmental standards.

For instance, the final use of the syngas limits the maximum concentrations of HCl, H_2S and NH_3 in syngas. Its use in a gas engine is the less restrictive application (80, 100 and 50 mg/m_n^3 of Cl, S and NH_3, respectively), followed by its use in boilers (72 and 35 mg/m_n^3 of Cl and S respectively) (29). More restrictive applications for syngas, requires a much lower level of pollutants such as its use in fuel cells (1 mg/m_n^3 of Cl or S) (4).

1.5. Aim and relevance of this work

1.5.1. Aim of this work

The purpose of this work is to study the gasification of waste-derived fuels establishing the main differences with respect to the gasification clean fuel, such as biomass. Therefore, the thesis was centred on the content of contaminant precursors in solid waste fuels – i.e., MSW, RDF and DSS – and their behaviour during the thermal conversion in the gasification process, with emphasis in fluidized bed conditions. In the following chapters, the literature will be reviewed, including the main techniques for the measurement of contaminants, their content in the fuel and in the product streams. Then, data from own-dedicated experiments both in laboratory and bench scale tests will be presented. Next, results of modelling simulations will be presented and, finally, the environmental assessment of continuous gasification processes using RDF will be shown.

1.5.2. Relevance of this work

This work contributes to the expansion of the current understanding of the inorganics and trace elements content in waste fuels and their distribution during thermal conversion, focusing on the gasification in fluidized bed reactors.

The results obtained contribute to a more accurate understanding of this subject, which can enable a better design of compatible equipment, the gasification process and downstream cleaning processes that can enable the upscaling of the technology to larger scaled, supporting the achievement of the current Sustainable Development Goals (SDGs).

Sampling and measuring gaseous contaminants formed in the output streams of the gasification process in a fluidized bed reactor is a challenging process. In the syngas, gaseous contaminants, such as H_2S, NH_3 and HCl are usually quantified since their content can significantly restrict the use of the syngas. Trace elements, especially heavy metals, are usually quantified in the product solid stream, because its content may also restrict their further use – such as soil amendment in the case of ashes from dried sewage sludge – or proper disposal. Therefore, gaseous species containing N, S and Cl and the content of trace elements in the solid streams are usually measured in the product streams from gasification experiments conducted in the literature. For the fluidized bed reactors, it is even more challenging to quantify the trace elements content in the solid residue, since it mixes with the bed material during the process. The sampling and measurement methods, as well as the reactor material may influence the results of such species, which might interfere in the realistic design of upscaled gasification process using waste fuels, in the environmental impact it causes, and in its associated costs.

Therefore, this study has been done focusing on two main aspects: literature review on the thermal conversion of waste fuels, specially fluidized bed gasification; and an experimental part that aimed at the understanding of the most fit-for-purpose lab-scale reactor materials, sampling and measurement methods and the influence of the process parameters on the distribution of inorganics and trace elements during the thermal conversion. The literature review presents the sampling and measurement methods presented in the literature, and the percentage of the recovery of N, S and Cl in the products compared to their parent fuel. Inconsistencies were found, pointing out potential inaccuracies in the materials, sampling and measurement methods presented in the selected studies. The experimental part of this thesis consists in tests designed for the understanding of how gaseous contaminants species and trace elements present in the solid residue could be properly quantified. Moreover, the distribution of species among gaseous and solid streams were also studied and continuous gasification tests were performed in order to better understand the chemistry and distribution of inorganic and trace elements during the thermal conversion.

Based on the results of the tests conducted on the fluidized bed gasification facility at bench scale, an environmental Life-Cycle Environmental Assessment (LCA) was performed, as well as a tecno-economic assessment. Results of fluidized bed gasification was compared to landfilling the same waste, which is the common practice in most countries worldwide.

Additionally, a thermodynamic analysis of the species that could be potentially formed during the gasification of wastes was performed through modelling, which is presented in Annex form in this thesis. The thermodynamic modelling was performed through the software *HSC Chemistry*®. Even though the residence time of gasification in fluidized bed is very low and the equilibrium is not reached in such conditions, results from equilibrium can support the understanding of which species could be potentially formed. Thermodynamic modelling is a very interesting topic; however, simulations might be very complex since waste derived fuels are composed by several elements that impact on the chemical reactions. Therefore, this topic was explored during this thesis only to a certain extent. A more detailed study of this topic was left for future work.

In summary, the relevance of this thesis lies on the assemble of valuable information regarding the inorganics and the trace elements content in solid waste fuels, mainly DSS and RDF.

1.6. Summary of the content of this thesis

In the next paragraphs the content of the following chapters of this thesis - Chapters 2 – 6 - will be summarized.

In chapter two (2), the measurement of the main inorganic contaminants on waste-derived fuels is studied. The purpose of this chapter is reviewing the most common methods for the measurement of contaminants of literature. Data from literature are thoroughly reviewed and discussed, and results from own-dedicated experiments for the evaluation of the measurement methods for contaminants are presented.

In chapter three (3), the results of discontinuous devolatilization experiments using Dried Sewage Sludge (DSS), Refuse Derived Fuel (RDF) and clean woody biomass (for comparison) is presented. The aim is the understanding of the behaviour of trace elements during the thermal conversion and the main influencing parameters.

In chapter four (4), the results of continuous tests carried out in a bench-scale fluidized-bed gasification plant is presented and discussed. The influence of process parameters, such as,

temperature, Equivalence Ratio (ER), and their effect on the main products – i.e., carbon dioxide, carbon monoxide, methane, hydrogen, tars, and char – as well as minor and trace species and contaminants is investigated. The effect of hot gas filtration on the trace elements is also studied.

In chapter five (5), the conclusions of this study will be presented, highlighting the main challenges that solid wastes gasification of fluidized bed face because of their higher content in trace elements and heavy metals, pointing out the most feasible solutions for their use in meaningful scales for energy production.

Additionally, two Annexes are included to this thesis. In Annex I, the thermodynamic analysis of the distribution of the trace elements present in waste fuels during gasification conditions is studied. The results from simulations carried out in the HSC Chemistry ® Software is shown and discussed for some cases of interest for gasification. The main focus in understanding the behaviour of inorganics and trace elements during gasification conditions by analysing their behaviour in equilibrium. In Annex II the Environmental Life Cycle Assessment (E-LCA) of the continuous gasification of RDF is presented. Some of the results obtained from experiments presented in chapter 4 are used.

Chapter 2

Measurement of the main inorganic contaminants on waste-derived fuels

2.1. Summary

Because of the heterogeneity and high content of contaminant precursors (Cl, S and N), the gasification of waste-derived fuels is challenging compared to clean biomass. A great deal of work has been published on wastes thermal conversion. However, reliable quantification of pollutants (i.e., HCl, H_2S, NH_3 and HCN) during gasification of wastes remains a difficult task. Particularly, it is hard to scale-up results from laboratory-scale to industrial reactors. This is because the materials and methods used in the former result in a significant interference with the gasification process, whereas in the latter the interaction is very limited.

These issues are investigated by: ***(i)*** analysing pilot/laboratory plant data from literature to calculate the recovery (ratio between the contaminant measured in the output streams and that in the input fuel); and ***(ii)*** conducting dedicated laboratory tests in various setups, doping a gas with the main inorganic contaminants in concentrations typical of waste-derived syngas. Outcomes from our tests elucidate the inconsistencies detected when analysing data from the literature. Recommendations for proper sampling and analysis of contaminants during the gasification of waste-derived fuels are given, so that the measurements from laboratory can be properly upscaled.

2.2. Methods for contaminants measurement

The traditional procedure used to measure contaminants in gas phase, such as HCl, H_2S, NH_3 and HCN in syngas, is the wet chemical technique, which is based on the syngas bubbling in impingers that contain an absorbing solution. For HCl capture, distilled water is widely applied as absorbing solution, although a sodium hydroxide (NaOH) solution is also an option due to its basicity. For the

capture of NH_3, dilute sulfuric acid (H_2SO_4) is normally used, while for H_2S and HCN, a basic solution is employed, commonly dilute NaOH.

The analyses of these species are made off-line, being the Ion Chromatography (IC) technique the most extensively applied. This is due to the IC capacity of tolerating a dirty gas without compromising the measurement reliability. However, condensate tars must be removed by filtering the collected content.

Moreover, H_2S can be analysed online through gas chromatography and UV based techniques. There are even more sophisticated methods available that enable online measurements of these contaminants, such as FTIR or mass spectroscopy, but these are less frequently applied in laboratory-scale and are more common in pilot or commercial gasification plants.

The simultaneous sampling of various species, i.e., using impingers in series, may result in inconsistencies. This is because one absorbing solution can capture other species in addition to the expected one (30).

Ståhlberg et al. (31) evaluated the storage time impact on results, finding that while NH_3 can be stored in a cold and dark place in an acid medium (pH=2, achieved through H_2SO_4 addition) for over a month, HCN should be preferably analysed immediately after sampling, with a maximum storage time of 6h. In order to guarantee the results accuracy, Ståhlberg et al. (31) also recommend a maximum storage time of 3-4 days for HCl.

2.3. Contaminants partitioning in literature

Several studies were selected from literature, in which the concentrations of HCl, H_2S, COS, NH_3 and HCN in gas phase were measured and clearly reported in Table 2.1 (4,11,17–19,32–36). The mass balances of Cl, S and N were made, and the recoveries (R, %) were calculated, defined as the ratio of the amount of element in the phase analysed and that in the parent fuel:

$$R_i = \frac{m_i{}^p}{m_i{}^f} \cdot 100\% \qquad \text{(Eq. 2.1)}$$

In which: $m_i{}^p$ is the mass of the element *i* in the phase (p) of interest (p: gas, solid) and $m_i{}^f$ is the mass of the element *i* in the fuel.

Information of fuel, temperature, reactor material, gasification agent, equivalence ratio (ER), mass balances, tar, and char (when available), are included in Table 2.1, as well as relevant details of the collection setup. All works deal with gasification, except for Ryu et al. (17), which covers pyrolysis. Particular assumptions were made for the calculations in order to assess Cl, S and N mass balances in some works (19,32–36), as indicated in the comments of Table 2.1. Most recoveries (R) were calculated considering only the gas phase (the only one reported), with the exception of Paasen et al. (4), Ryu et al. (17) and Arena and Gregorio et al. 2014 (32), in which data of tars and solid streams were provided and , thus, included in the mass balances.

Table 2.1. *Review and analysis of literature works measuring contaminants derived from Cl, N, and S.*

							Recovery (%)									
Reference	**Feedstock**	**Temperature**	**ER**	**Reactor / Material**	**Atmosphere**	**Bed material**	**Gas**	**Tar**	**Solid**		**Total**					**Summary of sampling setup**
		ºC					**Cl**	**S**	**N**	**Cl**	**Cl**	**S**	**Cl**	**S**	**N**	
Paasen et al [3]	SS + WP	750	0.22	FB/NS	Air	Silica Sand	6.1	108.6	41.4	1.2	5.0	5.3	12.2	113.9	41.4	** H_2S and COS in gas phase: Micro GC, when in low concentrations they were measured by GC*
	SS + WP	850	0.23	FB/NS	Air	Silica Sand	8.5	92.3	23.8	9.1	4.5	7.6	22.1	99.8	23.8	** HCl in gas phase: collected in impingers, HCl analysed by IC*
	RDF	725	0.21	FB/NS	Air	Silica Sand	16.3	57.4	3.3	35.9	1.7	1.5	53.9	58.8	3.3	*while NH_3 and HCN by FIA*
	RDF	820	0.21	FB/NS	Air	Silica Sand	53.4	27.0	11.4	44.2	8.6	6.8	106.2	33.8	11.4	**Cl in tar: EOX analyser, coulometry after combustion*
																**Solid phase: Cl same method used for tar, and S by ICP*
Ryu et al [15]	RDF*	350 - 700	-	Packed Bed/316SS	N2	-	-	-	-	-	0.0	50.6	1.6	53.4	-	**Pyrolysis tests* **S and Cl also measured in oil phase/ ICP and SEM analysis of char* **Cl: analysed by titration, using the Schöninger oxygen flask combustion*
Arena and Gregorio [16]	SRF	849	0.26	FB/NS	Air	Olivine	1.2	0.8	1.5	-	-	-	1.2	0.8	1.5	**NH_3, H_2S and HCl in gas phase: collected in impingers and analysed by IC*
	SRF	852	0.26	FB/NS	Air	Olivine	0.0	0.0	0.0	-	-	-	0.0	0.0	0.0	**Average of recovery rates, since contaminants content in fuel was in an interval*
	SRF	869	0.27	FB/NS	Air	Olivine	0.4	0.0	2.8	-	135.0	-	135.4	0.0	2.8	
	SRF	879	0.30	FB/NS	Air	Olivine	16.4	4.7	0.9	-	-	-	16.4	4.7	0.9	
	SRF	898	0.32	FB/NS	Air	Olivine	0.3	0.1	0.1	-	-	-	0.3	0.1	0.1	

	SRF	932	0.33	FB/NS	Air	Olivine	3.2	0.1	0.5	-	133.8	-	137.0	0.1	0.5	
Arena and Gregorio [17]	SRF	833	0.26	FB/NS	Air	Olivine*	885.2	63.6	117.6	-	-	-	885.2	63.6	117.6	** SRF type 1 / Bed material also contained Fe and Mg silicates*
	SRF	816	0.31	FB/NS	Air	Olivine*	432.3	80.4	371.3	-	-	-	432.3	80.4	371.3	** Same collection and measurement method of Arena & Gregorio, 2014*
	SRF	847	0.37	FB/NS	Air	Olivine*	412.8	77.2	250.3	-	-	-	412.8	77.2	250.3	
	SRF	850	0.39	FB/NS	Air	Olivine*	401.9	76.2	131.7	-	-	-	401.9	76.2	131.7	
Berrueco et al [18]	RT	700	0.30	FB/Hastelloy-X	Air	Silica Sand	19.6	5.2	3.2	-	-	-	19.6	5.2	3.2	**NH_3, H_2S and HCl in gas phase: collected in Tedlar bags, then pumped*
	RT	750	0.31	FB/Hastelloy-X	Air	Silica Sand	13.0	0.7	3.4	-	-	-	13.0	0.7	3.4	*into impingers and analysed by means of ISE*
	RT	800	0.31	FB/Hastelloy-X	Air	Silica Sand	13.7	7.7	2.6	-	-	-	13.7	7.7	2.6	
	RT	850	0.31	FB/Hastelloy-X	Air	Silica Sand	6.0	20.3	9.6	-	-	-	6.0	20.3	9.6	
Recari et al [19]	RT	750	0.31	FB/Hastelloy-X	Air	Silica Sand	13.1	0.0	3.2	-	-	-	13.1	0.0	3.2	** Same collection and measurement method of Berrueco et al, 2015*
	RT	850	0.31	FB/Hastelloy-X	Air	Silica Sand	7.3	21.5	10.8	-	-	-	7.3	21.5	10.8	
	FL	750	0.30	FB/Hastelloy-X	Air	Silica Sand	30.8	0.0	2.1	-	-	-	30.8	0.0	2.1	
	FL	850	0.30	FB/Hastelloy-X	Air	Silica Sand	34.8	0.0	2.5	-	-	-	34.8	0.0	2.5	
	RT	850	0.31	FB/Hastelloy-X	Air	Dolomite	6.1	21.6	0.0	-	-	-	6.1	21.6	0.0	
	FL	850	0.31	FB/Hastelloy-X	Air	Dolomite	4.5	0.0	0.0	-	-	-	4.5	0.0	0.0	
	RT	850	0.30	FB/Hastelloy-X	O2/Steam	Dolomite	6.8	0.0	4.3	-	-	-	6.8	0.0	4.3	
Recari et al [20]	FL290*	850	0.29	FB/Hastelloy-X	Air	Silica Sand	2.2	48.1	24.2	-	-	-	2.2	48.1	24.2	**FL290, FL320: Torrefacted SRF at 290 and 320ºC, respectively.*

	FL290	850	0.31	FB/Hastelloy-X	Air	Dolomite	0.9	32.6	8.3	-	-	-	0.9	32.6	8.3	* Same collection and measurement method of Berrueco et al, 2015
	FL320*	850	0.29	FB/Hastelloy-X	Air	Silica Sand	20.1	62.8	22.0	-	-	-	20.1	62.8	22.0	
	FL320	850	0.29	FB/Hastelloy-X	Air	Dolomite	14.1	49.5	23.9	-	-	-	14.1	49.5	23.9	
	FL290	850	0.32	FB/Hastelloy-X	O2/Steam	Silica Sand	1.9	24.3	30.0	-	-	-	1.9	24.3	30.0	
	FL290	850	0.32	FB/Hastelloy-X	O2/Steam	Dolomite	1.0	62.8	42.7	-	-	-	1.0	62.8	42.7	
	FL320	850	0.30	FB/Hastelloy-X	O2/Steam	Silica Sand	5.7	35.8	48.0	-	-	-	5.7	35.8	48.0	
	FL320	850	0.31	FB/Hastelloy-X	O2/Steam	Dolomite	6.5	118.8	64.3	-	-	-	6.5	118.8	64.3	
	FL320	850	0.31	FB/Hastelloy-X	O2/Steam	Olivine	2.3	78.1	38.7	-	-	-	2.3	78.1	38.7	
Recari et al [21]	RT	850	0.31	FB/Hastelloy-X	O2/Steam	Silica Sand	97.5	14.2	47.2	-	-	-	97.5	14.2	47.2	* Same collection and measurement method of Berrueco et al, 2015
	RT	850	0.34	FB/Hastelloy-X	O2/Steam	Dolomite	27.5	103.8	92.4	-	-	-	27.5	103.8	92.4	
	RT	850	0.29	FB/Hastelloy-X	O2/Steam	Olivine	98.5	3.7	47.7	-	-	-	98.5	3.7	47.7	
	FL	850	0.30	FB/Hastelloy-X	O2/Steam	Silica Sand	106.7	15.6	53.7	-	-	-	106.7	15.6	53.7	
	FL	850	0.31	FB/Hastelloy-X	O2/Steam	Dolomite	91.5	38.4	111.6	-	-	-	91.5	38.4	111.6	
	FL	850	0.30	FB/Hastelloy-X	O2/Steam	Olivine	93.0	34.0	44.1	-	-	-	93.0	34.0	44.1	
Pandey et al [22]	PL	700	0.18	FB/NS	Air+N2	Silica Sand	0.7	18.9	96.2	-	-	-	0.7	18.9	96.2	* H_2S and COS in gas phase: Micro GC
	PL	700	0.22	FB/NS	Air+N2	Silica Sand	0.7	27.6	96.2	-	-	-	0.7	27.6	96.2	* NH_3 and HCl in gas phase: Collected once a day in impingers and
	PL	700	0.30	FB/NS	Air+N2	Silica Sand	0.7	23.8	96.2	-	-	-	0.7	23.8	96.2	measured by means of IC, they were collected in the end of four tests,

	PL	700	0.30	FB/NS	Air+N2	Silica Sand	0.7	37.6	96.2	-	-	-	0.7	37.6	96.2	*so results are in average.*
	PL	700	0.29	FB/NS	Air+N2	Sand+Limestone	4.2	25.6	98.4	-	-	-	4.2	25.6	98.4	
	PL	700	0.35	FB/NS	Air+N2	Sand+Limestone	4.2	30.2	98.4	-	-	-	4.2	30.2	98.4	
	PL	700	0.41	FB/NS	Air+N2	Sand+Limestone	4.2	15.2	98.4	-	-	-	4.2	15.2	98.4	
	PL	700	0.35	FB/NS	Air+N2	Sand+Limestone	4.2	35.7	98.4	-	-	-	4.2	35.7	98.4	
	PL	750	0.23	FB/NS	Air+N2	Sand+Limestone	0.6	11.2	71.9	-	-	-	0.6	11.2	71.9	
	PL	750	0.28	FB/NS	Air+N2	Sand+Limestone	0.6	13.7	71.9	-	-	-	0.6	13.7	71.9	
	PL	750	0.33	FB/NS	Air+N2	Sand+Limestone	0.6	12.5	71.9	-	-	-	0.6	12.5	71.9	
	PL	750	0.28	FB/NS	Air+N2	Sand+Limestone	0.6	17.8	71.9	-	-	-	0.6	17.8	71.9	
	PL	800	0.25	FB/NS	Air+N2	Sand+Limestone	-	11.1	-	-	-	-	-	11.1	-	
	PL	800	0.30	FB/NS	Air+N2	Sand+Limestone	-	12.6	-	-	-	-	-	12.6	-	
Schweitzer et al [23]	*SS*	*800*	-	*CFB/NS*	*O2/Steam*	*Silica Sand**	*84.2*	*20.9*	*47.6*	-	-	-	*84.2*	*20.9*	*47.6*	**NH_3, H_2S and HCl in gas phase: collected in impingers*
	CM	*800*	-	*CFB/NS*	*O2/Steam*	*Silica Sand**	*9.6*	*80.0*	*37.0*	-	-	-	*9.6*	*80.0*	*37.0*	**Quantification: NH_3 by photometry analysis, HCl by coulometry and*
	PM	*800*	-	*CFB/NS*	*O2/Steam*	*Silica Sand**	*8.9*	*39.3*	*34.2*	-	-	-	*8.9*	*39.3*	*34.2*	*H_2S through the reaction with Zn, quantified by iodometric titration*

- *For Arena & Gregorio works, the MB in gas phase was done assuming that contaminants concentration (mg/nm^3) was referring to the same gas of the gas yield results provided in the papers, because in both works the product gas was not specified as wet or dry.*
- *For Berrueco et al and Recari et al works it was considered that, contaminants concentration was given for a syngas containing N_2. Both, gas yield and contaminants concentration were considered for a dry syngas.*
- *For the remaining papers included, the gas yield and contaminants concentrations were provided in a way that mass balance in gas phase could be assessed directly.*

The majority of authors collected contaminants containing Cl and N in impingers and then measured their concentrations by IC (4,18,19,32). In those works, H_2S was sampled and measured in the same way as Cl and N (32)(19), or online via micro-GC (4)(18). Berrueco et al. (33) and Recari et al. (34–36) also collected contaminants through impingers, but they analysed the solutions with a different method, the Ion-Selective Electrode (ISE).

Schweitzer et al. (11) used impingers as well, and measured contaminants by using three different methods: photometry (NH_3), coulometry (HCl), and reaction with Zn, followed by iodometric titration (H_2S). The concentrations of such species in syngas can be analysed online using more sophisticated technologies as mentioned before, i.e. mass spectroscopy (37)(38) or FTIR (39)(40). However, these methods are not included in Table 2.1 due to the lack of data for the calculation of elemental mass balances.

Although in most works presented in Table 2.1 data for calculations of the Cl, N and S contents in syngas were available, it was not possible to close the elemental balances considering all exit streams (tar in syngas, exit ash and char streams). This is because information was not available. Paasen et al. (4) measured contaminants in tars and in the solid residues, and Arena and Gregorio 2014 (32) and Ryu et al. (17) measured Cl in the solid residue. Generally, data provided is incomplete to establish the species partitioning.

In all works included in Table 2.1, contaminants in gas phase were collected in a liquid solution for posterior analysis. However, samples storage time was not included in any of them (unless for Paasen et al. (4)) which could be an additional source of inaccuracies in contaminants quantification.

2.4. Analysis and discussion of results from literature

From the analysis of works summarized in Table 2.1 it is observed that, for some tests, the calculated recoveries of contaminants are extremely low or exceed 100%. In some experiments, the release of gas contaminants was negligible, while in others, more Cl, S or N were found in the gas phase than in the parent fuel. Fuel heterogeneity together with the inherent difficulties in the measurement (sampling and/or analysis, and interaction with the reactor/piping material of the rig) of some species could explain these inconsistencies (30)(31).

Paasen et al. (4) measured contaminants derived from Cl, S and N, using two types of fuels: SRF and a blend of DSS and clean biomass (white pellets). They were focused on the Cl and S partitioning, and to our knowledge it was the only work found in literature in which the partitioning of contaminants into gas, tar and solid phases is reported in detail. They described the measurement methods for S and Cl in gas phase (tar included), the influence of Cl and S sampling points, as well as the impact of the tests duration on the results. The Cl and S in the solid residues were measured by sampling solids located in the freeboard and cyclone, showing that these species are more concentrated in the cyclone ash, due to their condensation on particulate matter surfaces.

They concluded that Cl in tar is overestimated, probably because some HCl is dissolved from the gas phase when sampling tars (4). Authors recognized that Cl and S mass balances were not closed in most tests, which was attributed to the partial recollection of ashes. They claimed that mass balances for Cl and S would have been closed if all ash had been collected.

Ryu et al. (17) performed pyrolysis tests and then quantified Cl and S in solid and oil phases. It can be concluded that most of Cl, and about 50% of S, were released to the gas phase, which agrees with the expected partitioning behaviour for these species (41). However, contaminants in gas phase were not quantified, so, in this case, the mass balance closure does not apply.

Mass balances calculations for the results reported by Arena and Gregorio (32) showed very low recoveries for Cl, S and N in the gas phase. Chlorine was measured in two tests in solid phase (fly ashes), with a recovery of around 134%. Therefore, it was concluded that Cl from the gas phase was condensed on ash, in agreement with observations from previous studies (4). Cl recovery for exceeds 100% and the surplus may be justified by the low content of Cl in the fuel and fuel heterogeneity. Also, several processes that samples are submitted to, which are susceptible to errors (i.e., sampling, storage and analysis).

These results contrast to the ones from Arena and Gregorio (19), who reported Cl and N recoveries much greater 100% (achieving 885.2% and 371.3% for Cl and N, respectively). HCl and NH_3 concentrations in the gas phase were not high. However, Cl and N contents in SRF were very low, which may explain the inconsistencies found. The outsized values may indicate the incorrect quantification of those species in the fuel. S recoveries are in the range of 63.6−80.4%, demonstrating that most fuel-S was released to gas phase, which is the expected partitioning behaviour of this element during gasification (4)(41).

Berrueco et al. (33) and Recari et al. (34–36) measurements were made applying the same sampling and analysis procedures, so results are discussed altogether. Recoveries from Berrueco et al. (33) are low for all contaminants in all tests, being the highest ones 19.6% and 20.3% for Cl and S, respectively. Recoveries from Recari et al. (34) were also small, even though, in some tests, Cl and S recoveries reached 34.8% and 21.6%, respectively. These range (19.6 – 34.8%) is still classified as low to moderate recoveries, especially for S, since at least over 90% of S is expected to be found in gas phase. Inconsistencies may be related to the measurement method, which was made by sampling the gas with Tedlar® bags, and the sampling of HCl, H_2S, NH_3 and HCN with impingers, analysed by ISE. As bags were maintained at ambient temperature, the water vapor in syngas may have condensed inside them together with some fraction of contaminants. Moreover, the ISE method is susceptible to interferences during measurements and may not quantify properly species in low concentrations (42), affecting results. Likewise, Norton and Brown (43) found negative deviations (up to 22%) in NH_3 concentrations using the ISE method when measuring ammonia in doped gas.

Recoveries calculated from data Recari et al. (35)(36) indicate that the gross of contaminants was captured from the gas phase in most of the tests, using the same measurement method discussed previously (33)(34). Chlorine recovery was very low for the results from Recari et al. (35), which they attributed to the effect of torrefaction, the process SRF was submitted to before gasification. By analysing the results of their last work (36), it can be observed that the measurement and sampling issues were improved.

In Pandey et al. (18) tests, Cl and N recoveries are identical for some tests, because they provided an average of HCl and NH_3 concentrations. That is because these compounds were sampled in the same impingers in several tests (tests 2 – 4) – using one set of impingers for each component NH_3 and HCl – and then, made an average of NH_3 and HCl concentrations in the product syngas from those experiments. Recoveries were high for N (up to 98.4%) but moderate for S (11.1 - 37.6%). Nonetheless, Cl recovery in the gas was very low, reaching only 4.2%. This may be related to the condensation of Cl in the hot filter because the contaminants' sampling point was after it. The S released to the gas phase was expected to be even higher (>37.6%), since in their experiments COS was also analysed in gas phase. H_2S and COS are the two major species found in syngas, and because all sulphur is supposed to be found in gas during gasification in the range of 700 – 800 ºC, S recovery should approach 100%. The reactor material plays a role in H_2S quantification, which may explain the low S recovery.

Results of Schweitzer et al. (11) show moderate recoveries for N (34.2 - 47.6%) and from moderate to high recoveries for S (20.9 - 80.0%). Authors alerted about the possible errors in the Cl measurement method, because coulometry also detects bromine, oxalate, thiosulphate or thiocyanate compounds. Thus, consequently, Cl concentration in gas could be overestimated. Conversely, Cl recuperation in gas was low when using cattle and pig manure as fuels – recoveries of 9.6 and 8.9%, respectively. For sewage sludge, Cl recovery was high (84.2%), though. They reported that the line before the impingers was maintained at 180°C. However, it is known that at this temperature the formation of NH_4Cl as solid is already favoured, due to its vapor pressure is very low (4). Thus, this could explain the low and moderate recoveries of Cl and N, respectively.

Chlorine and sulphur low recoveries can be associated to corrosion issues. Most works do not report the reactor material used in the gasification tests (Table 2.1). Berrueco et al. (33) and Recari et al. (34)(35)(36) used a reactor made of Hastelloy-X, which is known to be more resistant than other stainless steels (i.e. 316SS). Nevertheless, it can still suffer corrosion at gasification temperatures (700 – 900 ºC), as we later demonstrate in our experiments (presented in the next sections). Ståhlberg et al. (31) showed that stainless steel can be safely used for NH_3 and HCN up to 600-700 ºC, while it is not recommended for HCl and H_2S.

An overview of all these results suggests that inaccuracies in the contaminants evaluation are associated specially with their interaction with the material lining; uncontrolled condensation (water condensation, formation of Cl salts with Na and K, NH_4Cl formation) and issues with the contaminants measurement and sampling methods. All the presented issues are not considered in most works aiming at contaminants measurement in gas phase in the gasification community. These results are used in the experimental section of this chapter to explain the possible errors during measurements of contaminants derived from Cl, N and S.

2.5. Experiments to evaluate the accuracy of the measurement methods

To evaluate the precision of some of the measurement methods used in our facilities, tests were performed with typical contaminants concentrations in waste-derived syngas.

2.5.1. Materials

HCl aqueous solution (37% vol.), NH_3 aqueous solution (25% vol.) and H_2S 1000 ppmv (diluted in N_2) were used to simulate typical contaminants concentrations in syngas from waste-derived fuels. HCN was not studied due to its associated danger, to which our installations are not equipped for. The following compounds were used as absorption solutions: distillate water or NaOH (5% vol.) for HCl, and H_2SO_4 solution (0.05 mol/L) for NH_3. After ammonia sampling, the pH of the captured solution was checked (pH = 2). KOH was added in the impingers to increase pH to 3-4, since it is the necessary range for the operation of the IC column.

2.5.2. Experimental setup and operating conditions

The experiments were conducted in two different setups, shown in Figure 2.1. below.

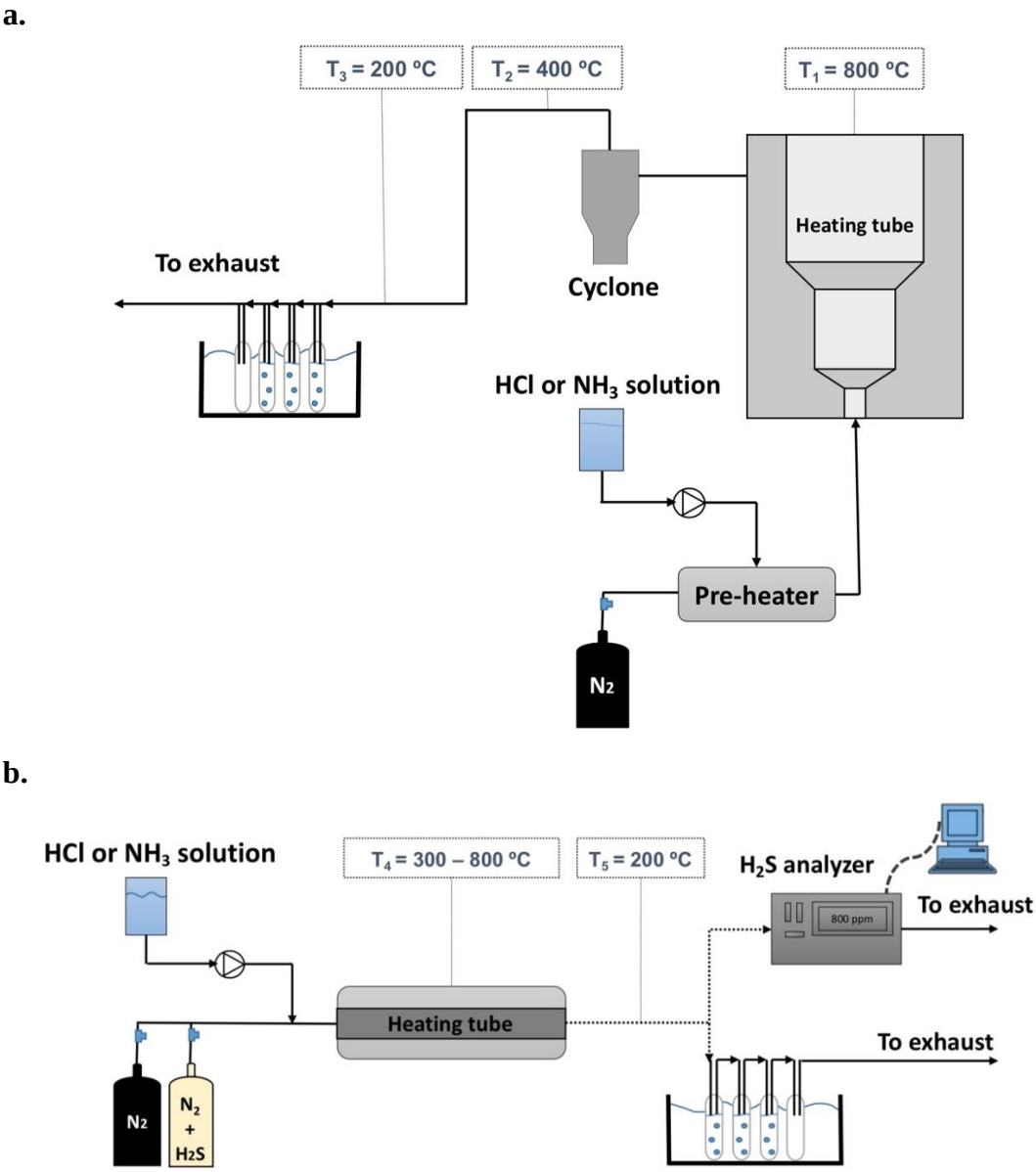

Figure 2.1. *Experimental setups:* ***a.*** *Rig1: first arrangement, in which indicated temperatures were kept at: T_1 = 800 ºC, T_2 = 400 ºC and T_3 = 200 ºC; and* ***b.*** *Rig2: second arrangement: in which T_4 varied accordingly to the test temperature T_4 = 300 – 800 ºC (100 ºC step) and T_5 was fixed at T_5 = 200 ºC.*

The reactor in the arrangement presented in Figure 2.1a is entirely made of 316 Stainless Steel (316SS) and had been previously used in in fluidized-bed mode for gasification and pyrolysis tests. It has two different internal diameters: 51 mm internal diameter (ID) with a length of 250 mm and 81 mm ID with a length of 257 mm (44). For these tests, the reactor was used as a heated tube, without any bed material inside. Bed material is essential for fluidized bed gasification (i.e. silica sand, dolomite, olivine, etc.), and it is known that they influence the contaminants partitioning (36). However, in our experiments we have not used any bed material, because our aim is to investigate possible effects of

the reactor material and methods. Bed material would be then an additional variable and, thus, generate another uncertainty in the analysis.

In this provision, pipes until contaminants sampling had 18 mm ID and 970 mm of length and were also made of 316SS. The area per unit of volume (A/V) was 57 m^{-1} for the reactor and 222 m^{-1} for the pipe.

Figure 2.1b displays Rig2, where various types of tubes were used - made of different alloys: 316 Stainless Steel (316SS), 310 Stainless Steel (310SS), Hastelloy ® C-276, Haynes® HR-160, Kanthal-APM, and quartz (all new). Tubes made of 316SS, C-276, HR-160 and quartz had an ID of one-inch (24.5 mm), while 310SS and Kanthal-APM had an ID of 21.6 and 20.9 mm, respectively. All tubes presented a heated length of 630 mm, and a length of 370 mm and same ID for each material, until the sampling point. The A/V ratio in this setup varied from 160 to 190 m^{-1}. 316SS and C-276 reactors were used for both NH_3 and HCl tests. HR-160 and quartz were also used for the HCl tests. 310SS and Kanthal-APM were employed for the H_2S tests, besides all the materials mentioned before (316SS, C-276, HR-160 and quartz). Kanthal-APM tube was pre-treated up to 800 °C in air atmosphere for two hours to generate an internal protective layer against corrosion (forming alumina).

The lab-scale tests were conducted doping the gas with typical contaminants concentrations in waste-derived syngas: HCl (30 – 250 ppmv), NH_3 (35 – 275 ppmv) and H_2S (500 and 1000 ppmv). Temperatures in the reactor were 500 ºC and 800 ºC for HCl and NH_3 tests, while the range of 300 – 800 ºC (100 ºC step) was tested for H_2S.

Gas flows varied between 10.3 to 17.8 NL/min in Rig1, while it went from 1.5 to 11.3 NL/min in Rig2. Gas residence time (τ) in the reactor varied from 1.5 to 2.8 s (2.3 s in average) in the first setup and from 0.4 to 3.2 s (0.9 s in average) in the second one. Some pre-tests were made to assess the impact of the experiments duration and no clear effect was observed varying the time from 5 to 30 min. Thus, the experimental time was set to 5 min, typical sampling time in gasification tests (5 - 10 min). Table 2.2 summarizes the characteristics of both arrangements and the tests condition.

Table 2.2. *Summary of the experimental conditions used on own dedicated tests*

Rig	A/V	Flow	τ	Material	Species	T	Concentrations	Method	Absorbing solution
	(m^{-1})	**(NL/min)**	**(s)**			**(°C)**	**(ppmv)**		
1	reactor: 57	10.3 – 17.8	1.6 - 2.8 (2.4 in average)	*316SS*	HCl	800	34 - 172	*IC*	*Water, NaOH (5% vol)*
	pipe: 222		1.5 - 2.5 (2.1 in average)		NH_3		38 - 272		*H_2SO_4 (0.05 mol/L)*
2	reactor and pipe: 160 - 190		0.4 - 0.7 (0.5 in average)	*316SS, C-276, HR-160, quartz*	HCl	500, 800	98 - 241	*IC*	*Water, NaOH (5% vol)*
		1.5 – 11.3	0.4 - 0.56 (0.5 in average)	*316SS, C-276*	NH_3		272		*H_2SO_4 (0.05 mol/L)*
			0.45 - 3.2 (1.4 in average)	*316SS, 310SS, C-276, HR-160, Khantal-APM, quartz*	H_2S	300 - 800	500, 1000	*UV*	-

Hydrogen chloride and ammonia tests were performed using aqueous solution of these components to simulate their concentration in the syngas. Then, the solutions were fed into the system with a carrier gas (N_2). Liquids were injected by a pump and the carrier of the gas flow rate was controlled by mass flows. The HCl and NH_3 concentrations in the gas were controlled by the concentrations of the species in the solutions and their flow rate, as well as the N_2 flow. The H_2S concentration was controlled by feeding 1000 ppmv in N_2 directly into the reactor or diluting the gas with pure N_2 (for 500 ppmv). The total amount of contaminants added into the system was controlled by the H_2S gas flow and the experiment time as well.

The temperature of the lines downstream the reactor until the impingers were kept above 200 ºC to avoid condensation of water-soluble compounds like HCl and NH_3. In gasification tests, it is also required to avoid the formation of Cl salts, such as salts with Na and K, and NH_4Cl.

Impingers were made of glass, with a capacity of 30 ml. The glass heads contained frits for bubble formations, enhancing the liquid-gas contact. They were interconnected using transparent plastic pipes and were sealed with metal clips to prevent gas leaks.

2.5.3. Methods used for sampling and analysis

HCl and NH_3 in gas phase were collected in impingers with a proper capture solution for each specie, described in Section 2.6.1. They were located after the heated tube used in the experiments (Figure 2.1a and 2.1b). The three first impingers were filled with 25 ml of the absorbing solution, while the last one was left empty to collect the discharged liquid, totalizing four impingers in each test. The set of impingers were maintained at 5 ºC during all experiments using a recirculating cold bath. As mentioned above, the streams that connected the heated tubes and the impingers were maintained at temperatures above 200 ºC to avoid condensation.

In the end of the tests the absorbing solutions were transferred to amber bottles and stored in the dark at 5 ºC for a couple of days until analysis. Before analysis, the solutions obtained from NH_3 tests in the impingers had their pH neutralized, through KOH addition, which was proved to cause no interferences during NH_4^+ measurement by IC. All solutions collected were diluted to reach a total volume of 250 ml, before contaminants quantification by means of IC. This dilution was accounted when calculating the concentrations.

Before the test campaigns started, solutions doped with HCl and NH_3 - with previously known concentrations - were analysed by IC to determine the reliability of the method. Results proved that the IC is accurate and suitable for even extremely low concentrations (≥ 1 ppmv). Moreover, the collected solutions were remeasured within a week, and some samples were analysed again in a month. Results show that storage time did not affect NH_3 and HCl concentrations for our tests.

H_2S was analysed online in gas phase using a UV apparatus ABB Limas11. Results were acquired in a data card and concentration was monitored online through the PicoLog® software.

2.6. Results and discussion

Results were studied in terms of recovery ratio defined in Eq.2.1: high recovery means that the reactor material is inert (it is not likely to interact with the contaminant); then, if a waste fuel is fed into the reactor, the release of contaminants will be completely characterized by measuring the concentration of the species in the outlet gas. Low recovery means high interaction between the reactor and contaminant and then, it will be difficult to characterize the release of contaminants because corrosion

may take place. In this case, as a result, besides the degradation of reactor lining, the concentration of the contaminant in the gas will be underestimated.

Discussions are then finalized with recommendations for proper sampling and analysis of the HCl, NH_3 and H_2S in lab scale tests, based on literature and experimental highlights.

2.7.1. Measurement of HCl in the lab-scale tests

Figure 2.2 displays the HCl recovery as a function of the HCl concentration in ppmv using reactors with different alloys.

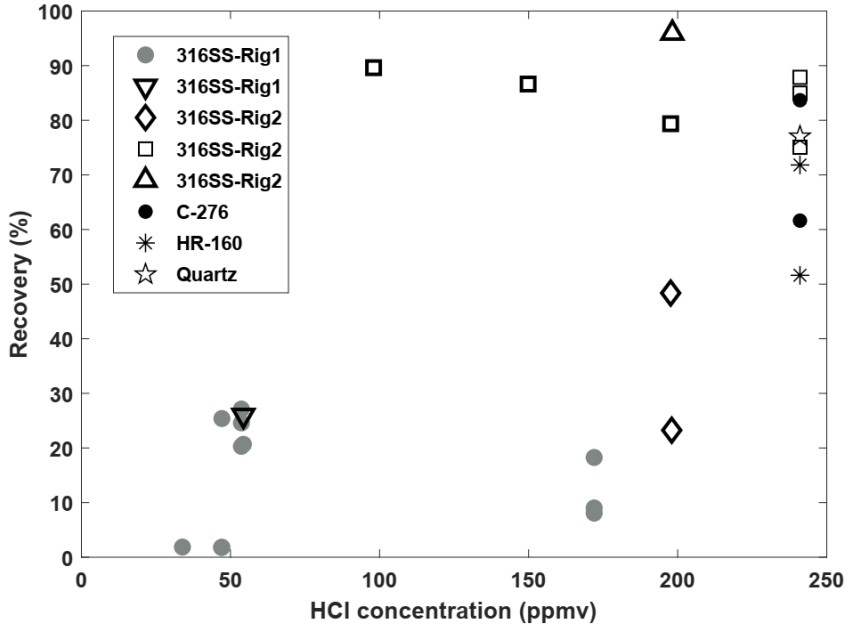

Figure 2.2. *Comparison of HCl recovery for different materials at 800 ºC, unless for ◇316SS-Rig2 tests, that were performed at 500 ºC. ▽316SS-Rig1 and △316SS-Rig2 tests were performed using NaOH as absorbing solution. Experimental time was set as 5 minutes.*

Very low recoveries were achieved during the tests conducted in the first setup (Rig1), reaching a maximum of 27.1%. The use of a NaOH as absorbing solution did not enhance the Cl recovery with respect to distilled water. In the second setup (Rig2), using 316SS, the overall recoveries were much higher, up to 96%. For the same temperature (800°C), it seems that the use of NaOH as absorbing solution performs as well as distilled water. However, it hinders Cl quantification by IC due to the addition of Na^+ ions in the solution. Therefore, the employment of distilled water is the best option, since it is inexpensive, harmless and the performance for HCl capture matches to the one using NaOH.

Comparing both rigs for the same material (316SS) focusing on the HCl recovery, it can be observed that recovery in Rig2 (Figure 2.1b) is higher than in Rig1 (Figure 2.1a). This is due to its higher contact surface area (1070 cm^2 in Rig 1 vs. 464 cm^2 in Rig2), even though it has a smaller A/V ratio in the heating zone (57 m^{-1} in Rig1 vs. 160-190 m^{-1} in Rig 2). Moreover, the reactor in Rig1 was previously used, while the one in Rig2 was new. Thus, the reactor lining in Rig1 was already affected by corrosion prior to the tests conducted in this work, losing its internal protective layer.

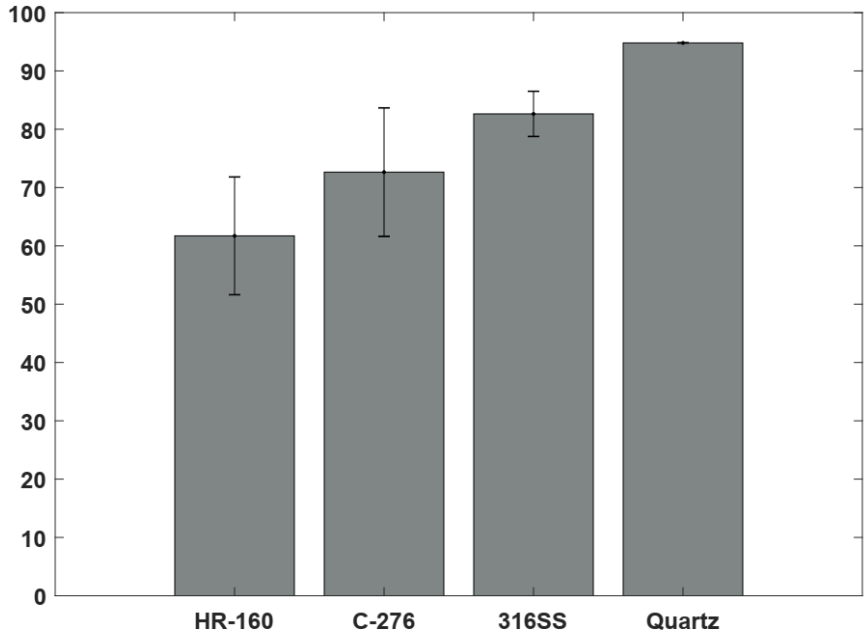

Figure 2.3. *Comparison of HCl recovery for different materials for Rig2 at the same conditions (T = 800 °C, 270 ppmv of HCl and 5 minutes of duration).*

Figure 2.3 compares HCl recoveries when using different materials at 800 °C, for a given HCl concentration in the inlet stream (271 ppmv). It was verified that HCl recovery drops when using C-276 and HR-160, although alloys C-276 and HR-160 are considered corrosion-resistant materials at high temperatures. HR-160 was reported to behave properly as a gasification material (45), but this was not corroborated in our tests.

In Rig2, 316SS performed better than the other alloys, but the highest Cl-recoveries were achieved using quartz (Figure 2.2). It can be inferred that 316SS may be initially suitable for gasification tests using fuels with high Cl. However, the reactor loses its protectiveness capacity against corrosion due

intensive use. Hence, the reactor internal layers should be checked periodically to guarantee the measurements validity.

2.7.2. Measurement of NH_3 in the lab-scale tests

Figure 2.4 contains the results of ammonia tests, showing low recovery of NH_3 when using the first setup (Rig1), which may be related to 316SS deterioration, as reported before. For the tests using the second arrangement (Rig2), the ammonia recovery was high when employing alloy C-276, around 80%. Nonetheless, even higher recoveries were initially expected using C-276, since Ni-based alloys and low Cr levels are likely to be better for nitridation (46).

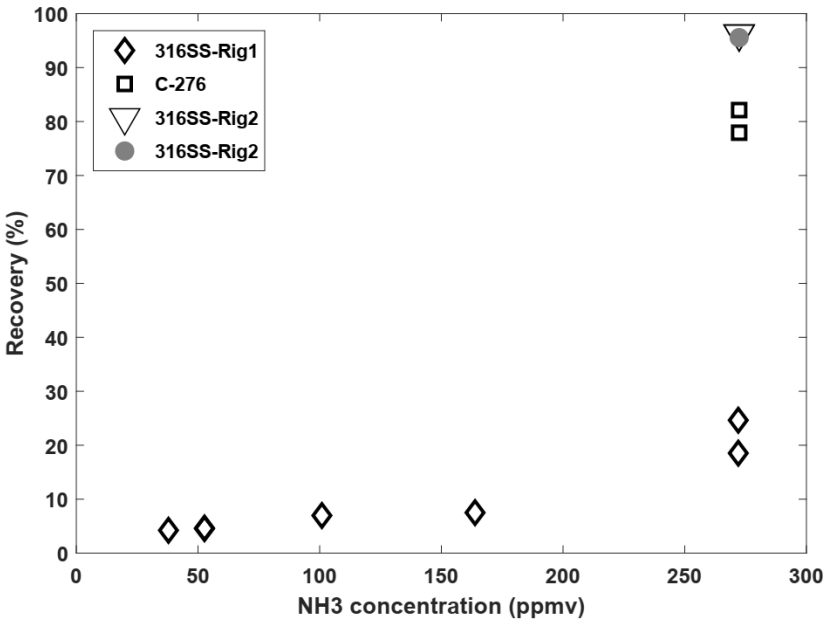

Figure 2.4. *Comparison of NH_3 recovery for different materials at 800 ºC, only ▽ 316SS-Rig2 tests were performed at 500 ºC. Experimental time was set as 5 minutes.*

Tests using the 316SS in Rig2 (new material) showed the highest NH_3 recoveries, higher than 95%. Additionally, steel lines do not seem to be a problem for transporting low amounts of NH_3 in low concentrations, at least it was validated between 25 and 200 ºC (43). Furthermore, steels were reported to be resistant to ammonia even at higher temperatures (600-700 ºC) (30). This agrees with our results, which shows that 316SS is an appropriate material for gases containing NH_3, when the reactor internal surface is preserved properly.

It can also be appreciated in Figure 2.4 that the decrease in temperature did not influence the recovery of ammonia, when comparing tests at 800 ºC and 500 ºC.

2.7.3. Measurement of H_2S in the lab-scale tests

Figure 2.5 displays the H_2S recovery from tests using different materials and temperatures.

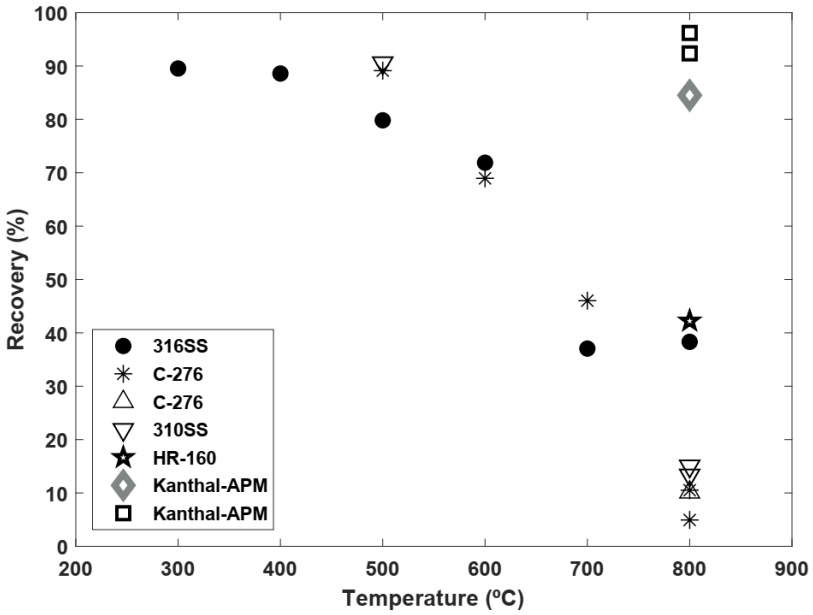

Figure 2.5. *Comparison of H_2S recovery for different materials using 1000 ppmv of H_2S (unless for ⧋, which was performed using 500 ppmv of H_2S) versus temperature. For □ Kanthal-APM tests the thermocouple protective cover –made of quartz was used. Experimental time was set as 5 minutes.*

For the 316SS, C-276 and 310SS, the decrease in the recovery with temperature is evident, explaining that these materials execute well in sulphur corrosive atmospheres at temperatures up to 500 °C, but they do not endure higher temperatures. Comparing these materials performance at 500 °C, 310SS was the best (R=90.6%), slightly better than C-276 (R=89.1%), while 316SS showed the worst behaviour (R=79.8%). Nevertheless, at 800 °C, alloy 316SS (R=38.3%) worked better than alloys 310SS (R=15.0%) and C-276 (R=10.5%).

Figure 2.6 compares the H_2S recovery at 800 °C for all the materials studied for 1000 ppmv of H_2S in the inlet stream.

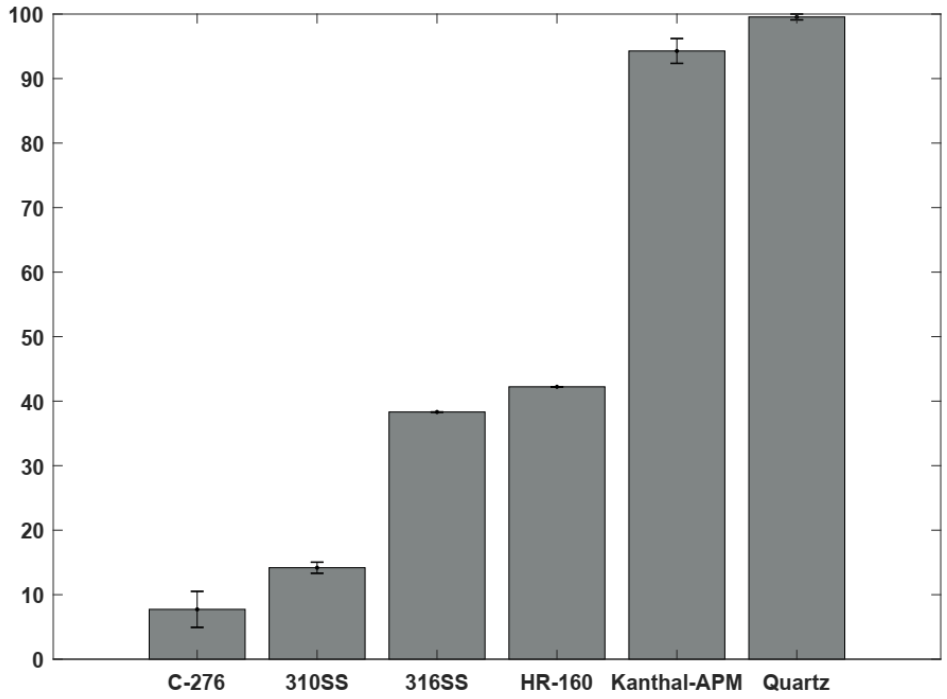

Figure 2.6. *Comparison of H_2S recovery for different materials at same conditions (T = 800 °C, 1000 ppmv of H_2S and 5 minutes of duration).*

For some materials, results were presented as the average from various tests conducted at same conditions (error bars added). Moreover, tests with quartz were also conducted, and results have shown complete recovery (R>99%).

Besides quartz, Kanthal-APM was the best performing material (and the best alloy among those investigated here). Two tests were conducted using a quartz cover on the thermocouple (which is made of alloy 310SS), to see its interference on the results. These tests revealed higher H_2S recovery compared to the test without thermocouple's cover, which remarks the importance of avoiding even small surfaces of materials that are prone to H_2S corrosion.

On the other hand, despite showing great endurance in the presence of H_2S, Kanthal-APM is not suitable in chlorine corrosive atmospheres (43). Nevertheless, it appears to be an appropriate choice for fuels containing high S and low Cl amounts.

2.7.4. General comments

The material selection for a lab-scale reactor for the analysis of waste-derived syngas can be quite complex, because certain alloys behave well in presence of S but not in Cl. Quartz is inert but is also fragile.

It can be concluded from Figures 3 and 6 that the most suitable choices for the analysis of gas containing both Cl and S at 800 °C – for instance, the case of MSW/RDF/SRF syngas – would be 316SS and HR-160. Alloy 316SS behaved better in presence of HCl, and, thus, it would be considered the best choice overall, between these alloys.

Nonetheless, even in this scenario, the measurement of H_2S would be severely compromised if those materials were employed at high temperature. This is because from the results of our own dedicated tests, a reduction of H_2S concentration up to 60% in the outlet stream was observed when using those materials. Even though this is a specific problem of laboratory or pilot scale devices, it is an important issue when scaling up the results (refractory lining is applied in full-scale reactors).

For a syngas containing low S and high Cl, 316SS is recommended, whereas Kanthal-APM is suggested when the syngas has high concentrations of these species. When carefully measurements of these species are required, the use of quartz is strongly encouraged.

2.8. Conclusions

Earlier studies on waste gasification at laboratory scale have shown inconsistencies regarding the measurement of the main pollutants formed from Cl, S and N, i.e., HCl, H_2S and NH_3. In this paper, the fate of these contaminants was analysed: (i) by formulating elemental balances of Cl, S and N from selected literature measurements, and (ii) by conducting dedicated tests employing different set-ups and reactor materials, doping a carrier gas (N_2) with HCl, NH_3 and H_2S with typical concentrations of waste-derived syngas. The analyses made in this paper explain some of the inconsistencies detected in literature. Thus, results enable recommendations for proper measuring of these contaminants in research facilities that focus on the partitioning of elements that form contaminants. The main findings are summarized as follows:

Concentrations of HCl, NH_3 and H_2S reported in literature during gasification of wastes vary from virtually zero, to well in excess to the maximum allowable (the Cl, S and N content in the parent fuel). The reasons for these inconsistencies may be related to interaction between the reactor material and some species; uncontrolled condensation in the lines between the reactor and sampling ports; or imperfections in the sampling and measurement techniques employed.

The method for sampling contaminants by using impingers and the posterior analysis of the solution by ion chromatography is reliable. It enables the detection of even small quantities of contaminants (≥1 ppmv), given that the temperature upstream the reactor is maintained above 200 ºC to avoid water condensation and, thus, the loss of NH_3 and HCl. This is because these species are soluble in water, and condensation of chlorine in the form of alkali salts (Na, K) or as NH_4Cl in the presence of NH_3 may occur. Samples storage time did not affect the species concentration.

Corrosion by H_2S and HCl was found in tests at high temperature (above 500˚C), impacting on the measurement of these species. Thus, the selection of adequate materials is required (i.e., one that does not interact with these species). Even alloys that are considered resistant to corrosion, such as Hastelloy® C-276, Haynes® HR-160 and Kanthal-APM, showed severe limitations for their use at high temperature and corrosive atmospheres.

The most suitable steel-based materials for waste-derived syngas containing both Cl and S, are 316 Stainless Steel (SS316) and Haynes® HR-160, even though it could result in under-prediction of both H_2S (a loss of 60% for both materials) and HCl (a loss of 20 and 40% for SS316 and HR-160, respectively). The use of Kanthal-APM was shown to be the most appropriate for syngas containing high H_2S and very low HCl, yielding S recovery above 95%. The use of C-276 and SS316 resulted in high recovery of NH_3 (above 96%, reaching recovery ratios using SS316). Hence, quartz is strongly recommended for pyrolysis and gasification tests aiming at contaminants measurement in syngas.

Chapter 3

Measurements and distribution of inorganics and trace elements during devolatilization of batch of fuel in a laboratory fluidized bed

Summary

The aim of this chapter is studying the fate of main inorganic precursors contaminants (Cl, N, S, and trace elements) during devolatilization tests in fluidized bed, using different solid wastes as fuels. The study was done by conducting batch-wise experiments using batch of fuels and measuring the transient response of the gas yield, using the following fuels: Dried Sewage Sludge (DSS), Refuse-Derived Fuel (RDF), and commercial wood pellets (for comparison) and N_2 as the carrier gas. Analyses were made to understand the results and to compare the measurements with previous literature works.

Two experimental campaigns using fluidized bed setups were conducted, the first one in 2017 and the second one in 2018 (1^{st}: 2017 / 2^{nd}: 2018). Additionally, muffle furnace tests were conducted. Further explanation about the tests are given below:

- In the **first experimental campaign of fluidized bed devolatilization tests (2017)**, devolatilization tests were conducted on the lab-scale fluidized bed (FB) reactor at 800 ºC using DSS (840µm – 2mm), RDF and commercial wood pellets as fuels.

- In the **second experimental campaign of fluidized bed devolatilization tests (2018)**, just DSS and wood pellets were employed as fuels. In this experimental campaign a wider temperature range was studied (600 – 900 °C), as well as some tests in air atmosphere. The differences of the second experimental campaign from the first one are: *new reactor*, although same design and material - Stainless Steel 316 (SS316); online measurement of the contaminants in gas phase by a *mass spectrometer* (previously these species were collected

using impingers - HCl - and an online UV analyser - H_2S); and smaller DSS particles sizes (500 – 840 μm).

Additional **muffle furnace tests using DSS particles** (the same used in the second experimental campaign, with particle size of 500 – 840 μm) were conducted. The muffle furnace was included because in this setup the solid residue mass could be easily measured, which enables the obtaining of more accurate volatilization results for trace elements. In this type of test, the focus was only on the solid residue, therefore, the gaseous product released during the thermal conversion was not collected and analysed.

The focus of the tests presented in Chapter 3 is on inorganics – N, S and Cl - and other trace elements – such as heavy metals - and the effect of temperature and atmosphere during the devolatilization step. Species containing N, S and Cl are usually measured in the gaseous phase, while trace elements are measured only in the solid residue. Additionally, main product gases from devolatilization, such as CO, CO_2, CH_4 and H_2, were measured in both fluidized bed experimental campaigns.

More details regarding the two fluidized bed experimental campaigns (1^{st}: 2017 / 2^{nd}: 2018) and the muffle furnace tests are given in the next sections.

3.1. Introduction

During gasification, the devolatilization is one of the first steps – after drying – that a fuel particle goes through (47). The products of the of devolatilization of biomass are usually grouped into light gases, which include CO, CO_2, H_2, CH_4 and other light hydrocarbons, other contaminant gases, HCl, NH_3, HCN, H_2S, condensable compounds, including organic compounds , water and char. Char is a carbonaceous solid that remains after thermal decomposition of the fuel, which is about 10-30 wt.% of the total mass fed (48), also depending on the initial fuel composition in ashes.

The distribution of products obtained during devolatilization is a consequence of both the primary generation due to the thermal decomposition of the fuel and secondary reactions involving the

produced volatiles. Secondary reactions may occur homogeneously or heterogeneously, both inside the fuel particle and in the reaction furnace, for example, with the water vapor that is released from the fuel drying. Devolatilization experiments are usually conducted in inert atmosphere, for example, using N_2 as carrier gas for the evolving volatiles (48).

3.1.1. Literature review

Ronda et al. (15) have presented a literature review of the partitioning of heavy metals during the thermal conversion of waste in 2019. The review included different types of waste fuels, such as doped sewage sludge, dried sewage sludge (DSS), food waste, PVC and municipal solid waste (MSW). For this work, a review of the advancements on the thermal conversion of solid waste was performed, analysing the literature from 2019 up to the present (January 2023).

Some works detailed studied the devolatilization process of waste, during pyrolysis, combustion, as well as the conversion by thermogravimetric analysis (TGA), but the content in inorganic or trace elements, including heavy metals were not assessed (49–54).

Other works found in recent literature studied the evolution of trace elements and polluting gases toward the clean co-combustion of coal and sewage sludge (55) and the co-combustion of torrefied municipal solid waste and coal in bubbling fluidized bed (56). Most works that study the trace elements behaviour during thermal conversion, focus on coal or solid waste as fuel, but during the combustion (57–60).

Additional works that did studied the gasification of solid waste and inorganics were included in the literature review presented in Chapter 4 (Table 4.1) (32,61–64).

Nevertheless, to the best of our knowledge, no recent work studying the devolatilization of waste derived fuels in fluidized bed focusing on inorganics and the partitioning of trace elements was published. Thus, the relevance of the results presented in this chapter are evidenced and can shed some light into the understanding of the conversion of solid waste - overall Dried Sewage Sludge (DSS) during its devolatilization in fluidized bed.

3.2. Experimental

Two types of experiments were conducted to analyse the devolatilization process: the first one is *devolatilization tests in fluidized bed reactors, and the second one* using a *muffle furnace* to analyse in detail the behaviour of the fuel. The tests conducted in the fluidized bed set up were conducted in two separate experimental campaigns (1st: 2017 / 2nd: 2018). Although the reactors used in both campaigns were made using the same design and material - Stainless Steel 316 (SS316) - in the second experimental campaign, the reactor was recently bought and new.

In the *first experimental campaign of fluidized bed devolatilization tests (2017)*, devolatilization tests were conducted on the lab-scale fluidized bed (FB) reactor at 800 ºC using DSS (840µm – 2mm), RDF and commercial wood pellets as fuels.

In the *second experimental campaign of fluidized bed devolatilization tests (2018)*, just DSS and wood pellets were employed as fuels. In this experimental campaign a wider temperature range was studied (600 – 900 °C), as well as some tests in air atmosphere. The differences of the second experimental campaign from the first one are: new reactor (although same design and material - Stainless Steel 316, SS316); online measurement of the contaminants in gas phase by a mass spectrometer (previously these species were collected using impingers - HCl - and an online UV analyser - H_2S); and smaller DSS particles size (500 – 840 µm).

Additionally, *muffle furnace tests* using DSS particles (the same used in the second experimental campaign, with particle size of 500 – 840 µm) were conducted. The muffle furnace was selected because in this setup the solid residue mass could be easily measured, which enables the obtaining of more accurate volatilization results for trace elements. In this type of test, the focus was only on the solid residue, the gaseous product released during the thermal conversion was not collected and measured.

3.2.1. Materials

Sand was used as bed material (250μm ≤ d ≤ 500μm) in both FB tests campaigns. When contaminants sampling was done with impingers, water or NaOH solution (%) was used for HCl capture, and H_2SO_4 (%) with a buffer solution was used for HCN.

Fuels proximate and elemental compositions are shown in Table 3.1, while Table 3.2 displays concentrations of trace elements.

The DSS particles used in the muffle furnace experiment and in the last experimental campaign using the fluidized bed reactor, the DSS particles were smaller (500 - 840μm) than the DSS particles used in the first experimental campaign (840μm – 2mm). Nevertheless, they were considered to have the same composition in ash, fixed carbon, volatiles, moisture, and main elements (C, H, N, Cl, S, O), because they were from the same source. Different particles sizes were used in experimental campaigns due to fuel availability in the moment that experiments were being conducted.

Table 3.1. *Proximate and elemental composition of fuels*

Fuel	DSS (0.5-2mm)	RDF pellets	Wood pellets	Analysis Method
% weight, as received				
Moisture	6.53	8.05	4.96	CEN/TS 14744-1
% weight, dry basis				
Ash	27.76	11.48	0.63	CEN/TS 14775
Fixed Carbon	10.06	11.24	15.59	*
Volatiles	62.18	77.28	83.78	CEN/TS 15148
% weight, dry and ash free basis				
C	53.60	60.40	51.05	CEN/TS 15104
H	8.32	7.85	6.55	CEN/TS 15104
N	8.46	1.18	0.12	CEN/TS 15104
Cl	0.05	0.13	0.01	UNE ISO 16994
S	1.25	0.15	0.02	**
O	28.32	30.29	42.25	*

** Calculated by difference, for RDF and DSS at 750°C, and for wood at 550°C*

*** Measured by ICP*

Table 3.2. *Trace elements composition of fuels*

	DSS (840µm – 2mm) *1st exp. campaign*	**DSS (500 - 840µm)** *2nd exp. campaign muffle furnace tests*	**RDF**	**Wood**
		g/kg of fuel		
Al	14.34	5.13	3.28	2.00
As	0.01	0.01	3.47	0.33
Ba	-	0.25	-	-
Ca	46.54	23.89	17.24	1.90
Cd	0.00	0.00	0.01	0.01
Co	0.01	0.01	0.00	0.03
Cr	0.14	0.08	0.04	0.03
Cu	0.73	0.40	0.17	0.19
Fe	21.52	11.50	1.58	0.23
Hg	-	0.01	-	-
In	-	0.00	-	-
K	4.96	7.72	2.90	0.89
Mg	7.55	3.74	1.33	0.67
Mn	0.20	0.19	0.01	0.07
Na	2.25	6.95	2.33	2.78
Ni	0.17	0.13	0.25	0.25
P	30.06	23.94	-	-
Pb	0.09	0.07	0.00	-
S	8.44	9.58	1.24	0.11
Sb	0.01	0.02	0.03	0.01
Se	-	0.00	-	-
Si	16.58	-	9.49	0.89
Sn	0.06	1.06	0.08	0.00
Sr	-	0.35	-	-
Te	-	0.00	-	-
Ti	1.29	1.16	1.67	0.01
V	0.02	0.02	0.00	0.00
Zn	1.17	1.18	0.24	0.16
Total	156.14	97.38	41.89	10.23

Comparing the two trace elements analyses for DSS, results are in the same order of magnitude. Most elements have their content very similar in both (As, Cd, Co, Mn, Ni, P, Pb, S, Sb, Ti, V and Zn), while other elements concentration differ considerably (Al, Ca, Cr, Cu, Fe, K, Mg, Na, Sn). The differences are explained by both the heterogeneity of the fuel, and particles size interval.

Total trace elements content is about 33-53% of ash composition for DSS, 34% for RDF and about 154% for wood. As trace elements content exceeded 100%, inaccuracies may have happened during elements measurement or the ash content determination.

3.2.2. Experimental set-ups

3.2.2.1. Fluidized Bed tests

The general setup for the fluidized bed tests is shown in Figure 3.1. FB reactor is made of SS316 and consists of a 51mm internal diameter (ID) bottom bed and 81mm ID freeboard. The reactor is surrounded by an electrical oven, which allows temperature control. The only modification made from Figure 3.1 is in the fuel feeding system which, in this case, was made manually in the reactor top.

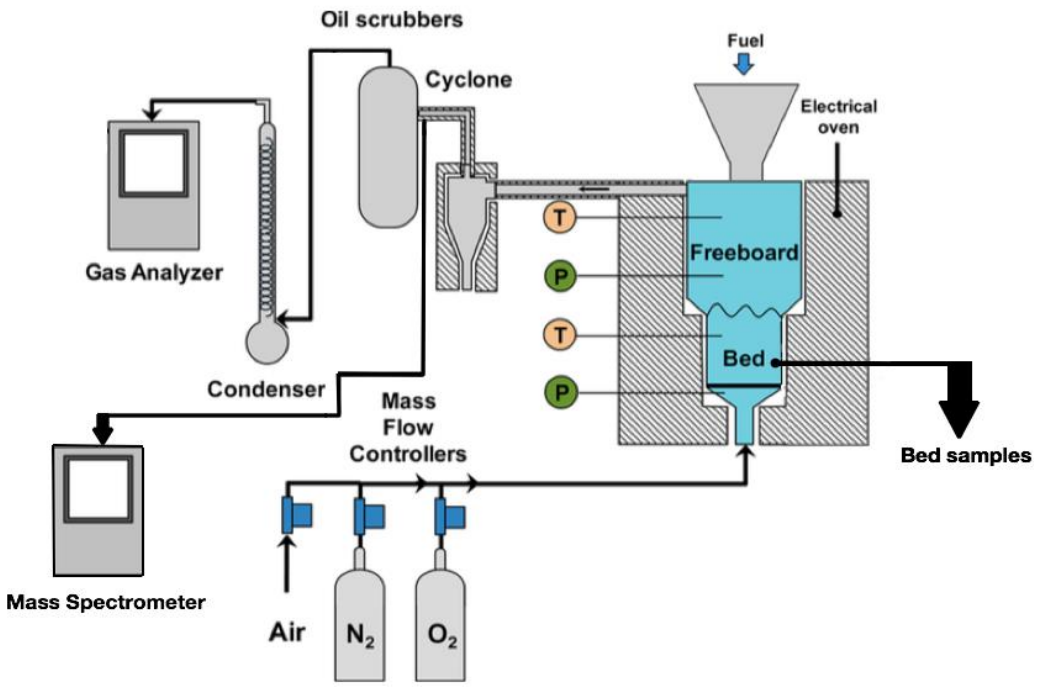

Figure 3.1. *Experimental setup for the fluidized bed tests.*

The gas feeding system can supply air, N_2 or gas mixes, using mass flows. At the exit of the reactor a cyclone is placed for entraining particles collection. After that, there is the impingers filled with water to collect Cl, and then there is a condenser operating at 0 ºC for tar and other components elimination before gas analysis.

In the first fluidized bed experimental campaign, impingers were used to collect NH_3 and HCl for further analysis. Nondispersive infrared absorption was used to measure CO, CO_2, and CH_4; while H_2 and O_2 were measured by thermal conductivity and a magneto-mechanical oxygen analyser, respectively. Additionally, a UV analyser (ABB AO2020) for the measurement of H_2S.

First experimental campaign

The first experimental campaign was conducted in 2017. In this round of experiments, impingers were placed after the cyclone, filled with water to collect some species (NH_3 or HCl). Then, there is a condenser operating at 0 ºC for tar and other components elimination before gas analysis. The clean gas stream was then divided into three streams, one that went to the main gas analyser (nondispersive infrared absorption was used to measure CO, CO_2, and CH_4; while H_2 and O_2 were measured by thermal conductivity and a magneto-mechanical oxygen analyser, respectively). The second stream went to the UV analyser (ABB AO2020) for the measurement of H_2S. The last stream was discarded.

Second experimental campaign

In the second test campaign (2018), a new reactor was used, made with the same material (316SS) and the same design. Moreover, instead of the UV analyser for the measurement the stream goes to the mass spectrometer. Bed samples were collected in the reactor bottom using a sample probe or in the end of tests by opening the reactor after cooling down with an inert gas (N_2).

3.2.2.2. Muffle furnace tests

The muffle furnace tests were performed in a set up that allowed rapid heating (Carbolite) and allows temperatures up to 1200°C. The heating rate capacity of the muffle furnace is 100°C per minute. The samples were place in porcelain crucibles of 30 ml of capacity, measuring 30 mm high per 50 mm of diameter.

3.2.3. Operating conditions

3.2.3.1. Fluidized bed tests

First experimental campaign

FB experiments were performed at 800 ºC, and the experimental design of FB tests is displayed in Table 3.3:

Table 3.3. *Experimental design of the first batch of experiments*

Test	Fuel	Test type	Batch mass	Bed removal*	Temperature	Gas	Flow	Fluidizing velocity
			(g)		(ºC)		(NL/min)	(m/s)
1	DSS	P	9	Full	800	N_2	11.75	0.33
2	DSS	P+C	9	Sample				
3	RDF pellets	P	3	Full				
4	RDF pellets	P+C	9	Sample				
5	Wood pellets	P	9	Full				
6	Wood pellets	P+C	9	Sample				

P= pyrolysis tests, P+C= 3 pyrolysis tests, bed sample collection followed by combustion of the final material

Bed removal = Full: the reactor was cooled down in inert atmosphere and then the solid residue was removed / Sample: after the devolatilization test, a sampling valve place on the reactor bed was open to take a small sample to the solid residue. The sample was placed in an additional vessel without contacting the outside atmosphere until it was cooled down.

Second experimental campaign

In the second experimental campaign, the tests were conducted using a temperature interval of 600 – 900 °C, and gas velocity was maintained as 0.35m/s in all tests. The gas flows were 15.6, 14.0, 12.7 and 11.6 NL/min for the following temperatures 600, 700, 800 and 900°C, respectively. The experimental design is displayed in the following Table 3.4:

Table 3.4. *Experimental design of the first batch of experiments*

Test number	Fuel	Batch mass	Bed removal*	Temperature	Flow	Fluidizing velocity	Gas
		(g)		(ºC)	(NL/min)	(m/s)	
1	DSS		Sample	600			
2	DSS		Sample	600	15.6		
3	DSS		Sample	600			
4	DSS		Sample	700			
5	DSS		Sample	700			
6	DSS		Sample	700	14.0		
7	DSS		Sample	700			
8	DSS		Sample	700			
9	DSS		Full	700			
10	DSS		Sample	800			
11	DSS		Sample	800			
12	DSS		Sample	800	12.7	0.35	N_2
13	DSS		Sample	800			
14	DSS		Full	800			
15	DSS		Sample	900			
16	DSS		Sample	900			
17	DSS		Sample	900	11.6		
18	DSS		Sample	900			
19	DSS		Sample	900			
20	Wood pellets		Sample	700	14.0		
21	Wood pellets		Sample	800	12.7		
22	Wood pellets		Sample	900	11.6		

Bed removal = Full: the reactor was cooled down in inert atmosphere and then the solid residue was removed / Sample: after the devolatilization test, a sampling valve place on the reactor bed was open to take a small sample to the solid residue. The sample was placed in an additional vessel without contacting the outside atmosphere until it was cooled down.

3.2.3.2. Muffle furnace tests

These tests were performed in triplicate using three different temperatures: 500, 700 and 900 °C.

3.2.4. Sampling and analytical methods

3.2.4.2. First batch of experiments in a fluidized bed reactor

The exit gas composition was measured online with a gas analyser using a no dispersed infrared method for CO, CO_2, and CH_4 and thermal conductivity and paramagnetic methods for H_2; and off-line using a micro-GC (the species mentioned as well as light gases and N_2). H_2S was analysed online using Limas11 UV analyser.

Chlorine content was collected using impingers and then was quantified using IC. The set of impingers used to sample water in some tests were located after the reactor. The three first impingers were filled with 25ml of the absorbing solution, while the last one was left empty to collect discharged liquid, totalizing four impingers in each test. The set of impingers were maintained at 5 ºC during all experiment using a recirculating cold bath. The streams that connected the heated tubes and the impingers were maintained at temperatures above 200 ºC to avoid condensation outside of the impingers. In the end of the tests, the absorbing solutions were transferred to amber bottles and stored in dark at 5 ºC until analysis. All solutions collected from impingers were dissolved to reach a total volume of 200 ml or 250 ml.

Bed sampling was performed as follows: 2NL/min of N_2 gas was added in the sampling probe (point indicated in Figure 1) during 10s with the sampling valve closed. Then N_2 feeding was suppressed, the valve was opened and closed instantly. The valve was opened again during 10s for the collection of approximatively 100-120g of bed material.

The collected samples were maintained inside a sampling probe, in a specific point until samples cooled, to prevent their burning when in contact to air. In some tests, the whole bed material was collected, after having cooled the plant with nitrogen until 150°C, to preserve the solid residue. The solid residue from the fuels were separated manually from the bed material, and then stored until analysis.

The composition of the solid residue was determined using the ICP technique. Samples were first disaggregated using an acidic solution before analysis. C, H and N solid residues compositions were analysed by a combustion-based technique, the same as muffle furnace solid residue samples.

3.2.4.3. Second batch of experiments in a fluidized bed reactor

In the second experimental campaign, the exit gas composition was also measured online using a no disperse infrared method (CO, CO_2 and CH_4) and a mass spectrometer (CO_2, CH_4, H_2, H_2O, H_2S, NH_3 and HCl). In some tests, Cl was also collected by impingers and then measured by IC. H_2O was also collected in some tests using impingers filled with isopropanol and then measured by Karl Fisher.

Bed material samples were also taken under the same procedure in 2017. The composition of solid residue samples was determined the same way as in 2017, however ICP analyses were conducted in Granada due to schedule issues at Seville. Their ICP equipment allows the more precise measurements of a wider selection of elements, thus some of them was added (Ba, Hg, In, Se, Sr and Te).

3.2.4.2. Muffle furnace experiments

Trace elements composition were analysed by ICP, while C, H and N by in accordance with the European standard CEN/TS 15104 using a LECO apparatus, which consists of the sample combustion (at 1050ºC) and elementals to measure in the flue gas.

3.2.5. Description of experiments

3.2.5.1. First batch of experiments in a fluidized bed reactor

FB tests were operated in two different ways, explained as follows. The first one consisted in the sequential pyrolysis of several batches of fuel particles (1g of fuel added/batch) and then, at the end, the removal of the whole reactor bed material after cooling the reactor down using an inert gas (N_2 gas).

The second type of tests consisted in three (3) batches of pyrolysis (3g of fuel added/batch), bed sampling, followed by the combustion of the remaining fuel to start a new set of experiments. After combustion, it was considered that all solid material was consumed, and another pyrolysis-combustion cycle was performed. This type of tests maximized the number of experiments it was possible to execute in a day, since in the other type of experiments, the reactor needed to be cooled down and opened to remove the whole final bed material, which takes about six hours to occur.

3.2.5.2. Second batch of experiments in a fluidized bed reactor

Each test consisted in ten (10) additions of approximately 500 mg of fuel, waiting 90 seconds between one addition and the following one. After the test, 10 minutes were waited until a sample of the bed material was taken in the point indicated in the experimental setup (Figure 3.1) and then, before

starting the new test, combustion was performed to burn the remaining solid material in the bed. Bed sampling was conducted the same way as in the first experimental campaign.

3.2.5.3. Muffle furnace experiments

In these experiments, samples of approximatively 1g of DSS were placed in the ceramic crucible, covered, and then placed in the furnace once the desired experimental temperature was reached. The sample was maintained in the furnace for 15 min and the removed to cool at ambient temperature. Finally, the sample was weighted and stored until analysis. These tests can be considered as exempt of oxygen since the air amount inside the ceramic crucible is so low and can be considered as zero. .

3.2.6. Definitions for calculation methods

The definition of recovery and volatility used in this chapter are described in the next topics, so they can be

3.2.6.1. Recovery

Recovery is defined as the percentage of element *i* in the phase of interest, and it is calculated dividing its amount in this phase by the amount of the same element in the fuel:

$$R_i = \frac{m_i^p}{m_i^f} * 100 \qquad \textbf{(Eq. 3.1)}$$

Where $\mathbf{m_i^p}$ is the mass of the element ***i*** in the analysed phase (gas/solid) after the thermochemical conversion and $\mathbf{m_i^f}$ is the mass of the element ***i*** in the fuel.

3.2.6.2. Volatility

Volatility is calculated using the following equation:

$$V_i = \frac{(m_i^f - m_i^p)}{m_i^f}.100 \qquad \textbf{(Eq. 3.2)}$$

Where $\mathbf{m_i^f}$ is the component ***i*** mass in the fuel, while $\mathbf{m_i^p}$ is the mass of the element ***i*** in the phase of interest (in this case, solid phase) after the thermochemical conversion, what is called solid residue.

3.3. Results and discussion

In the next topics, the results obtained in both experimental campaigns using the fluidizing bed set ups and the tests using the muffle furnace will be described.

First, at *Section 3.3.1 "Product gas containing S, Cl and N"*, the content in contaminants derived from S, Cl and N in the gaseous phase in both FB experimental campaigns will be presented.

Next, at *Section 3.3.2 "Solid residue: analysis their content in major and trace elements"* the content of C, H and N as well as trace elements is presented and discussed for the muffle furnace and the two experimental campaigns for the FB devolatilization tests. In this section, the trend of elements with temperature, and the elemental mass balances for the measured trace elements were also presented and discussed.

3.3.1. Product gas containing S, Cl and N

In this section, the product gases containing S, Cl and N were analysed for both experimental campaigns of devolatilization tests conducted in the FB facilities.

The results of the *first experimental campaign* conducted in 2017 are related to the content of Chapter 2, since they were being studied simultaneously, i.e., when analysing the results presented in Chapter 2 and learning about the measurement of inorganics in the syngas, the devolatilization tests were being made, therefore, potential measurement inconsistencies were not yet detected.

The results of the *second experimental campaign* conducted in 2018 are also related to the content of Chapter 2. Even though it does not use the same sampling methods, because a mass spectrometer is used to measure the inorganics product gas online (not using impingers as in the first campaign), the issues with corrosive compounds and the reactor material at high temperatures are corroborated and in line with the findings of the second chapter of this thesis.

Either way, these results are not part of Chapter 2, because its aim is to review the literature and to analyse the measurement methodology, without including the additional step of the fuel thermochemical conversion and all the inherent complexity it brings to the measurement dynamics, by including, for example, tars and other major gases.

Nevertheless, most of the findings presented below reflect the results

3.3.1.1. First batch of devolatilization experiments

H_2S

As H_2S was selected to be measured in the first experimental campaign, since it is the main product gas of devolatilization step. The H_2S concentration results are not reliable and so were not included here. They were extremely high and far exceeded the S content in the fuel. Later, it was detected that the UV analyser cannot properly measure H_2S with other species, besides N_2. In this case, S release to the gas phase was calculated from the S content in the solid residue.

HCl

Chlorine results in gas phase are available in Table 3.5 below:

Table 3.5. *Chlorine content in the fuel and syngas.*

Experiment	Fuel	Cl in the fuel (mg)	Cl in the product gas (mg)
1	DSS	3.51	4.87
2	DSS	2.39	14.91
3	RDF	3.27	9.01
4	RDF	9.92	11.66
5	Wood	0.97	4.47
6	Wood	0.96	4.69

From the analysis of Table 3.5, it is shown that the Cl content measured in the gas phase exceeded the Cl content in the fuel in all tests. This analysis leads to the conclusion - extensively discussed previously - that either the Cl measure in the fuel is not accurate, or the sampling method (bubblers) or analysis method are not suitable. From the previous work included in this thesis – Chapter 2 - HCl sampling with bubblers was proved to be a reliable method, as well as IC. Furthermore, the effect of

316 stainless steel (316SS) on the Cl capture was proved to be very low (~15% loss of Cl), and to decrease its recovery when the material is new (65).

Nevertheless, in the work of de Almeida et al (65), HCl was fed into the reactor just with N_2, and in these experiments HCl was sampled in a gas containing other compounds, by instance CO, CO_2, CH_4, H_2 and tars in an experiment that HCl is released from a solid fuel particle.

This difference may lead to the overall conclusion that Cl is not properly measured in the fuels, or other ions may interfere in Cl measurement by IC and, thus, Cl content in the gas is overestimated. Following our knowledge and experience in analytical chemistry, for instance, there is no evidence that other ions affect Cl measurement by IC, but this possibility must be further investigated.

The measurement of fuel-Cl is not simple, since Cl is very volatile, and there is evidence of inaccurate results of Cl in the fuel, even when following European standards (24). Furthermore, the issue reported in Table 3.5 may be a mix of the hypotheses mentioned.

An additional option to further investigate this issue would be, besides measuring again the fuel-Cl content by the European standard method based on fuel combustion, would be conducting devolatilization tests using an inert reactor (i.e., a quartz reactor).

3.3.1.2. Second batch of devolatilization experiments

H_2S

During pyrolysis the main products in the gas are H_2S and COS. The gas analysis was focused just on hydrogen sulphide because it is the main product, like the first experimental campaign. H_2S yields were extremely low compared with the S content in the fuel. In the figure below are present H_2S recovery ratios with temperature.

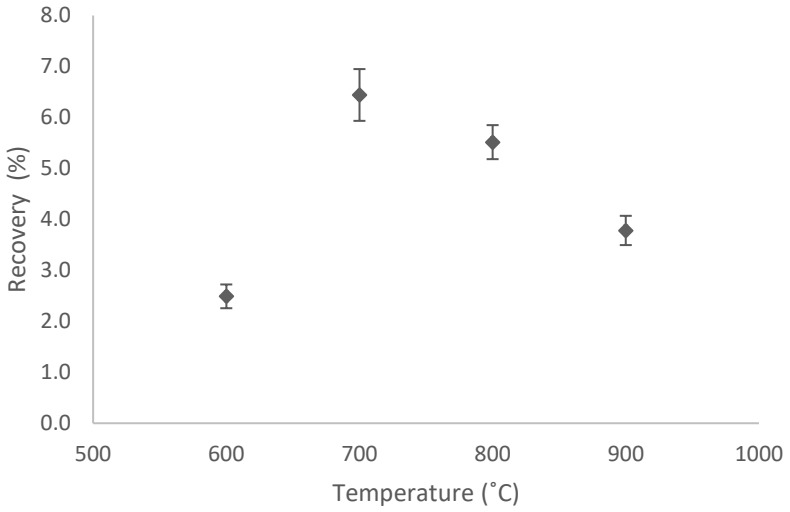

Figure 3.2. *H_2S recovery at different temperatures for DSS.*

The recoveries of S in the gas phase were very low compared to literature because for DSS, almost the 95% of S-fuel should be found in the gas phase (4). This low recovery could be, to a minor extent, associated to the lack of the analysis of COS in the gas phase (usually about 5-10%). However, it is mainly linked to potential corrosion issues at a reducing environment and high temperatures (700 - 900°C). This is because, according to the literature, stainless steel is not free from corrosion at such high temperatures. It was reported a reduction of H_2S concentration up to 60% in the outlet gas when using a reactor of 316SS (4).

In fact, it can be seen the pattern of the H_2S increasing until 700°C and then it starts to decrease in the recovery with temperature and this is in accordance with kinetic studies because the reaction rate of H_2S with the reactor material increase with temperature, while it is not high enough below the 700°C (4).

Several studies on different reactor materials were made and it was found that the quartz reactor is the one that allow almost the 100% of H_2S recovery because quartz is an inert material. Kanthal-APM is also suitable when in the fuel contains only S, and not Cl. The use of SS316 for similar tests – fuels containing a high content of sulphur, reducing environment and high temperatures - the results of H_2S can be severely compromised.

The release of S to the gas phase can also be estimated measuring S in both fuel and solid residues. This is discussed in another topic, because this one is only focused on gas phase measurements.

HCl

The recovery results of HCl for the devolatilization tests made are showed in the following Figure 3.3:

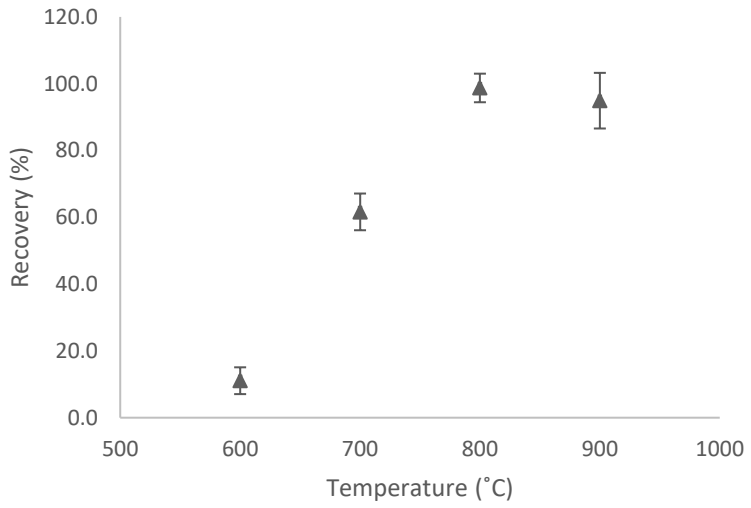

Figure 3.3. *HCl recovery at different temperatures for DSS.*

These results were obtained using the mass-spectrometry technique to measure HCl online at the outlet stream.

At 600°C the recovery is very low, because inorganic chlorine that needs higher temperature to be released into the gas phase. At 800 and 900°C, it can be observed that recovery ratios reach approximately 100%, which means that all the HCl in the fuel is released into the gas phase, and this allows to close the mass balance for this compound.

In some tests, complementary to the mass-spectrometer tests, HCl was also sampled offline by impingers, and Cl was measured afterwards using the IC technique, as the data obtained in the first experimental campaign. Like the first experimental campaign, more Cl was determined in the product gas phase than in the original fuels (recoveries that surpass 100%), when using the bubblers (impingers) as a sampling method.

Figure 3.4 shows HCl recoveries trend with temperature for both methods:

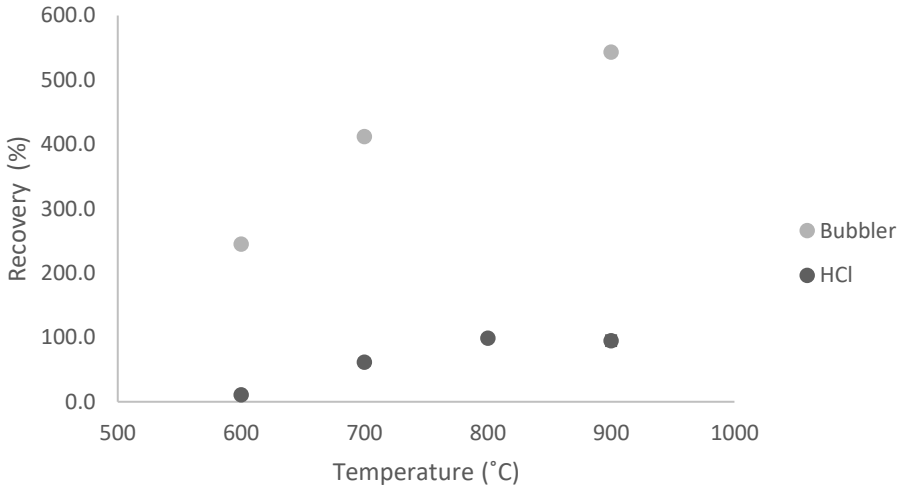

Figure 3.4. *HCl recovery ratio at different temperatures for DSS using bubblers (orange) and mass spectrometer for HCl (green).*

The same trend of Cl recovery increasing with temperature was observed for both methods: mass spectrometer (green points) and bubblers (orange points). However, as mentioned before, with impingers, the recovery is much higher and thus not acceptable as a reliable result.

Cl release to the gas phase is very complex to be estimated by measuring fuel-Cl and the Cl content in the product solid residue. This is because the Cl content is very low in the product solid residue, due to the high volatility of Cl. Therefore, measurement of Cl in the product solid residue was not included in this study.

NH_3 and HCN

HCN was not measured with MS, because it was not possible to calibrate the equipment for this compound because HCN is a dangerous species. HCN was sampled in some tests with impingers, but it was impossible to analyse its content in the recovered solution due to the influence of other ions (buffer solution added to maintain the basic pH). Just NH_3 was measured with MS and Figure 3.5 below shows the tendency of N-recovery from it:

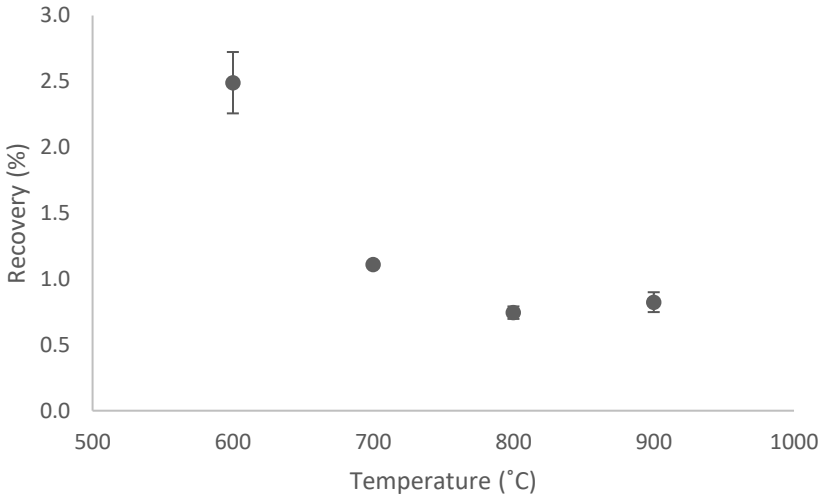

Figure 3.5. *NH_3 recovery ratio at different temperatures for DSS.*

Results show very low recovery of NH_3. The decrease in NH_3 with temperature is in accordance with equilibrium studies that show the same behaviour.

A hypothesis that might explain the low recovery of fuel-N in form of ammonia is that the DSS ash might have a catalytic effect on NH_3 production due to its high content in metals, resulting in a very low amount of NH_3 in the product gas (66).

A similar example, not of the catalytic effect of ash, but of another component, is dolomite. When used as bed material, dolomite might increase the conversion of fuel-N into NH_3 by affecting the whole gasification process, including the char conversion, steam conversion, gas composition, etc. Furthermore, it can catalyse the transformation of other nitrogenous compounds into ammonia (67).

N release to the gas phase can also be estimated by measuring fuel-N and the N content in the solid residue, as for S, and this will be further discussed in another topic (solid samples).

3.3.2. Solid residue: analysis their content in C, H, N and trace elements

3.3.2.1. Muffle furnace tests

Tests in muffle furnace were made only for DSS. Results are shown in terms of metals concentration in the solid residue and metals volatility. Table 3.6 shows the DSS initial mass, solid residue mass and R, which is the ratio of the mass of the solid residue and the mass of the initial fuel, for all the tests performed.

Table 3.6. *Initial mass of fuel, solid residue mass and the ratio for all the tests performed for DSS.*

Test	T (ºC)	Fuel initial mass (g)	Solid residue mass (g)	Ratio	Average	Error (%)
1	500	1.08	0.52	0.48		
2	500	1.03	0.47	0.46	0.46	2.33
3	500	1.03	0.46	0.45		
4	700	1.04	0.40	0.38		
5	700	1.00	0.41	0.41	0.43	4.14
6	700	0.96	0.35	0.36		
7	900	0.97	0.33	0.34		
8	900	0.98	0.30	0.31	0.41	2.61
9	900	1.06	0.35	0.33		

Ratio means the solid residue mass divided by the fuel initial mass. It slightly varies for tests at the same temperature, and the associated errors are below 5%.

The solid residues compositions in terms of C, H, N, and trace elements are presented in Tables 3.7 and 3.8 below.

Table 3.7. *Elemental composition in C, H, N for the solid residues in wt% for DSS.*

Test	1	2	3	Average	Error (%)	4	5	6	Average	Error (%)	7	8	9	Average	Error (%)
T (ºC)		**500**						**700**					**900**		
C (%)	33.27	31.8	31.66	**32.24**	**1.96**	26.03	25.5	24.63	**25.39**	**1.97**	17.95	17.86	21.00	**18.94**	**6.67**
H (%)	2.07	1.76	1.93	**1.92**	**5.72**	0.65	0.57	0.60	**0.60**	**4.76**	0.24	0.12	0.32	**0.23**	**30.95**
N (%)	5.01	4.84	4.89	**4.91**	**1.26**	3.58	3.34	3.18	**3.37**	**4.22**	1.18	1.15	1.41	**1.25**	**8.05**

Table 3.8. *Metals concentration in the solid residue samples (g/kg of sample) for DSS.*

Test	1	2	3	Average	Error (%)	4	5	6	Average	Error (%)	7	8	9	Average	Error (%)
T (ºC)		**500**					**700**					**900**			
Al	18.81	19.31	19.47	19.20	1.27	24.66	27.04	26.00	25.90	3.26	29.90	30.31	28.13	29.45	2.78
As	0.01	0.01	0.02	0.01	30.62	0.02	0.02	0.02	0.02	0.00	0.01	0.01	0.01	0.01	0.00
Ca	72.72	68.16	105.34	82.07	17.47	99.23	99.55	109.92	102.90	4.18	117.93	117.89	104.57	113.46	4.80
Cd	0.01	0.01	0.01	0.01	0.00	0.01	0.01	0.01	0.01	0.00	0.01	0.01	0.01	0.01	0.00
Co	0.02	0.02	0.02	0.02	0.00	0.02	0.03	0.02	0.02	17.50	0.03	0.03	0.03	0.03	0.00
Cr	0.21	0.21	0.20	0.21	1.98	0.25	0.27	0.26	0.26	2.72	0.31	0.30	0.29	0.30	2.36
Cu	0.88	0.89	0.88	0.88	0.46	1.14	1.22	1.16	1.17	2.51	1.41	1.31	1.17	1.30	6.57
Fe	35.47	37.53	36.58	36.53	2.00	46.88	52.61	54.44	51.31	5.44	56.10	56.82	48.50	53.81	6.06
K	7.03	7.94	7.38	7.45	4.36	9.81	9.44	11.11	10.12	6.13	14.03	14.10	19.21	15.78	13.31
Mg	12.87	12.57	13.58	13.01	2.82	16.35	17.47	16.78	16.87	2.37	19.93	19.71	17.94	19.19	4.02
Mn	0.40	0.41	0.41	0.41	1.00	0.53	0.56	0.54	0.54	1.99	0.61	0.59	0.53	0.58	5.11
Na	4.05	4.17	4.22	4.15	1.49	5.00	5.29	5.31	5.20	2.36	5.84	6.05	5.38	5.76	4.21
Ni	0.65	0.63	0.68	0.65	2.72	0.63	0.83	0.67	0.71	10.54	0.86	0.87	0.75	0.83	5.70
P	58.28	58.90	57.85	58.34	0.64	76.20	86.29	81.12	81.20	4.39	99.78	95.25	89.53	94.85	3.83
Pb	0.13	0.13	0.12	0.13	3.22	0.16	0.16	0.16	0.16	0.00	0.05	0.05	0.04	0.05	8.75
S	9.73	9.83	9.42	9.66	1.56	8.61	9.38	9.09	9.03	3.05	10.21	10.67	9.95	10.28	2.51
Sb	0.00	0.01	0.01	0.01	0.00	0.01	0.01	0.01	0.01	0.00	0.01	0.01	0.01	0.01	0.00
Si	26.49	31.82	28.27	28.86	6.65	36.39	41.26	36.62	38.09	5.10	46.44	42.60	40.39	43.14	5.02
V	0.03	0.03	0.03	0.03	0.00	0.04	0.04	0.04	0.04	0.00	0.05	0.05	0.04	0.05	8.75
Zn	1.85	1.87	1.87	1.86	0.44	2.42	2.63	2.45	2.50	3.21	1.77	1.92	1.79	1.83	3.15
Total	249.65	254.45	286.36	263.49	5.35	328.34	354.13	355.74	346.07	3.14	405.29	398.55	368.28	390.71	3.57

The analysis of Table 3.7 shows that the elemental composition in C, H, N results show low error (≤ 5% for most results). The highest associated errors appear for hydrogen. For all elements, the highest errors are associated with tests conducted at the highest temperature, 900°C. It is possible that the increase in the associated error with the temperature is due to the lower amount of material that is analysed. This is because, at higher temperatures, more volatiles are release, reducing the solid residue mass (see Table 3.6).

From the analysis of Table 3.8, it is observed that results for the same temperature are reproducible for most elements since most errors are low and under 10%. Errors associated with the measurement of As and Ca are high for tests at 500°C (30.6% and 17.5%, respectively); of Co for tests at 700°C (17.5%) and of K for tests at 900°C (13.3%). Errors, in general, may be linked to the nature of the fuel, which is a waste and, therefore, its composition is not standardized, and deviation might occur from one sample to another.

3.3.2.2. First batch of devolatilization experiments

Table 3.9 below contain solid residue composition in terms of C, H and N content in the solid residue for DSS, RDF and wood, respectively, for the tests conducted in the fluidized bed reactor in the first batch of experiments.

Test three (3) - using RDF as fuel - was not analysed, because not enough solid residue was collected from the bed material sampling. During the thermal conversion the RDF pellets disintegrated and, thus, it was not possible to separate it from bed material (sand) for analyses, even though bed samples were collected successfully. It was possible just for the fourth test four (4).

Table 3.9. *Elemental composition in C, H, N for the solid residues.*

Parent fuel	Test run	C (%)	H (%)	N (%)
DSS	**1**	16.62	≤0.02	1.14
DSS	**2**	13.89	≤0.02	1.12
RDF	**4**	48.42	0.52	1.15
Wood	**5**	86.24	0.36	0.26
Wood	**6**	80.88	0.36	0.23

Table 3.10 shows the concentration of metals in the solid residue samples in grams of element per kg of sample analysed.

Table 3.10. *Metals concentration in the solid residue*

Fuel	DSS	DSS	RDF	Wood	Wood
Test run	**1**	**2**	**4**	**5**	**6**
Element	**g/kg of solid residue**				
Al	18.19	30.82	14.19	3.35	3.40
As	0.01	0.00	0.01	0.01	0.00
Ca	114.68	128.38	80.15	11.12	11.28
Cd	0.01	0.01	0.01	0.01	0.01
Co	0.02	0.02	0.03	0.00	0.01
Cr	0.69	0.44	0.41	0.24	0.24
Cu	3.03	1.57	10.38	1.22	0.93
Fe	65.97	70.50	16.57	4.50	3.60
K	9.67	13.16	11.01	4.88	3.46
Mg	22.72	24.80	68.43	8.95	19.16
Mn	0.84	0.59	0.16	0.39	0.30
Na	2.18	2.89	6.97	1.29	13.24
Ni	0.60	0.64	1.97	0.30	1.46
Pb	0.01	0.01	0.00	0.00	0.00
S	7.11	6.78	2.62	0.39	0.26
Sb	0.01	0.01	0.10	0.01	0.01
Si	55.66	48.55	49.22	6.42	9.03
Sn	0.04	0.05	0.01	0.00	0.00
Ti	3.65	4.22	6.34	0.17	0.17
V	0.05	0.04	0.01	0.00	0.00
Zn	1.04	1.08	1.46	0.92	0.10
Total	306.16	334.55	270.04	44.16	66.66

Phosphorous (P) was not measured in any of the solid residue samples. As, Cd, Co, Pb, Sb, Sn, V, Ti content were bellow ICP limit detection (≤0,005 g/kg of sample) for some samples, so their concentration appears as zero in Table 3.11.

From Table 3.11, some comparisons can be made for the same fuels, tests one (1) and two (2) for DSS and tests five (5) and six (6) for wood.

For DSS, comparing the results from tests one (1) and two (2), it is observed that the concentrations of some elements are higher in test two (Al, Ca, Fe, K, Na, Ti), while the concentration of other elements are similar in both tests (Ca, Co, Ni, Pb, S, Sb, Sn, V, Zn). Also, the concentrations of other elements are lower in test two than in the first test (As, Cr, Cu, Mg, Mn, Si). However, concentrations do not vary considerably for tests number one (1) and two (2). Differences are related to the intrinsic heterogeneity of the fuel since it is derived from waste.

For wood, comparing the tests five (5) and six (6), it is observed that concentrations do not vary substantially. Only Mg, Na and Si concentrations are slightly higher in test number six (6).

For RDF, it is not possible to compare results, because there is just one test run. The solid residues masses are not possible to be measured with accuracy, because of the mixing and entrainment of the particles in the fluidized bed, and the separation of the solid residue particles from the bed material (sand). Therefore, solid residue masses are inaccurate to some extent even in the tests the full bed material was removed.

3.3.2.3. Second batch of devolatilization experiments

For the results of the second batch of devolatilization experiments, the elements were divided by major, intermediate, and minor elements, depending on their concentration (C, in mg/kg of sample). The concentration of these elements in the parent fuel is reported in Table 3.2.

For DSS, this classification was followed (C: concentration in mg/kg of sample):

- Major: $C \geq 10000$
- Intermediate: $10000 < C \leq 100$
- Minor: $C < 100$.

Table 3.11 shows the average trace elements concentrations in DSS solid residues (mg/kg of sample) from devolatilization tests in N_2 atmosphere and their associated errors (%) for the tests at 600 - 900°C. Every sample was measured twice.

Table 3.11. *Average trace elements concentrations in DSS solid residues (mg/kg of sample) from devolatilization tests in N_2 atmosphere and their associated errors (%). Major: C ≥ 10000 / Intermediate: 10000 < C ≤ 100 / Minor: C < 100 in mg/kg of sample.*

T (ºC)	600		700		800		900	
Element	**Concentration**	**Error (%)**	**Concentration**	**Error (%)**	**Concentration**	**error (%)**	**Concentration**	**Error (%)**
				Major				
Al	25855.5	3.9	24824.6	5.5	26153.0	4.7	29021.3	8.3
Ca	105002.2	9.9	101333.0	4.6	114400.9	5.2	114118.8	3.8
Fe	54014.3	5.5	53800.0	3.6	54445.2	8.9	62864.9	5.5
Mg	15352.2	9.2	14889.8	4.4	16872.6	4.9	17471.8	1.7
P	90326.3	2.9	81974.2	4.2	80891.0	5.5	74922.4	**12.7**
				Intermediate				
Ba	815.1	3.2	864.2	2.7	853.6	14.2	925.1	7.4
Cr	485.1	22.1	473.2	12.3	431.5	4.0	591.1	19.1
Cu	921.2	4.0	933.3	3.1	942.5	2.0	973.2	4.6
K	4136.5	6.6	3930.8	10.2	4661.5	29.0	6710.0	26.5
Mn	570.6	1.9	625.8	6.8	702.0	5.5	717.1	3.8
Na	5369.8	4.5	5032.8	5.7	5587.1	13.3	5682.1	21.4
Ni	468.6	15.3	454.0	9.3	460.9	4.5	555.6	9.3
Sn	2228.9	1.3	1811.2	5.8	730.0	20.1	125.9	48.4
Sr	1122.1	4.7	1144.3	1.9	1255.2	3.3	1226.0	5.9
Ti	4304.4	3.1	4366.1	2.4	3999.9	16.7	5193.1	8.2
Zn	1806.6	6.9	1084.6	11.4	302.9	4.8	177.1	52.1
				Minor				
As	17.5	12.0	18.2	5.3	17.4	9.5	20.4	25.2
Cd	0.2	8.0	0.1	12.2	0.1	15.6	0.1	18.6
Co	23.9	3.2	25.0	3.9	26.5	4.3	28.6	7.2
Pb	98.8	10.8	48.1	6.8	11.3	13.4	18.6	57.7
Sb	52.4	6.4	48.9	1.4	47.7	6.8	47.3	10.8
Se	1.7	7.8	1.5	6.1	1.4	18.1	1.5	14.4
Te	0.3	5.5	0.3	6.1	0.2	6.0	0.3	6.8
V	61.2	7.9	64.9	5.8	61.6	7.4	68.2	16.5

For wood, the classification of major, intermediate, and minor elements was different (C: concentration in mg/kg of sample):

- Major: C > 100
- Intermediate 100 ≤ C ≤ 5
- Minor: C< 5

This scale uses lower values than the ones for DSS, because trace elements concentration is lower in wood pellets, since it is a commercial and, thus, cleaner, and standardized fuel.

Table 3.12 shows the trace elements concentrations in wood solid residues (mg/kg of sample).

Table 3.12. *Trace elements concentrations in wood solid residues (mg/kg of sample). Major: C ≥ 100 / Intermediate: 100 < C ≤ 5 / Minor: C < 5 in mg/kg of sample.*

T (ºC)	700	800	900
Element	**Concentration (mg/kg of sample)**		
	Major		
Al	1106.0	2147.1	1790.9
Ca	2432.6	4661.1	4169.8
Fe	392.0	559.5	506.3
K	2492.2	7296.9	22783.0
Na	1854.2	7759.1	20959.1
Mg	1089.0	2060.2	1871.1
Mn	327.0	361.7	383.2
P	294.2	1380.3	3394.7
	Intermediate		
Ba	23.6	23.0	32.1
Cr	25.7	0.0	0.0
Cu	7.5	9.9	12.4
Ni	14.6	3.2	2.1
Sr	34.7	38.5	47.0
Ti	65.8	0.0	0.0
Zn	15.1	2.0	0.7
	Minor		
As	1.8	0.0	0.0
Cd	0.01	0.0	0.0
Co	1.4	1.0	1.0
Pb	1.7	1.5	2.2
Sb	0.6	0.9	3.0
Sn	0.0	0.0	0.0
Se	0.0	0.0	1.3
Te	0.0	0.1	0.0
V	6.2	0.0	2.0

For the solid residues from the tests using wood pellets as fuel, it was not possible to calculate an associated error, because there just one test was performed at each temperature.

3.3.2.4. Analysis of the behaviour of trace elements by their concentration with the temperature

From the results of all tests performed in the different experimental campaigns - one in the muffle furnace, and two using fluidized bed reactors - it is possible to analyse the concentration of the elements in the solid residue, and then comparing its change with the tests' parameters, for instance: fuel, temperature, and rig type (muffle furnace or fluidized bed).

To enable the analysis of the behaviour of the different trace elements during the devolatilization tests, it is possible to observe the change in their concentration depending on the process conditions, in this case, the temperature. To better understand how the concentrations are expected to change compared to their concentration in the fuel, or to another process condition, the following principles are proposed with temperature increase for a given element ***i***:

- **The concentration of an element *i* decreases:** the component has volatilized and was released to the gas phase. It can condensate on flying ash particles downstream or be released to the atmosphere, if not captured in gas cleaning systems. This behaviour is expected for volatile components, such as: As, Hg, Pb and Cd.
- **The concentration of an element *i* remains the same or slightly changes:** the component has volatilized, but not as much as in the previous case. It means that the component loss was the same as the solid residue mass loss. This behaviour is expected for less volatile components, such as Zn.
- **The concentration of an element *i* increases:** the volatility of the component ***i*** is very low, or the component ***i*** has completely remained in the solid (volatility = 0). This behaviour is expected for low/no volatile components, such as: Mn, Cu, Cr, Ni.

Therefore, the following sections compare:

- The concentration of trace elements in the solid residues from the tests conducted at the *second experimental campaign in the fluidized reactor (2018)* at different temperatures and for each fuel type (DSS and wood pellets).
- The *first (2017)* and the *second (2018)* experimental campaigns at the fluidized bed reactors at different temperatures, using DSS as fuel.
- The *muffle furnace tests* and the *second experimental campaign (2018)* at the fluidized bed reactor at different temperatures, using DSS as fuel.

Second experimental campaign at the fluidized bed reactor

Figure 3.6 below enables the analysis of temperature effect on DSS devolatilization at N_2 atmosphere.

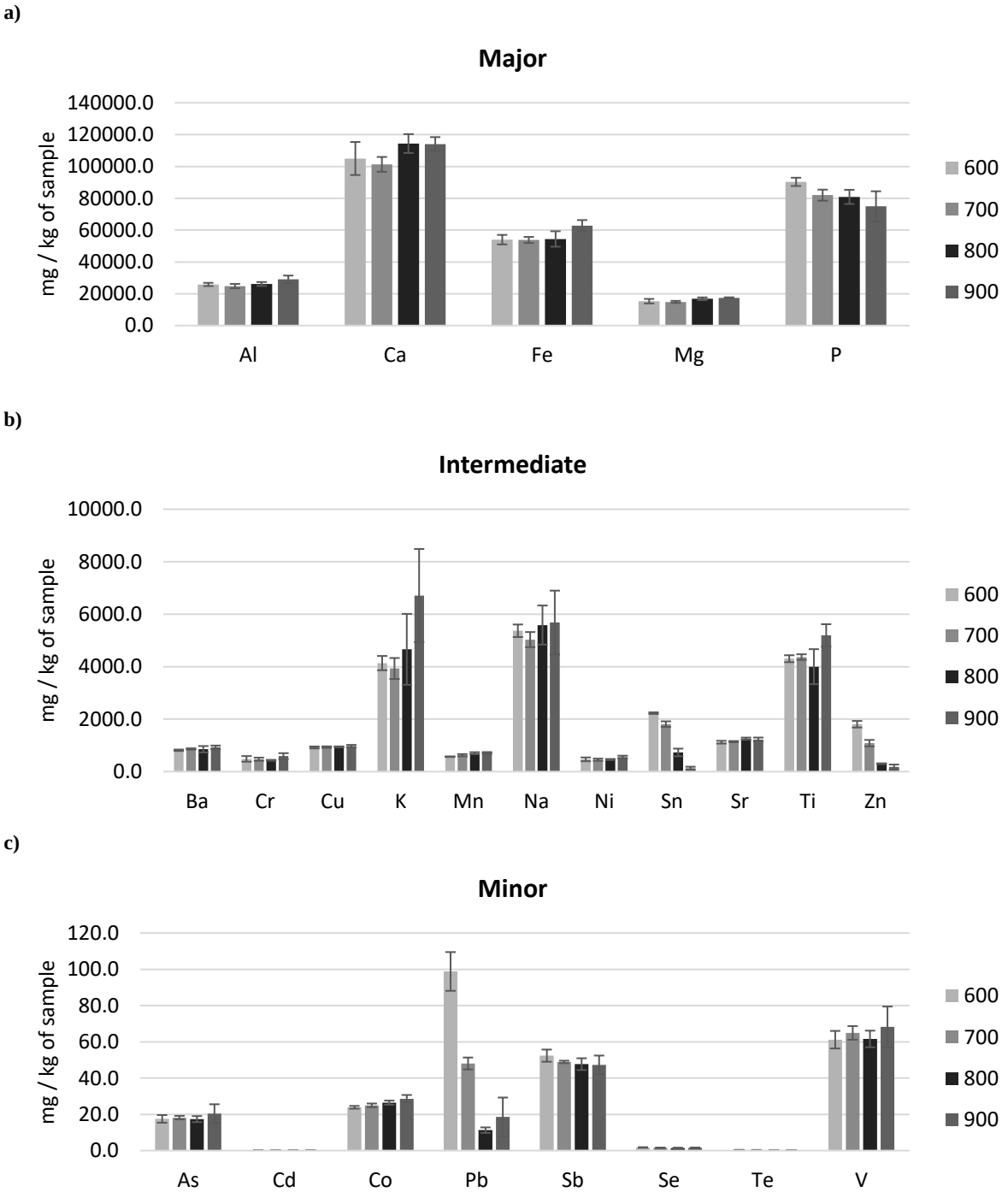

Figure 3.6. *Concentration of trace elements – a) major, b) intermediate, and c) minor elements - in the solid residue from devolatilization tests at N2 atmosphere using DSS as fuel, at different temperatures: 600, 700, 800, and 900 ºC. Major: C ≥ 10000 / Intermediate: 10000 < C ≤ 100 / Minor: C < 100 in mg/kg of sample.*

Based on the Figure 3.6 above and the explanation about trace elements behaviour, it can be observed that for DSS that the elements behaviours are the following:

- Most volatile elements: P, Sn, Zn and Pb.
- Least volatile elements: Ca, Fe, Mg, Al, K, Na, Ti, Co, and V.
- Elements which concentration remain the same with temperature increase: Ba, Cu, Ni and Sr. This indicates that the element ***i*** presents the same mass loss trend as the fuel during devolatilization.

Figure 3.7 below enables the analysis of temperature effect on wood devolatilization at N_2 atmosphere.

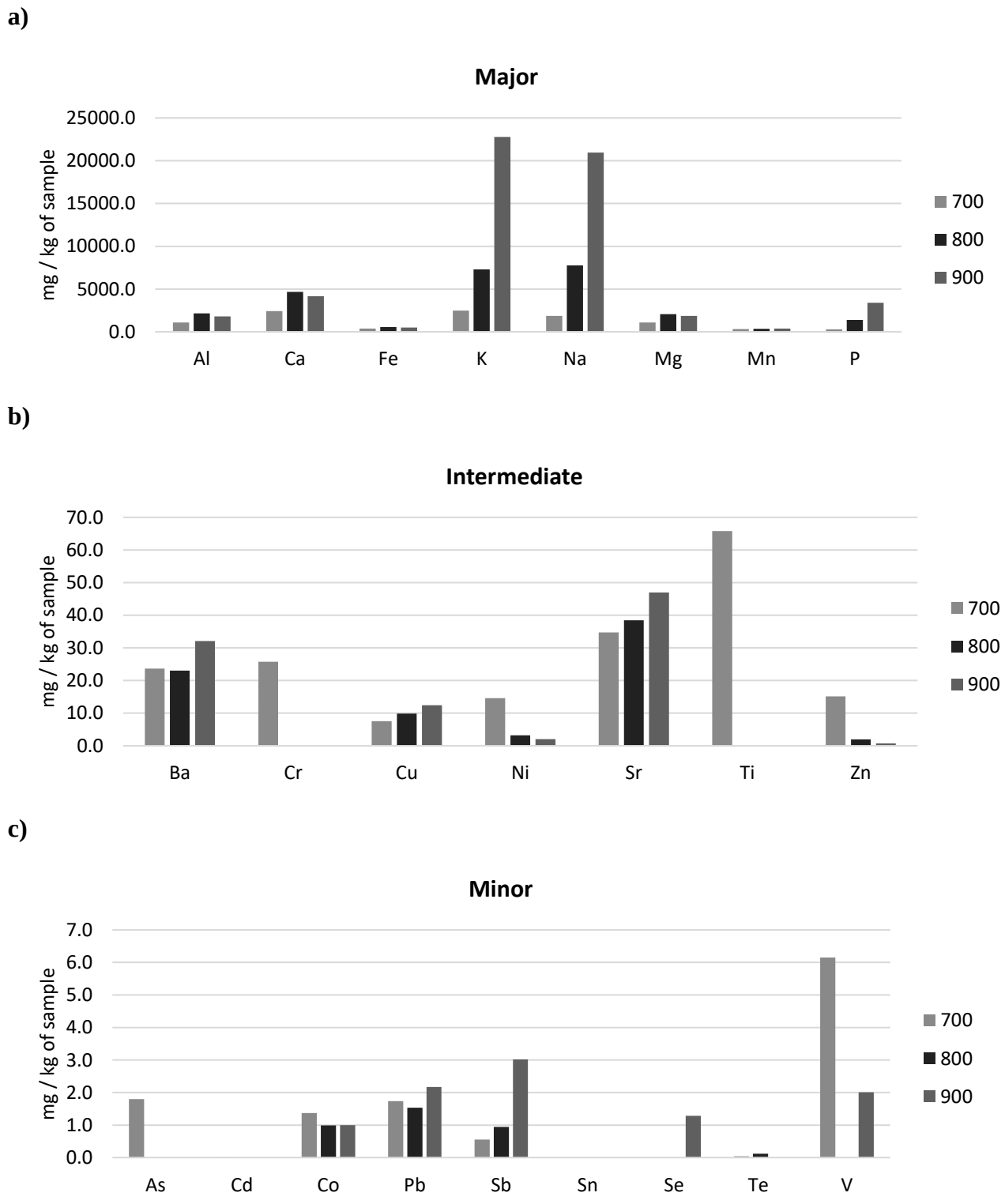

Figure 3.7. *Concentration of trace elements – a) major, b) intermediate, and c) minor elements - in the solid residue from devolatilization tests at N_2 atmosphere using wood pellets as fuel, at different temperatures: 700, 800, and 900ºC. Major: C ≥ 100 / Intermediate: 100 < C ≤ 5 / Minor: C < 5 in mg/kg of sample.*

First (2017) and second experimental (2018) campaigns at the fluidized bed reactor

Figure 3.8 below presents the results for DSS devolatilization at 800°C for the *first (2017)* and the *second (2018)* experimental campaigns.

a)

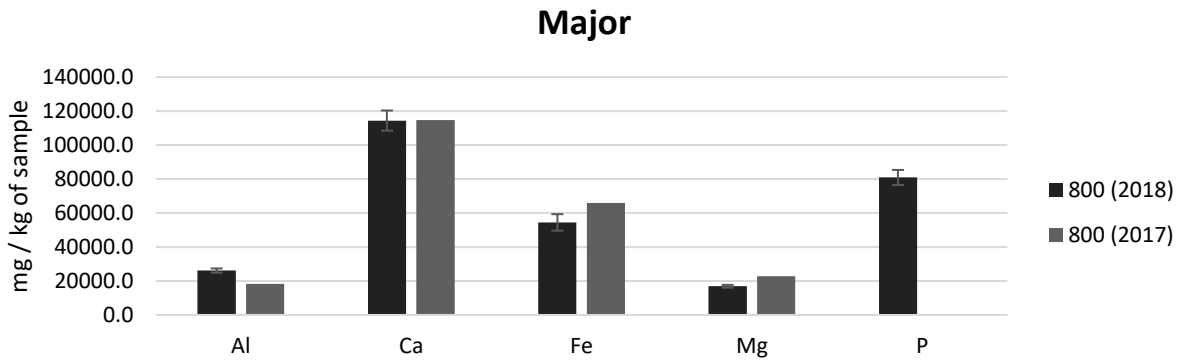

b)

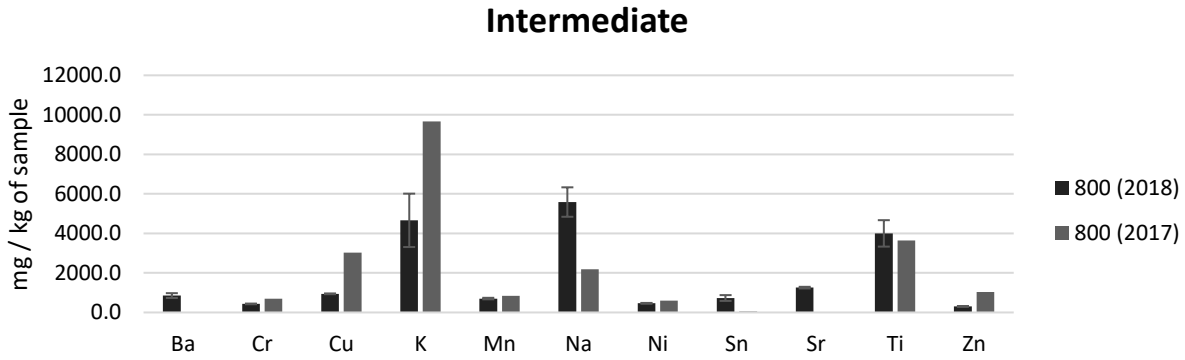

c)

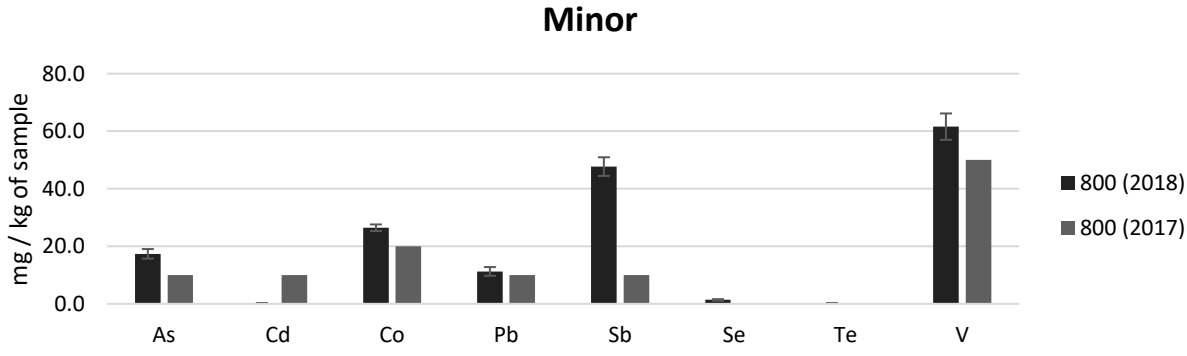

Figure 3.8. *Concentration of trace elements – a) major, b) intermediate, and c) minor elements - in the solid residue from devolatilization tests at N_2 atmosphere using DSS as fuel at 800ºC, at different experimental campaigns: the first one conducted in 2017 (particle size: 840μm ≤ DSS ≤ 2mm) and the second one conducted in 2018 (particle size: 500μm ≤ DSS ≤ 840μm). Phosphorous (P) was measured only in the second experimental campaign and, thus, its concentration is zero for the first one.*

Comparing results for devolatilization tests at 800°C and N_2 atmosphere, results in terms of concentration of trace elements in the solid residue are similar. Variations can be attributed to the differences of trace element in the fuel (2017/2018), the fuel size (particles from the last experimental campaign are smaller) and the intrinsic fuel heterogeneity.

Major elements results are very similar. Note that P was not quantified in 2017, so comparisons could not be made.

For intermediate elements, the most accentuated differences are found for Cu, K and Na, being the concentrations of Cu and K lower in 2018, while Na concentration was higher.

In the case of minor elements, Sb is the only element which concentrations differ considerably, being much higher in 2018.

Muffle furnace and last experimental campaign (2018) at the fluidized bed reactor

The following Figure 3.9 compares trace elements concentrations for tests using DSS at the *muffle furnace (mf)* and the *fluidized bed (FB) reactor in the second experimental campaign (2018).*

a)

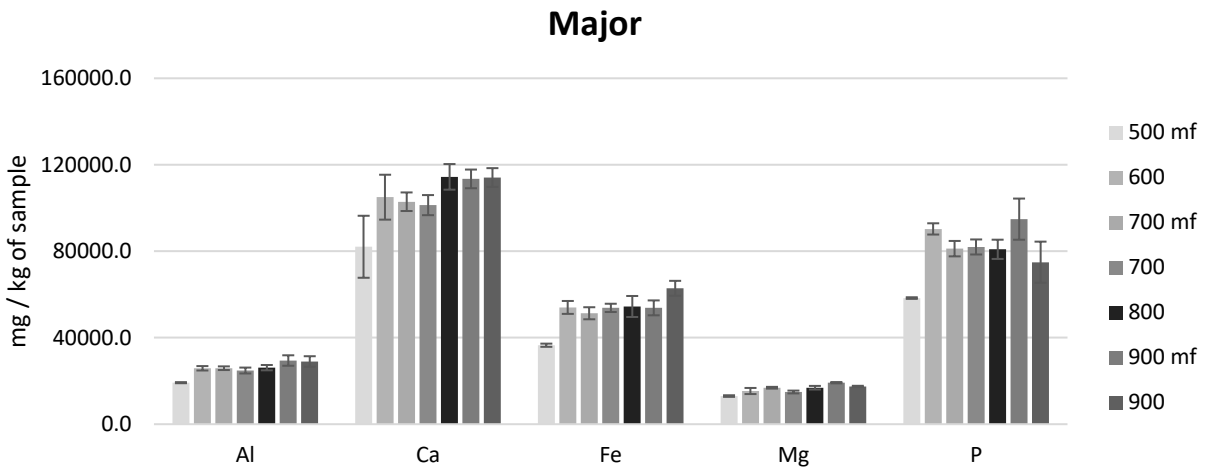

b)

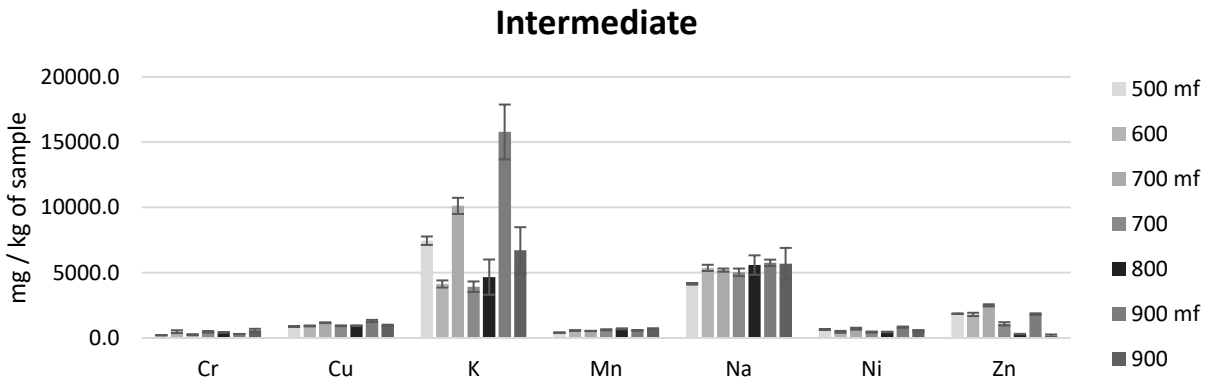

c)

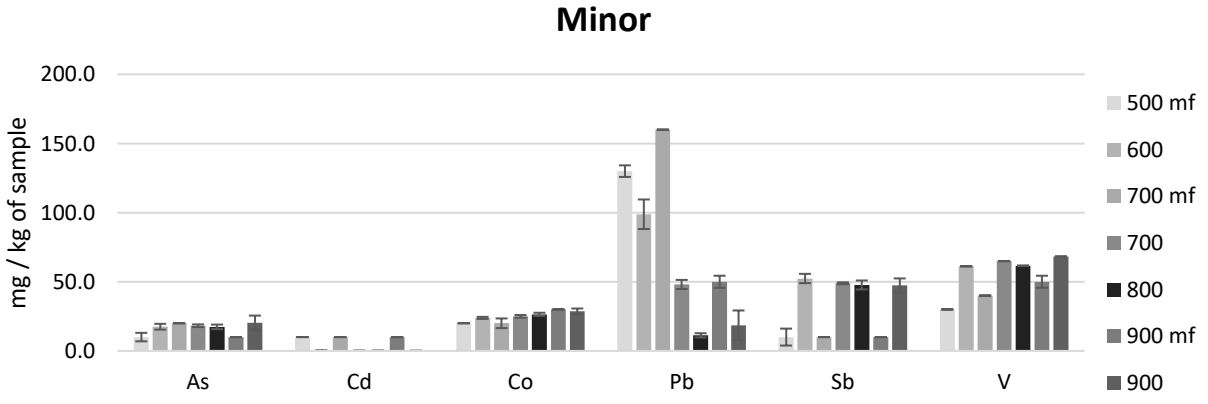

Figure 3.9. *Concentration of trace elements – a) major, b) intermediate, and c) minor elements - in the solid residues from DSS devolatilization tests at N_2 atmosphere: comparison between different temperatures from muffle furnace (mf) tests - 500ºC, 700ºC and 900ºC - at and fluidized bed tests (2018) - 600ºC, 700ºC, 800ºC and 900ºC. Major: C ≥ 10000 / Intermediate: 10000 < C ≤ 100 / Minor: C < 100 in mg/kg of sample.*

The concentration of major elements (Al, Ca, Fe, Mg, P) are very similar for both type of tests (mf/FB). All elements show the tendency of slightly increasing their concentration with temperature, which shows that they are not volatile, since they tend to stay in the solid.

Moreover, it is possible to conclude that the high concentrations of major elements, for instance, at least Al, Ca, and Fe in the samples of the solid residues from the fluidized bed tests, are not because a potential contamination from bed material, in this case, sand, which present a high content in these species, since concentrations do not differ from the muffle furnace tests.

The concentrations of most elements that are in the *"intermediate"* scale were not affected by the difference in the experiment rig (mf/FB). K and Zn were the ones in which some differences were noted, being their concentrations higher in muffle tests.

The concentration of minor elements in the solid residues varied more for both type of experiments and same conditions. The following observations are highlighted:

- As concentration is not affected either by temperature or experiment configuration (mf/FB). As is very volatile, so it is released at low temperatures. The temperature increases ($\geq 500°C$) or the fluidization effect cannot increase its volatility since it is soon released to the gas phase.
- The concentrations of Cd and Pb are higher in the muffle furnace experiments. This might be explained that the effect of fluidization supports their release, decreasing their concentration in the FB solid residue. During the fluidization, the particles are heated faster, which might contribute their release to the gas phase.
- Sb and V concentrations are lower in muffle furnace experiments, which suggests that the fluidization decrease their volatility.
- Pb and Sb are the elements which concentrations are more affected by experiment type. Pb lower concentrations in FB could be due to particles mixing, since they break and move, volatility could be favoured. However, this do not explain Sb higher concentration in FB.

It can be observed that the concentrations of the major elements are not affected by the experimental setup, since they tend to have low volatility. Furthermore, the similar result for both configurations suggests that the solid residues from the fluidized bed tests are not contaminated by the bed material, sand.

3.3.2.5. Elemental mass balance for the trace elements in the fluidized bed tests

It is known that with temperature increase, the resulting solid residue mass decrease. This is mainly due to carbon and other major elements loss/release to the gas phase, the release of volatiles to the gas phase (68).

In the muffle furnace tests, it was possible to collect all the solid in the end of the test (called here as "solid residue"). However, in the tests performed in the fluidized bed reactors, it was not possible to collect all the solid residue in the end of the test and, thus, determining the final mass of the solid residue with precision, enabling the calculation of a precise elemental mass balance.

This is because, during the fluidized bed tests, there are several events that prevent the full collection of the solid residue, being the most important: the solid residue break down into smaller particles and its mixing with the bed material. If the solid residue particles are very small, like dust, and it is impossible to recollect it.

Furthermore, collecting all the bed material in the end of each test and then separating the solid residue from the bed is a very time-consuming task, which delays the experiments schedule considerably. That is why the masses of solid residues are unknown in the fluidized bed tests.

The expected final mass of the solid residue be done by using the results from the muffle furnace tests (see Table 3.6), since in this type of tests the solid residue can be collected and weighted. Even if the fuel does not behave the same way in a fluidized bed reactor compared to a fixed bed test, it is possible to estimate the solid residue mass with high precision using this approach.

Figure 3.10 below shows the ratio of the mass of the solid residue with the mass of the fuel (axis y) versus the temperature in degree Celsius for the muffle furnace tests using DSS as fuel.

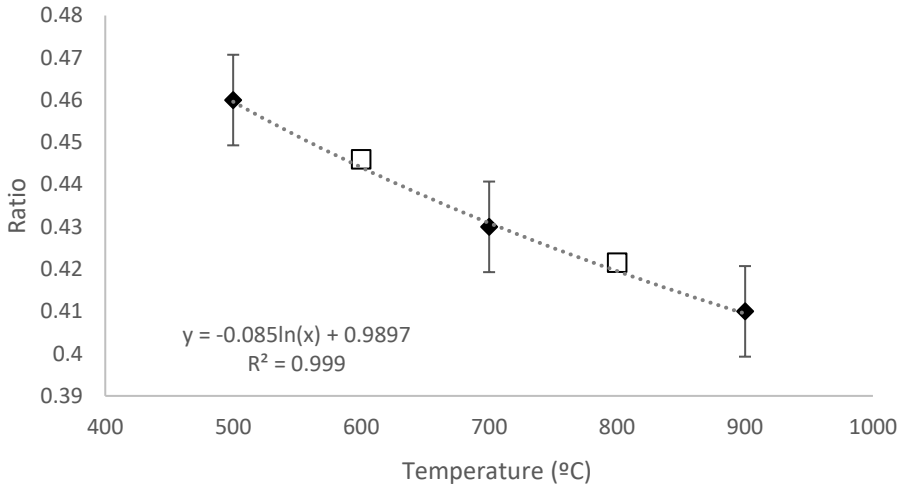

Figure 3.10. *Ratio between the solid residue mass and the initial mass of the fuel versus the temperature for the muffle furnace tests using DSS as fuel. The square points were calculated by using the estimation provided by the experimental points (black diamonds).*

In any case, it is important to highlight that both the fuel and the solid residue analyses in content of main (i.e., C, H, N) and trace elements (i.e., As, Cu, Ni) are done by using samples of these solids. As in this thesis the focus is on wastes, their content is not homogenous and may vary, i.e., the content of DSS or RDF is not standardized as the woody biomass pellets.

Therefore, a very precise elemental mass balance is very challenging in this scope, even in the muffle furnace tests, leading to variations in the results. For instance, by establishing that the solid mass residue for the fluidized bed tests follows the trend with temperature as for the muffle furnace tests and using the elements' concentrations both in the fuel and in the solid residues, variations in the mass balances can be encountered (i.e., finding that the amount of an element i is higher in the output stream than its initial content in the inlet stream, which is not possible). However, as explained, such inconsistencies are linked to the intrinsic heterogeneity found when using waste-derived fuels (15).

By estimating the mass of the solid residue, it is possible to estimate the mass of the elements in the solid at the end of the process. This way it is possible to analyse the elemental mass balance of such elements and estimate, for each element ***i***, how much stayed in the solid, and how much went to the gas phase. Through equation 3.2, it is possible to calculate the volatility of an element ***i***.

However, this approach does not give good results, since when the elemental mass balances are performed, for most elements, the masses of the elements in the solid stream are higher than in the

entrance. According to the loss of conservation of mass "*the mass in an isolated system can neither be created nor be destroyed but can be transformed from one form to another*". Therefore, it suggests that the solid residue masses are much lower in the fluidizing bed experiments than in the muffle furnace tests, suggesting that the fluidization may increase the release of volatiles.

Another option was that the solid residue samples from the fluidizing bed experiments were contaminated with the reactor material (SS316), which contains some of the elements that are in the fuel as well: Cr (16-18%), Ni (10-14%), Mo (2-3%), C (0.08%), Mn (2%), P (0.045%), S (0.03%), Si (0.75%), N (0.1%), Fe (balance). Other hypothesis was the contamination with the bed material, in this case sand, since it also contains elements present in the fuel SiO_2 (98.4%), Al_2O_3 (0.18%), Fe_2O_3 (<0.1%), TiO_2 (0.02%), CaO (0.28%), MgO (<0.10%), Na_2O (0.022%) and K_2O (<0.10%). However, by comparing the concentrations of the solid residues from the muffle furnace and fluidized bed experiments (see Figure 3.9) for the same temperatures, similar concentrations were found and, therefore, these hypotheses were discarded.

To estimate the mass of the solid residues for the fluidized bed experiments and calculate the elemental mass balances for the trace elements and, thus, understand their behaviours during the devolatilization tests, the *Key Element Method* was proposed, which will be explained below.

Key Element Method

The other way to analyse it is by applying the "Key Element Method (KEM)" in which, one *key element* is assumed to remain completely in the solid residue (69). The key element method (KEM) is based on the principle that the key element (KE) is not volatile (volatility is zero) and thus remains entirely in the solid residue. Then, by knowing its concentration in the fuel and in the solid residue, it is possible to determine all elements volatilities.

The following Figure 3.11 shows the element volatilities using Ni as the key element for different temperatures (600 – 900°C).

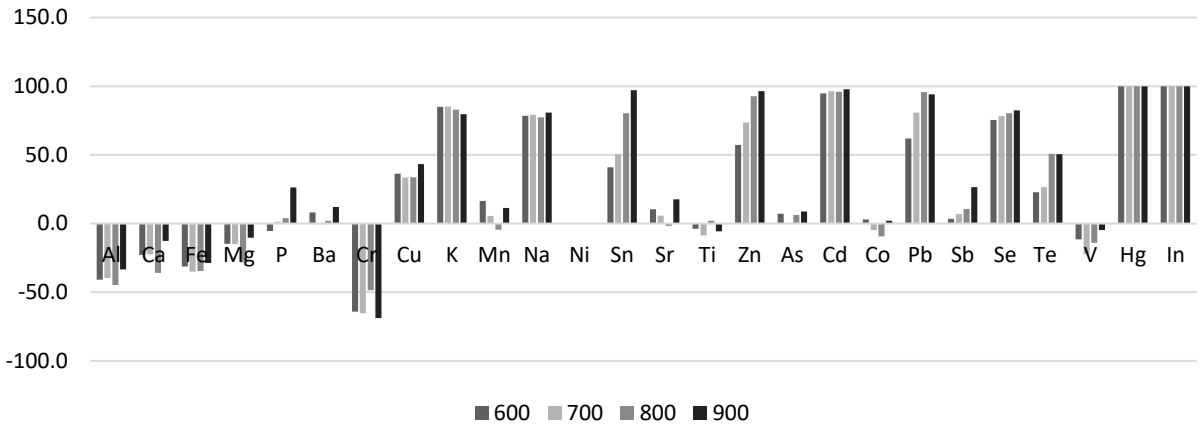

Figure 3.11. *TE volatilities for DSS devolatilization tests at N_2 atmosphere. Ni as a key element, comparison of results using initial concentrations of TE.*

From the graphics comparison, it shows that Al, Ca, Fe, Mg, Cr, Mn, Ti, Co, and V still present negative volatilities. Overall, elements that are very volatile (i.e., Pb, Cd, Hg and In) present high volatility, which is a positive result.

Cr was the critical compound, presenting the most negative volatilities. Thus, one analysis was carried considering it Cr as the key element. Figure 3.12 presents the results:

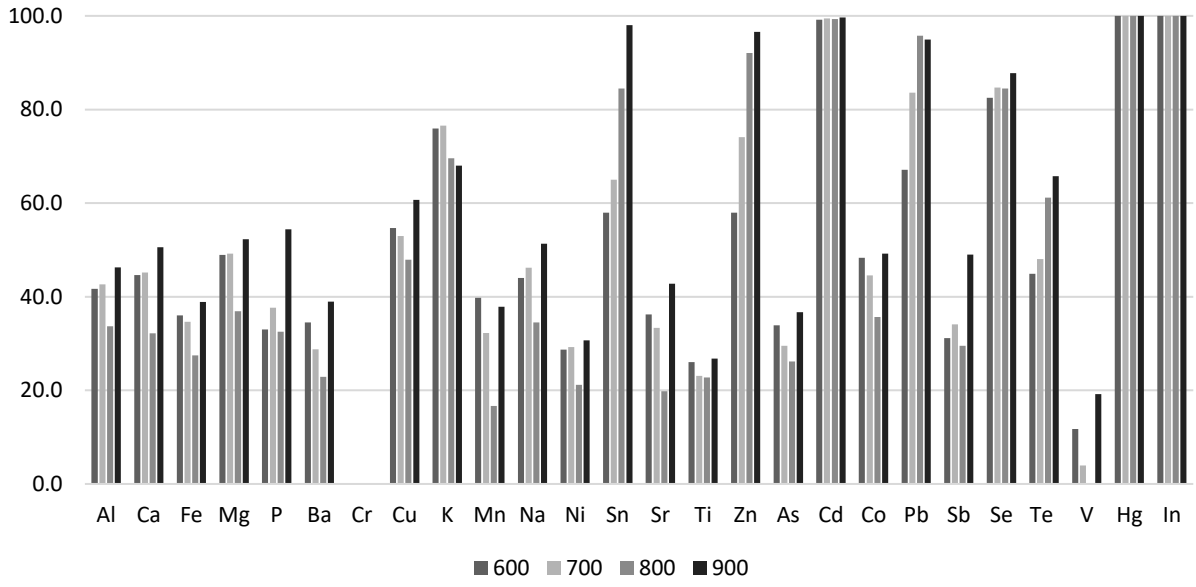

Figure 3.12. *TE volatilities for DSS devolatilization tests at N_2 atmosphere using Cr.*

These results look very attractive since now no negative volatilities were obtained. For this, it was obtained a solid residue mass of about 22% from the initial fuel mass, while for Ni, it was about 28%.

This method supports the calculation of the metal volatilities which, overall, agrees with their expected behaviour from literature. To enable the proof of this method, dedicated lab-scale devolatilization experiments in which the solid residue mass was fully recovered should be performed.

The muffle furnace tests gave a good insight into the elemental mass balances of the trace components. As they were carefully carried out, if no external interference found in the FB experiments (i.e., bed and reactor materials, fluidization, difficulty in measuring the mass of the solid residue), the elemental mass balances should be satisfactory. However, for those experiments, the volatilities were also negative for several elements. This result led to the hypothesis that the measurement of the trace elements in the fuel might have interferences with volatiles from the biomass, since when the fuel is characterized in terms of its concentration in those elements, it is the original fuel, with its volatile, fixed carbon and ashes. When it is measured in the solid residue, these volatiles were already released, and the potential interference is eliminated. Unfortunately, in the scope of this thesis it was not possible to explain the inconsistencies in the mass balances studied. Nevertheless, the behaviour of the elements concentration with experimental conditions was studied, as it is commonly analysed in the literature (15), supporting the understanding of the partitioning of these elements, including heavy metals, during the thermal conversion.

3.4. Conclusions

The devolatilization experiments performed along the two experimental campaigns in the fluidized bed and the experiments carried out in the muffle furnace enable to shed some light about the partitioning comportment of inorganic and trace elements during the thermal conversion. These are valuable results, since devolatilization, after drying, is the first step the fuel passes through during the gasification process.

Due to fuel availability, Dried Sewage Sludge (DSS) was the focus of the experiments. In the first experimental campaign in the fluidized bed RDF was used as well, but the difficulty of recovering its solid residue in the end of the experiment precluded further experiments using this fuel. Wood was used in both experimental campaigns using the fluidized bed reactor for comparison.

The inorganics, S, Cl were measured in in the outlet gaseous streams in both fluidized bed experimental campaigns. N was measured only in the second one. The compounds containing these elements S, Cl and N were measured by using a mass spectrometer:

- **Sulphur**: The measurement of H_2S using an UV spectrometer in the first experimental campaign was not successful due to the interference with other compounds. It was properly measured with the mass spectrometer, but its recovery in the outlet stream was low, reaching up to 6 wt.% and decreasing with the temperature. This suggested a potential reaction of S and the reactor material and the sulphur retention in the internal reactor surface, decreasing the H_2S content in the outlet stream.
- **Chlorine**: The measurement of Cl was not successful in the first experimental campaign using impingers. More Cl was obtained in the outlet stream than it was detected in the fuel, suggesting that maybe another ion was interfering in the result. During the second experimental campaign in the FB reactor, the recovery of Cl in the outlet stream was up to 100% and increased with the temperature, which agrees with its expected behaviour.
- **Nitrogen**: Nitrogen was measured only in the second experimental campaign in FB tests, only in NH_3 form. Its recovery was very low, up to only 2.5% and decreasing with the temperature. The ammonia decrease with temperature is in accordance with equilibrium studies that show the same behaviour with temperature. This leads to the hypothesis that DSS ash might have a catalytic effect on NH_3 production due to its high content in metals.

The solid products, in this thesis called as "*solid residues*" of the tests were extensive studied in this chapter. They were characterized both in terms of C, H, N and in trace elements. The concentration of trace elements was studied and compared between different test conditions: i.e., temperature, fuel, and rig type and some tendencies were identified:

- The concentration of non-volatile elements increased with temperature, suggesting their accumulation in the solid residue: i.e., Mn, Cu, Cr and Ni.
- The concentration of volatile elements decreased in the solid residue with the temperature, suggesting their release to the gas phase: i.e., As, Hg, Pb and Cd.

The elemental mass balances of the selected trace elements was performed, so the volatilization behaviour of such elements could be characterized. However, inconsistencies were found. For some

elements, more was calculated in the output solid stream than in the fuel. The muffle furnace tests eliminated hypothesis that this might be due contamination and other external factors during the fluidized bed experiments. Thus, a final hypothesis suggests that the volatile content in the fuel might interfere the measurement of trace elements in the fuel. Nevertheless, the study of trace elements is very complex (70) and in order to obtain a satisfactory overview of the elemental mass balances, it would be further necessary to study both the fuel and the solid residues, by including imagery analysis and determining the chemical form in which such elements are found both in the fuel and in the solid residues.

Unfortunately, such studies are not in the scope of this thesis. However, it is expected that the extensive and careful analyses conducted here, and the hypothesis tested can shed some light on the understanding of their behaviour during the thermal conversion of wastes and biomass.

Chapter 4

Experimental: Results of continuous gasification tests using RDF as fuel

4.1. Summary

In this chapter, the gasification of refused-derived fuel (RDF) in a fluidized-bed gasifier followed by a high-temperature filter in a bench-scale plant will be investigated by presenting and discussing experimental tests conducted at VTT Bioruukki Pilot Centre in Espoo, Finland. It aims to study the effect of process operation conditions during gasification of refused derived fuel (RDF).

The gasification performance is analysed by measurements of gas and solid streams: the main species in the product gas are characterized, including tars, but the main contribution of this chapter is the analysis of the fate of nitrogen, sulphur, and chlorine in the fuel into gaseous pollutants, bottom, and filter ashes, as well as the distribution of the main trace elements in the bottom and filter ashes.

4.2. Introduction

Six bench-scale air or air/steam gasification tests were carried out using RDF in the form of crushed, pellets as feedstock and changing the temperature, equivalence ratio (ER), composition of gasification agent, bed material and filter temperature. The tests were performed at fixed reactor (bed and freeboard) temperature of 850°C, filter temperature of 450°C and 550°C, using air-N_2 and air-steam mixtures as gasification agent with equivalence ratio (ER) in the range of 0.24 – 0.32) and sand and sand/dolomite mixtures as bed material. The influence of these parameters on gasification performance was studied, with the primary objective of understanding the fate of fuel-N, fuel-S, fuel-Cl, and fuel-trace elements distribution into the gas and ash streams (both filter and bottom ashes).

It was found that steam addition, besides increasing the yield of H_2, promoted the yields of NH_3, H_2S and tars. The catalytic effect of dolomite on decreasing tar production was not observed in our

experiments. The fuel-N and fuel-S were mainly converted into ammonia (≥ 40%) and H_2S (≥ 20%). Most of fuel-Cl was measured in the filter ash, whereas only a fraction of the fuel-S was detected in the filter ash, which decreased with higher filter temperature.

The distribution of trace elements into the filter and bottom ashes was consistent with their inherent volatile behaviour, although precise quantification was difficult due to the heterogeneity of the fuel. Preliminary assessment of ash utilization/disposal options of filter and bottom ashes generated was made by studying the enrichment factor.

4.3. Literature review

Several works in the literature have studied the content of inorganics and trace elements during the fluidized bed gasification of solid waste in the last years. Table 4.1 below shows a selection of these works.

Table 4.1. *Literature review of the inorganics and trace elements during the gasification of waste in fluidized bed. NA: Not applicable / NM: not measured*

Waste fuel	Studied elements in the product gas and solid			System mode	Analysed parameters	Year	Reference
	Inorganics	Trace elements *					
		Major	Minor				
Sewage Sludge	NM	NM	Cd, Cu, Ni, Pb, Zn	Fluidized bed reactor (continuous)	Residence time	2011	*Syc et al.* (71)
Municipal solid waste (MSW)	HCl, H_2S, NH_3	Al, Ca, Fe, K, Mg, Mn, Na, P, Si	As, Cd, Co, Cr, Cu, Hg, Ni, Pb, Sb, Si, V, Zn	Pilot scale bubbling fluidized bed (continuous)	Temperature	2014	*Arena & Di Gregorio* (72)
Solid recovered fuel and woody biomass (waste wood and beech wood)	H_2S, COS / N and Cl **	NM	NM	Lab scale fluidized bed air gasification (continuous)	Temperature and atmosphere	2019	*Valin et al.* (8)
Poultry litter	H_2S, NH_3, S (solid)	Al, Ca, Fe, K, Mg, Mn, Na, P, Si	As, Ba, Cd, Co, Cr, Cu, Hg, Mo, Ni, Pb, Sb, Si, Tl, Ti, V, Zn	Bench scale bubbling fluidized bed (continuous)	Temperature for inorganics in gaseous form	2020	*Pandey et al.* (63)
N-rich fibreboard	HCN and NH_3	Al, Ca, Fe, K, Mg, Mn, Na, P, Si	Zn	Air blown fluidized bed gasification	Hot gas filtration on hydrogen cyanide and ammonia and distribution of trace elements between cyclone and filter	2021	*Ruiz et al.* (64)

References: Valin et al. (8)*; Syc et al.*(71)*; Arena & Di Gregorio* (72)*; Pandey et al.* (63)*; Ruiz et al.* (64)*;*

** Minor elements are considered the ones in concentrations lower than 0.1% (<0.1% or <100mg/kg or <0.1g/kg)*

*** The measurements of nitrogen and chlorine were not satisfactory, with elemental balances far from being closed, so results were not reported*

4.4. Experimental

4.4.1. Test rig

Gasification experiments were conducted as part of the Brisk2 program at VTT's bench-scale gasification, which consists of an atmospheric bubbling fluidized-bed gasifier connected to a gas filter and a reformer/gas residence time tube (Figure 4.1). The so-called gas residence time tube is an electrically heated pipe that can also be operated as a catalytic reformer. In this work, our interest was on the gasification step and subsequent filtration, so the reformer was used as a gas residence time tube. The maximum fuel feeding rate is 5 kg/h, and the gasification tests can be conducted with air, air/steam, oxygen/steam or at steam-blown mode.

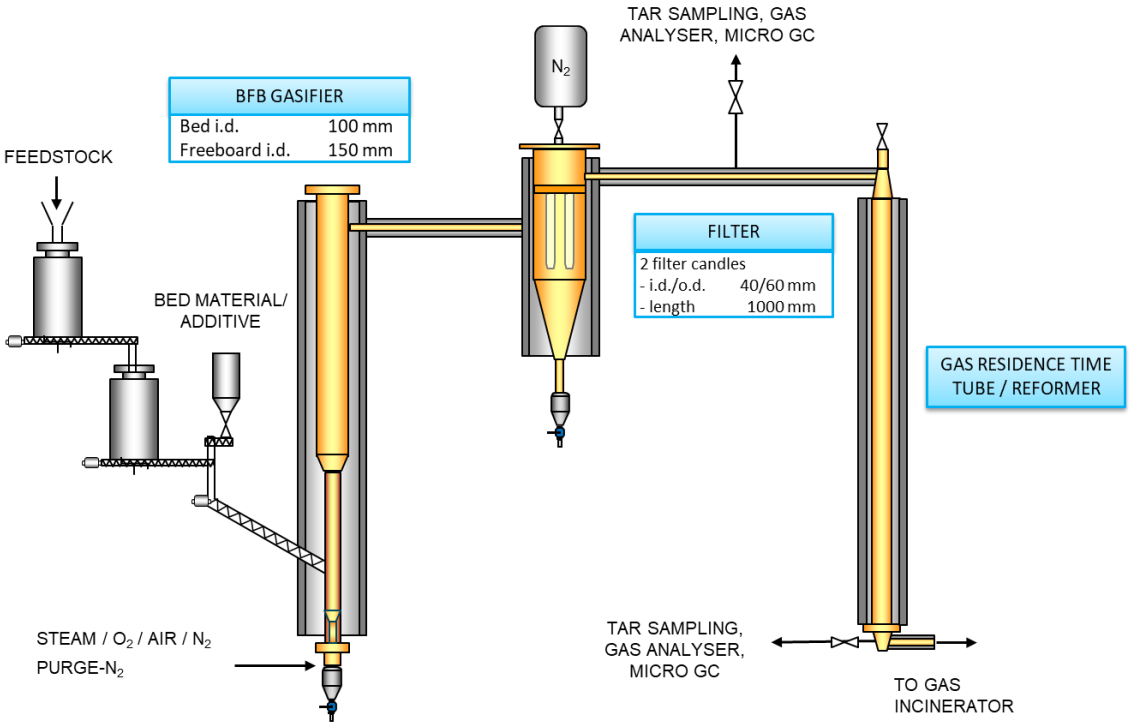

Figure 4.1. *VTT's bench-scale, atmospheric pressure gasification test facility BFB100.*

The gasifier (bottom bed i.d. 100 mm, freeboard i.d. 150 mm) is surrounded by electrically heated ovens, which compensate thermal losses and supply extra heat to operate at a pre-set gasification temperature. Gasifying agents (steam, air, nitrogen) are introduced into the reactor's bottom through a multi orifice plate distributor and controlled through mass flows. The gases are pre-heated before

entering the reactor and, in this study, water was introduced directly with the pre-heated air to generate steam (since the steam concentration was only about 20 vol-% of fluidizing gases).

Temperature is continuously measured in the gasifier at different points in the bottom bed (125, 225 and 425 mm from the plate distributor) and in the freeboard (1270 and 1470 mm from the plate distributor). Pressure drop in the bed and distributor plate; freeboard and the whole reactor are continuously monitored. A small amount of purge nitrogen (about 7 vol-% of the total feed gas flow) is fed with the fuel for inertization and pressure stabilization purposes. Adding this nitrogen aims to flush the measurement lines (pressure or temperature) in the bed and prevent the loss of bed material into these lines. Bed material is added as a batch at the beginning of each experiment.

The fuel feeding system is composed of two subsequent tanks and feeding screws. The first one is located at the tank bottom and adjusts the fuel feeding rate. The second feeding screw adjusts the first screw speed, and it is located inside water-cooled jackets. Fuel feeding is located 101 mm above the plate distributor.

The hot gas filter downstream of the reactor separates the elutriated bed material and fly ashes from the gas. Inside the vessel, two rigid ceramic filter elements (Pall Corporation: Pall Dia-Schumalith 10-20 KK). The filter is electrically heated with two-zone oven (upper and lower zone), with a maximum temperature of 850°C. The solids are detached from the filter through nitrogen pulses (2 bars and 150 ms) and then collected in the bottom container. Temperature is measured both at filter inlet ("dirty" side) and outlet ("clean" side).

The dust-free gas then flows into a gas residence time tube (i.d. 100 mm) covered by electrically heated ovens. It was maintained at 350 – 400°C to prevent tar condensation in the pipeline. The gas is then incinerated for final combustion.

4.4.2. Materials

4.4.2.1. Feedstock and bed materials

Crushed Refuse Derived Fuel (RDF) pellets were used as feedstock. The original pellets (2 cm of diameter) were ground with Weima WL 2 Labor crusher (with a 15 mm sieve). The final RDF particles were ≤ 15 mm. The proximate and ultimate analyses of the feedstock are presented in Table 4.1.

Table 4.1. *Proximate and ultimate analysis of the feedstock*

Feedstock	**RDF pellets**	**Error (+/-), %**	**Standard applied**
Moisture content, wt%	4.1	2	*SFS-EN ISO 18134-2*
LHV, MJ/kg (dry)*	23.9	1	-
Proximate analysis, wt% (d.b.)			
Volatile matter	80.5	1	*SFS-EN ISO 18123*
Fixed carbon	10.2	3	*Calculated*
Ash (550 °C)	9.3	2	*SFS-EN ISO 18122*
Ultimate analysis, wt% (d.b.)			
C	55.3	1	*SFS-EN ISO 16948*
H	7.9	2	*SFS-EN ISO 16948*
N	0.5	7	*SFS-EN ISO 16948*
S	0.1	6	*ASTM D 4239 (mod), SFS-EN ISO 16994*
Cl	0.7	13	*SFS-EN ISO 10304-1*
O *(cal. as difference)*	26.3	3	*Calculated*
Ash (550 °C)	9.3	2	*SFS-EN ISO 18122*

**LHV was calculated based on fuel composition* (73)

Table 4.2 contains the composition of RDF pellets in inorganic elements in mg/kg of dry fuel. Major elements were measured by Inductively Coupled Plasma Optical Emission Spectroscopy (ICP-OES) by applying the SFS-EN ISO 17294-2 standard (74). Minor elements by ICP Mass Spectroscopy (ICP-MS), using the SFS-EN ISO 11885 standard (75). By following the standards, the samples were digested using an acid solution.

Table 4.2. *RDF composition in major and minor inorganic elements (mg/kg of dry fuel)*

Major elements, mg/kg dry fuel		**Error (+/-), mg/kg dry fuel**	**Error (+/-), %**
Al	17600.0	200.0	1
Ba	1150.0	50.0	4
Ca	2550.0	50.0	2
Fe	1700.0	10.0	1
K	415.0	15.0	4
Mg	1150.0	50.0	4
Na	7450.0	550.0	7
P	8150.0	450.0	6
Si	2050.0	50.0	2
Ti	210	10.0	5
Minor elements, mg/kg dry fuel			
As	1.0	0.1	10
Cd	3.4	2.0	59
Co	7.1	0.8	11
Cr	58.5	28.5	49
Cu	43.0	1.0	2
Hg	2.2	0.1	5
Mn	47.0	4.0	9
Mo	4.3	1.1	26
Ni	6.3	0.7	11
Pb	35.0	3.0	9
Rb	4.3	0.1	2
Sb	31.5	8.5	27
Sn	7.4	0.4	5
Sr	39.0	0.1	<1
V	2.9	0.1	3
Zn	215.0	45.0	21

Silica sand and dolomite (Myanit B by Björka Mineral) were used as bed material, with a particle size of ≤ 0.25 mm and 0.28 – 0.55 mm, respectively. The Sauter mean diameter (d_{32}) of the RDF particles is 10 mm, while the sand d_{32} is 0.18 mm and the dolomite d_{32} is 0.40 mm, with a minimum fluidization velocity (u_{mf}) of 0.016 m/s for sand and 0.099 m/s for dolomite at 25°C, calculated using Wen and Yu's correlation (76).

4.4.2.2. Filter elements

Pall Dia-Schumalith 10-20 KK filter elements (o.d./i.d. 60/40 mm, length 1000 mm) by Pall Corporation were employed in this work. It consists of a coarser support body (material: SL 20) with a porosity of 38% and a dense membrane (material: mullite grains) as a top layer (77).

4.4.3. Sampling and analytical methods

The composition of the product gas was measured after the filter unit (Figure 4.1). The sampling lines were heated to 350-400°C. Continuous gas analyser (ABB AO2020) was used to measure CO, CO_2, H_2, CH_4 and O_2. Non-dispersive infrared absorption was used to measure CO, CO_2 and CH_4. H_2 and O_2 were measured by thermal conductivity and a magneto-mechanical oxygen analyser, respectively. The hot gas filter's sampling line to the gas analyser consisted of a condenser and a filter. The condenser is used to cool the gas to 2°C to condense the heaviest tar compounds and water vapor (78). Afterwards, the gas is led to the filter, consisting of a filter case filled with cotton wool.

After the analyser (ABB AO2020), the gas was transferred through a Teflon tube to an online micro gas chromatograph (HP3000, equipped with a TC detector), which was used to analyse CO, CO_2, O_2, N_2 and light hydrocarbons (C_2 – C_5 hydrocarbons). Samples were taken every 7 min. The continuous gas analyser is focused on monitoring the process's stability, while the micro gas chromatographs results are used to calculate the mass balances discussed in the next section.

Tars were sampled according to the European Tar protocol (79). Isopropanol was used as an absorbent. Samples were analysed by a gas chromatograph (Agilent 6890A, column: Agilent 19091B-112 Ultra 2) equipped with a Flame Ionization Detector (FID) detector, for benzene and compounds up to coronene ($C_{24}H_{12}$, 300.35g/mol). A complete list of the 52 compounds analysed is available in the Appendix section. Water content was determined from the tar samples using a gas chromatograph (HP 5890 series II, column: PoraPLOT U) equipped with a TC detector.

Gaseous pollutants such as H_2S, COS, NH_3, HCN and HCl were also analysed during the tests, all collected after the filter unit. Ammonia (NH_3), hydrogen cyanide (HCN) and hydrogen chloride (HCl) were collected in a set of impingers. A gas stream of 5-6 l/min was drawn from the process and led through six impinger bottles placed in series. The first three bottles were filled with their proper capture solution for each substance, described separately below. The last three impingers were washing bottles used to extract water and tars from the gas for all substances. The fourth impinger contained 70 ml of isopropanol, the fifth one was filled with 70 ml of isopropanol and glass beads, and the last impinger contained only glass beads. The first four impingers were placed in an ice/water bath (< 5 °C) and the last two in an ice/water/NaCl bath (< -15 °C).

For ammonia capture, the first three impingers contained 70 ml (each) of 5% H_2SO_4 solution. The first three impingers' contents were combined after sampling, and the glassware was also rinsed with a small amount of 5% H_2SO_4 solution and added to the collected sample. The final sample was preserved in a tightly sealed glass bottle before analysis (away from sunlight and below 5 °C). The pH of the sample was kept below 2. The sample was analysed using the Kjeldahl distillation method according to ASTM D1426-93 standard.

For hydrogen cyanide, the first three bottles were filled with 70 ml of 5% NaOH solution (each). The pH of the washing liquid was maintained at above 10.5 during sampling. The three impingers' contents were combined after sampling, and the glassware was also rinsed with a small amount of 5% NaOH solution, which was added to the final sample. The sample was analysed within 6 hours of sampling to prevent cyanide from reacting further with sulphur compounds. The sample was analysed with a static headspace method using a gas chromatograph equipped with FID.

Hydrogen chloride sampling was performed by using six impingers. The first three impingers were filled with 100 ml of ion-exchanged water and glass beads (each). The fourth and the fifth impingers contained 70 ml of isopropanol and glass beads each, and the sixth one contained only glass beads. The contents of the first three impingers were combined after sampling. The quartz probe was also washed with ion-exchanged water, and the washing liquid was poured into the sample bottle. The sample was preserved below 5°C (and away from sunlight) before analysis. The sample was analysed by ICP-OES.

Gaseous H_2S and COS samples were collected in Teflon gas bags and analysed for sulphur compounds using a gas chromatograph equipped with FPD (Agilent 7890B) and analysed within a few hours of sampling. Note that H_2S was also measured online using Dräger tubes, but this method is not as accurate as offline methods. Thus, sulphur elemental mass balances were performed using offline results.

4.4.4. Description of experiments and calculation methods

The gasification tests were conducted under air/N_2 and air/steam conditions with crushed RDF pellets as feedstock and sand and dolomite (Myanit B) as bed materials. All tests were carried out at the same gasifier temperature, using varying the Equivalence Ratio (ER), bed material, hot filter temperature

and fluidizing agent. In each test, one of these parameters was varied separately to appreciate their effect on the results. The operating conditions are summarized in Table 4.3.

Table 4.3. *Target conditions in the air+N_2 and steam/air gasification experiments*

Gasification experiments	**1**	**2**	**3**	**4**	**5**	**6**
Feedstock	RDF	RDF	RDF	RDF	RDF	RDF
Particle size, mm	≤ 15	≤ 15	≤ 15	≤ 15	≤ 15	≤ 15
Bed material	Sand	Sand	Sand	Sand	Sand	Dolomite
Particle size, mm	0.15 - 0.25	0.15 - 0.25	0.15 - 0.25	0.15 - 0.25	0.15 - 0.25	0.28 - 0.56
Target conditions						
Bed temperature, °C	850	850	850	850	850	850
Freeboard temperature, °C	850	850	850	850	850	850
Filter temperature, °C	450	450	450	550	450	450
Fluidizing velocity*, m/s	0.40	0.40	0.40	0.40	0.40	0.40
ER	0.30	0.25	0.30	0.30	0.25	0.30
steam in fluidizing gases, vol-%	-	0.20	-	-	-	-
Steam-to-fuel feed ratio, kg H2O/kg fuel (daf)	-	0.40	-	-	-	-
Target compounds to be measured	N, S	N, S	Cl	Cl	N, S	N, S

daf: dry and ash-free
**calculated*

Six gasification tests were conducted with fuel particle size ≤15mm, and each experiment lasted at least 4h at steady state except for experiment 6, which lasted only 3h. The filter temperature was kept at 450°C, except for one test, in which it was increased to 550°C.

Before each experiment, the rig was electrically heated up close to the test target temperature in nitrogen atmosphere. The bed material was added at the beginning of each test, and a static bed height was maintained at 35 cm in all tests. For the test using dolomite, the loss of solids during calcination was considered and, thus, more bed material was added, so the bed height was 35 cm after calcination. The dolomite was calcinated in-situ before the test start, by adding a batch of the bed material (dolomite) in the reactor that was maintained there for approximately 2h at 800°C. The CO_2 released was monitored and when the CO_2 stopped being detected we proceeded to the experiment.

No additional bed material was added during the tests using sand as bed material. Fuel feeding was initiated to start the gasification experiments, and the feed gas was switched to the fluidization agent selected for each test (air/N_2, air/steam). The operation conditions were kept stable during the tests. Every hour the filter was pulse cleaned by the addition of nitrogen. The particulate matter entrained by the gas (fly ash and bed material) were collected at a nitrogen pressurized vessel to cool, and then,

the detached solids were stored for further analysis. The bottom ash was removed only after the experiment completion and the cooling process in N_2 atmosphere. Both filter and bottom ash samples were analysed in C, H, N, O, S, Cl, and ash for all tests.

Nevertheless, for test 6, bottom ash results cannot be used directly, as C comes from the $CaCO_3$ used as bed material. Trace elements (Table 5) were measured in both filter and bottom ash samples for tests 3 and 4. After each test run and the removal of the bed material, the remaining carbon-containing matter in the filter was oxidized with nitrogen/air mixture. The oxidation data was used to calculate the carbon release in the filter.

Mass balance calculations were conducted for all experiments using average values from the measured data (solid and gas streams). The dry gas flow rate was calculated from nitrogen balance in all tests. The water content in gas was calculated by measuring the water content in the tar samples and hydrogen balance. Carbon conversion to gas and tars was calculated by two methods: (1) directly by the C content in gas and tars divided by the total carbon input in the fuel, and (2) indirectly by the total carbon input in the fuel, deducting the carbon losses (C in fly ash, bottom ash, and residual in the gasifier and on the filter), and dividing it by the total carbon in the fuel. Average dust content in gas (g/s) was calculated by dividing the mass of the accumulated dust in the filter (g), divided by the setpoint duration (s).

The cold gas efficiency, CGE (lower heating value in the syngas/lower heating value of the fuel) and the hot gas efficiency, HGE, (sensible energy plus the lower heating value of the syngas/lower heating value of the fuel) were calculated for all tests. The species considered for calculating the syngas lower heating value were CO, CO_2, H_2, CH_4, C_2H_2, C_2H_4, C_2H_6, C_4H_{10} (n-butane, representing C3 – C5 fraction).

4.4.5. Tars classification

Tars were classified based on their molecular weight, divided into four groups: (1) benzene, (2) light tars, (3) naphthalene and (4) heavier tars: tars heavier than naphthalene, up to coronene. GC-unidentified tars were also included as they were present in high amounts and were described as

"unknown". The total tars concentration is the sum of GC-identified and unidentified tar compounds (78).

4.4.6. Species containing nitrogen, sulphur, and chlorine

The following species were sampled and quantified in the syngas: NH_3, HCN, H_2S, COS and HCl. All samples were taken after the filter unit. Nitrogen species were measured during experiments 1, 2, 5 and 6; while HCl was measured only for experiments 3 and 4. Three samples of NH_3, HCN and HCl; four samples of H_2S and COS were taken in each test.

4.4.7. Fate of trace elements in solid streams

Filter dust and bottom ashes were analysed in tests 3 and 4. For each test, two samples of filter dust, collected at different times, were analysed. Only one sample of bottom ash was analysed for each experiment since bottom ashes are collected at the end of the experiment.

The fate of trace elements for experiments 3 and 4 was calculated by the mass balance of the elements entering the reactor in the fuel (F) and the bed material (BM) and leaving the reactor as filter ash (FA) and bottom ash (BA). The conversion into filter ash and bottom ash was calculated by the ratio of a specific element leaving the reactor in FA or BA and the total amount entered in the reactor.

$$E_i = F_i + BM_i \quad \textbf{(Eq. 4.1)}$$

$$E_i = Q \times h \times C_{F_i} + BM \times C_{BM_i} \quad \textbf{(Eq. 4.2)}$$

$$Conversion = \left(\frac{Ash \times C_{ash_i}}{E_i}\right) \times 100\% \quad \textbf{(Eq. 4.3)}$$

The conversion in percentage is calculated by the amount of ash (filter/bottom), the concentration of the element *i* in the referred ash, divided by the total amount of element *i* that entered the reactor. Both concentrations of ashes (filter/bottom) were taken at the end of the experiment. It is expected that the

difference between 100% and the sum of conversions into filter and bottom ashes is the conversion to the gaseous phase that was not retained in the filter.

The Enrichment Factor (EF) is used to quantify the relative volatile behaviour of trace elements (15)(19)(80)(81) and is defined as:

$$EF = \left(\frac{C_{ash\ i}}{C_{F_i}}\right) \times \frac{\%ash\ in\ the\ fuel}{100} \qquad \textbf{(Eq. 4.4)}$$

4.5. Results and discussion

The main operating conditions and results for the six tests conducted are summarized in Table 4.4.

Table 4.4. *Main operating conditions in steam and air/steam experiments with wood and bark pellets*

TEST RUN	**1**	**2**	**3**	**4**	**5**	**6**
GASIFICATION	air+N_2	air+steam	air+N_2	air+N_2	air+N_2	air+N_2
Bed material	Sand	Sand	Sand	Sand	Sand	dolomite
GASIFIER						
Fuel feed rate, kg/s x 10^6	422	464	374	374	463	406
Air feed rate, kg/s x 10^6	915	861	915	915	861	915
Nitrogen feed rate, kg/s x 10^6	154	0	154	154	208	154
Steam feed rate, kg/s x 10^6	0	133	0	0	0	0
Purge nitrogen feed rate, kg/s x 10^6	202	202	202	202	201	202
Steam-to-fuel feed ratio, kg/kg-daf	0.00	0.33	0.00	0.00	0.00	0.00
Bed/freeboard temperature, °C	847 / 849	854 / 854	846 / 849	852 / 848	850 / 851	859 / 849
Fluidizing velocity, m/s	0.42	0.42	0.42	0.42	0.42	0.42
Gas velocity in freeboard, m/s	0.30	0.31	0.29	0.29	0.31	0.29
Equivalence ratio (ER)	0.28	0.24	0.32	0.32	0.25	0.30
Carbon conversion to gas and tar, % **	97.9	97.9	98.3	98.4	97.6	96.6
FILTER						
Filter temperature, °C (inlet/outlet)	457 / 444	457 / 442	454 / 439	553 / 532	455 / 441	455 / 443
Face velocity on the filter, cm/s	0.9	0.9	0.9	1.0	0.9	0.9
Filter dust, g/h	97	109	96	96	117	228
DRY PRODUCT GAS COMPOSITION						
After filter, vol-% (purge N_2 -free) +						
CO	9.9	9.4	10.0	9.3	11.3	6.6
CO_2	13.4	14.7	13.6	14.0	13.3	15.7
H_2	8.2	10.9	7.0	7.4	7.9	7.1
N_2	60.2	55.7	62.3	62.7	58.0	62.0
CH_4	5.1	5.8	4.5	4.2	5.7	4.9
C_2H_2	0.1	0.2	0.1	0.1	0.3	0.1
C_2H_4	2.8	2.9	2.4	2.2	3.0	3.1
C_2H_6	0.10	0.11	0.07	0.07	0.09	0.10
C_3-C_5 hydrocarbons	0.03	0.02	0.11	0.05	0.22	0.13
NH_3, ppmv*+	1638	2088	nm	nm	1712	2165
HCN, ppmv *+	104	125	nm	nm	213	61
H_2S, ppmv*+	79	182	nm	nm	161	130
COS, ppmv *+	11	15	nm	nm	15	9
HCl, ppmv *+	nm	nm	49	172	nm	nm
H_2O content in wet gas, vol-% - After filter (measured)	11.1	21.3	11.2	10.6	12.3	10.0
Gas flow rate						
Dry gas flow rate, m^3n/h +	3.4	3.4	3.3	3.2	3.3	3.3
Wet gas flow rate, m^3n/h +	3.7	4.3	3.7	3.6	3.7	3.6

***** *average*

****** *Calculated from Carbon losses*

In experiments 1 and 3-6, nitrogen was added as a gasification agent to reach the desired gasification velocity, since airflow is a limiting factor (maximum is 1 g/s).

Carbon conversion (CC) was high for all experiments (96.6 – 98.4 %) and seemed to increase with ER and steam addition, although the small variation makes it difficult to obtain clear trends. The CC was lowest for the experiment using dolomite as bed material.

Carbon, hydrogen, nitrogen and oxygen, balances closures were within +-3%. Sulphur elemental balance varied from -91% (test 4) to – 38% (test 2). Chlorine elemental balance varied from -64% (test 1) to -21% (test 6). The negative values mean that the respective percentage is missing in the products considered in the balance, respect to the quantity of element entering in the fuel. For both sulphur and chlorine, this is related to their lower content in the fuel and the feedstock heterogeneity, causing their measurement to be more sensitive to variations. Ash balances (out/in) did not reach 100% in experiments 1 to 5, using sand as bed material. In test 6, ash balance was 150%, in which dolomite was used as bed material. The negative deviation in experiments 1 to 5 is possibly related to the fact that some dust may have stuck in the filter vessel's bottom cone section.

4.3.1. Analysis of syngas composition and gasification performance

Figure 4.2 below shows the tendencies of the main species' yields in the syngas (mg/g of daf fuel) with the ER. The yields of the different species represent the amount of those species expressed per unit of dry and ash free fuel. The authors intentionally represent this per unit of dry and ash free fuel to facilitate comparison between fuels and the scaling up process (47,68,82).

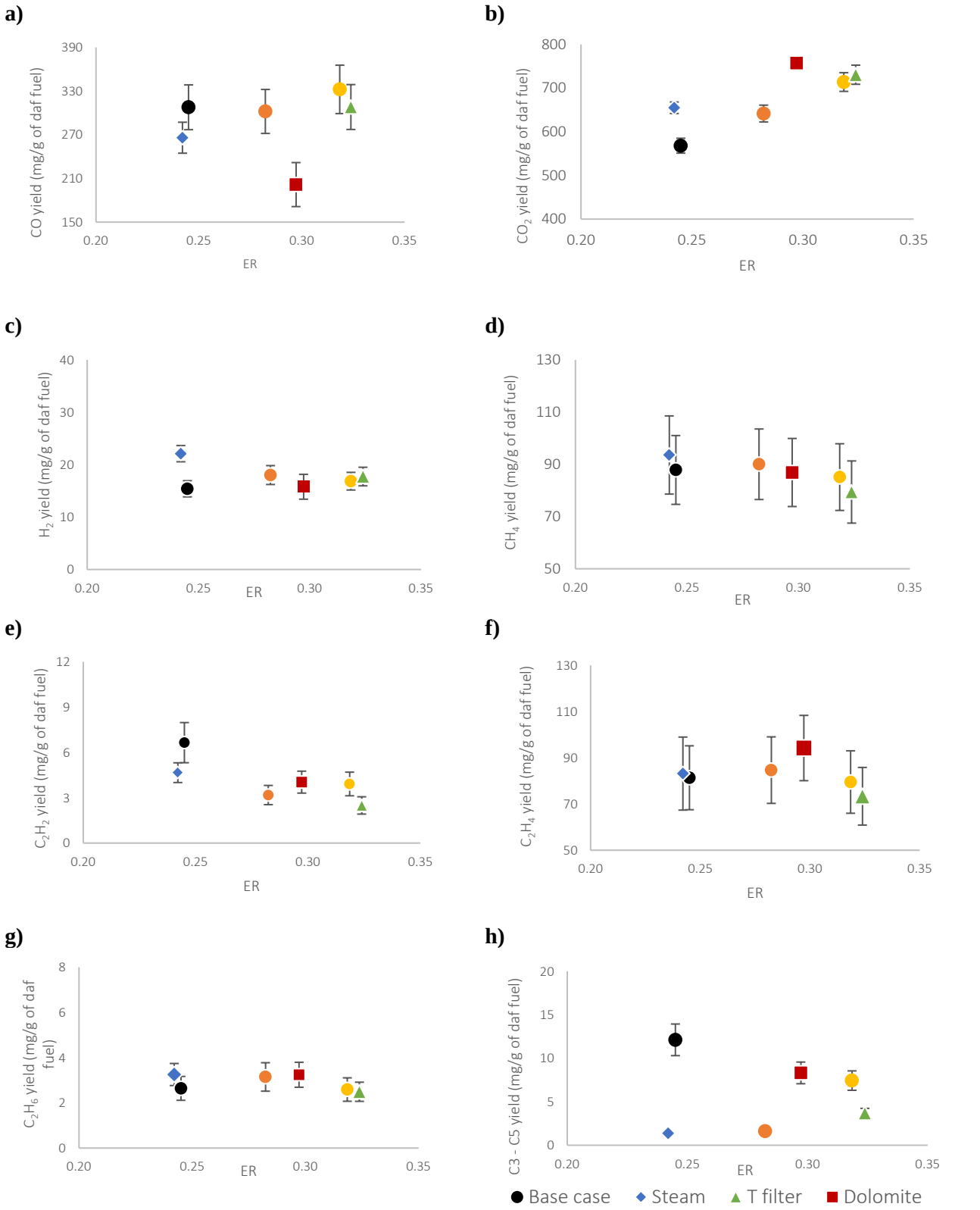

Figure 4.2. *The yield of major components as a function of ER:* ***a)*** *CO,* ***b)*** *CO_2,* ***c)*** *H_2,* ***d)*** *CH_4,* ***e)*** *C_2H_2,* ***f)*** *C_2H_4,* ***g)*** *C_2H_6 and* ***h)*** *C3-C5. All experiments were performed at 850°C. The base case (circles) operates using air/N_2 as gasification agent, sand as bed material and filter temperature at 450°C. The other tests vary in only one parameter from it: steam (diamond); higher filter temperature (550°C, triangle) and dolomite as bed material (square). Test number (1 – 6) can be detected by colour: (1) orange, (2) blue, (3) yellow, (4) green, (5) black and (6) red.*

The increase in ER slightly increased the yield of CO (Figure 4.3a) but showed a higher and apparent increase in the CO_2 yield (Figure 3b) due to the greater char oxidation (68)(83). Figures 4.3a and 4.3b show that while steam decreased the CO, it increased the CO_2 yields. Steam shifts the WGS reaction towards the production of CO_2 and H_2 (84). Regarding the bed material, Figures 3a and 3b show that the use of dolomite ($CaMg(CO_3)_2$) decreased the CO yield, while it increased the yield of CO_2.

In general, an increase of ER is expected to result in lower light gas yields, since it increases their combustion by adding more oxygen (68). Figure 2c shows that it is impossible to define a tendency for hydrogen yield and ER change. The use of dolomite as bed material seemed not to affect hydrogen yield either. On the other hand, steam use gave higher H_2 yield, as expected by the shift in the WGS reaction.

Based on the measured yields, the gasification performance was characterized by calculating the LHV of the gas and the cold and hot gas efficiencies (CGE and HGE). Figure 4.3 shows the LHV of the product gas and the gasification efficiency as a function of ER.

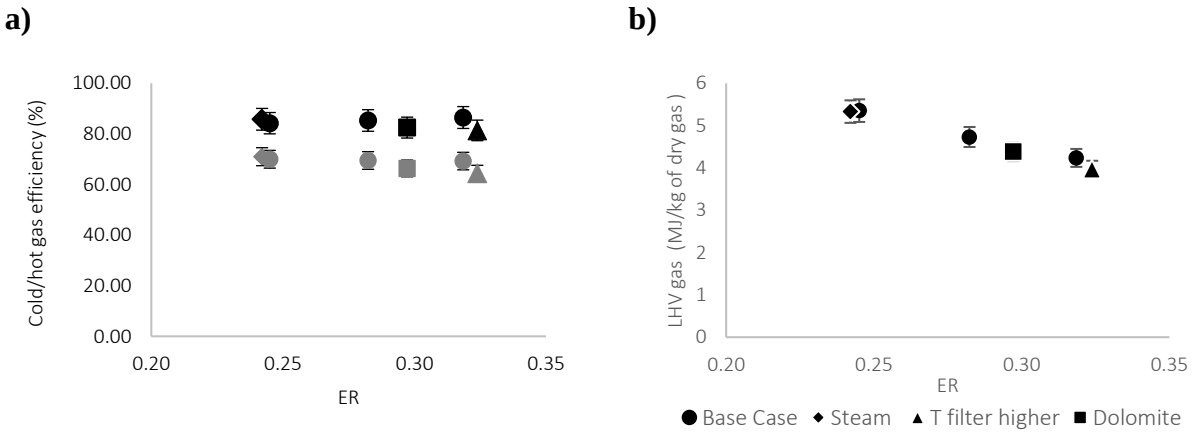

Figure 4.3. a) *CGE (grey) and HGE (black) and* ***b)*** *LHV of the product gas as function of ER. Legend: base case (circle), steam (diamond), triangle (T_{filter} higher) and dolomite (square).*

LHV of the product gas varies from 4.0 – 5.3 MJ/kg of dry gas. Results shown in Figure 4.3a shows a tendency of a linear decrease in the LHV with ER increase, which is explained by the higher gas combustion with the increase in oxygen and the gas dilution with the increase in N_2 (68)(28). The steam addition, filter temperature and bed material did neither impact the LHV nor gasification efficiency. The CGE varies from 64.4 – 71.0% and, in agreement with previous observations, the CGE

decreases with ER (68)(85). The same tendency is observed for the HGE, which varied from 81.4 – 85.8%.

4.3.2. Tars

The average concentration (mg/m^{3}n) of different tar groups and benzene sampled after the filter is presented in Figure 4. Tars were separated in the following groups: light, heavier, unknown, naphthalene and benzene (78).

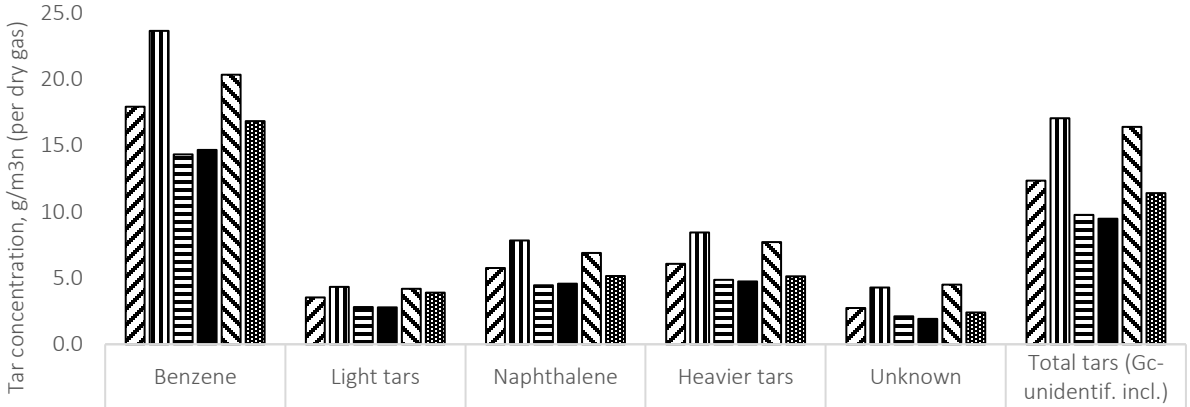

	Benzene	Light tars	Naphthalene	Heavier tars	Unknown	Total tars (Gc-unidentif. incl.)
Test 1	17.9	3.5	5.8	6.1	2.7	12.3
Test 2	23.6	4.3	7.8	8.4	4.3	17.0
Test 3	14.3	2.8	4.5	4.8	2.1	9.8
Test 4	14.7	2.8	4.6	4.8	1.9	9.5
Test 5	20.3	4.2	6.9	7.7	4.5	16.4
Test 6	16.8	3.9	5.2	5.1	2.4	11.4

Figure 4.4. *The concentration of different tar groups and benzene after the filter in air/steam and air+N_2 gasification experiments with RDF and sand or dolomite (Myanit B) as bed material. Total tars stands for the sum of light, heavier and unknown tar groups.*

Benzene was the predominant species in all experiments (Figure 4), followed by heavier tars, naphthalene, light tars, and unknown groups. Due to the lower presence of oxygen, the lower the ER, the higher the yield of tars produced. Even though in-bed dolomite is expected to decrease tar concentration due to its catalytic effect (78)(86)(28), the effect of dolomite decreasing the tars was not observed in our experiment (6, ER=0.3), comparing with experiments 1 and 3 with similar conditions. More experiments should be conducted to evaluate the catalytic effect of dolomite on tar cracking.

Different filter temperatures were set in experiments 3 (T_{filter} = 450°C) and 4 (T_{filter} = 550°C) at the same ER (0.32). At lower filter temperature, it is expected that the heavier tars may condense more in the filter. Nevertheless, the reduction of tar concentrations has been only reported at a higher filter temperature (87). In our experiments, the tars concentrations in tests 3 and 4 were very similar, since conditions are the same (T and ER) and the filter temperature gap was only 100°C.

4.3.3. Conversion of fuel-N

Figure 4.5 shows the fuel-N conversion into filter dust-N, tar-N, HCN and NH_3. HCN and NH_3 are expected to be the main species derived from fuel-N. Quantification of NOx and HNCO were not included in the paper, because NOx is not formed in reducing conditions at large scale and HNCO is not stable so it would ultimately be transformed to NH_3 and HCN (88)(41).

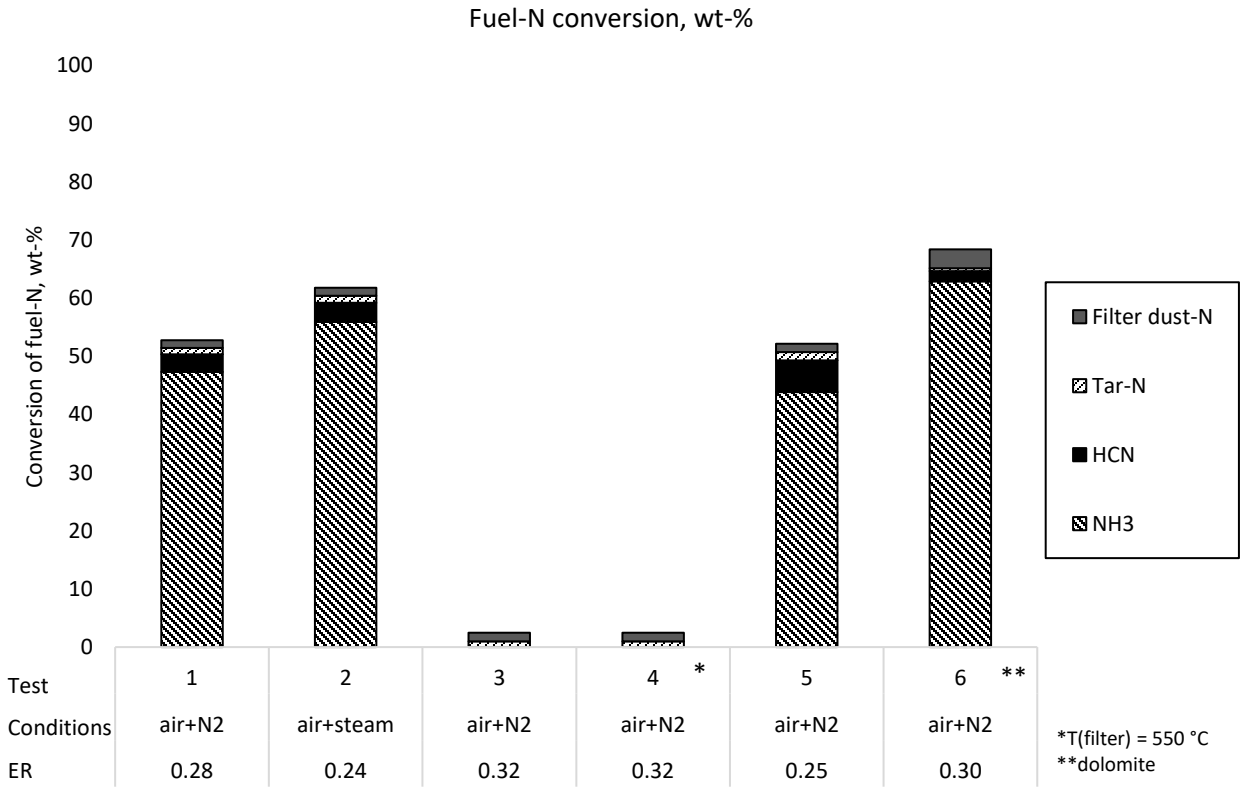

Figure 4.5. *Conversion of fuel-N (wt-%) into N_2 (calculated by difference), filter dust-N, tar-N, HCN and NH_3.*

In experiments 3 and 4 ammonia and hydrogen cyanide were not sampled. In all experiments in which ammonia was measured (1, 2, 5 and 6), it was the main measured product from the conversion of fuel-

N. Ammonia concentration was much more significant than hydrogen cyanide, as expected for several types of feedstocks (4).

Nevertheless, higher concentrations of HCN than NH_3 during solid recovered fuel (SRF) gasification have been reported (33). Although the chemistry of Fuel-N evolution during gasification is not yet completely understood, it is known that HCN is formed during the pyrolytic conversion of pyrrolic and pyridinic forms (from polyamides and polyacrylonitriles, present in textile). In contrast, NH_3 is formed from amino-groups (biomass). RDF is a mix of different fractions - for instance, organic, plastic and textile – the Fuel-N conversion from different sources must be understood. In this work, ammonia was the predominant species probably due to the high content in organic matter in the fuel.

Besides the effect of the feedstock, experimental conditions, such as temperature, residence time, ER, fuel feeding location and heating rate also affect Fuel-N conversion (33)(89)(90). By comparing Tests 1 and 5, the ER increase is found to boost ammonia production, probably concerning higher char conversion, in agreement with previous findings (65)(91).

The addition of steam (test 2) increased the ammonia production, due to the higher availability of hydrogen. HCN can react with H_2O to produce ammonia and CO, and also HNCO (isocyanic acid) can react with steam to form ammonia and CO_2, explaining the higher NH_3 content found in this experiment (90)(92)(93)(94)(95). The conversion of fuel-N into HCN decreased with the increase in ER. This may be explained by the ammonia production being favored over HCN when more oxygen is available.

Fuel-N conversion into ammonia was highest in experiment 6, in which dolomite was used as bed material, while the conversion into HCN was the lowest for this test. Dolomite has also increased NH3 and decreased HCN in peat gasification in fluidized bed (96). This seems to be related to the catalytic properties of calcined dolomite in converting char and producing ammonia, as calcium oxide (CaO) is known to enhance the conversion of HCN into NH_3 (90)(95).

Regarding the filter dust, it increases when using dolomite as bed material, and this can be related to smaller particles being formed during the gasification, due to attrition, and then being elutriated from the bed and collected in the filter, which could explain the higher amount of filter dust-N (36). The conversion into tar-N was the lowest in experiment 6 (0.5 wt-%), while it did not considerably vary in experiments 1 (1.3 wt-%), 2 (1.4 wt-%) and 3 (1.4 wt-%).

This result may be related to the lower tar production in experiment 6 due to dolomite's catalytic properties for tar conversion, even though a reduction of total tars was not observed in experiment 6 (see Figure 4). For instance, two N-tar compounds – benzonitrile and quinoline - showed lower concentration in experiment 6 compared to all other experiments (see Supporting Information). Furthermore, the increase in filter temperature from 450°C (test 3) to 550°C (test 4) did not affect fuel-N conversion into filter dust-N and tar-N.

4.3.4. Conversion of fuel-S

Figure 4.6 shows the fuel-S conversion into bottom ash-S, filter dust-S, COS and H_2S.

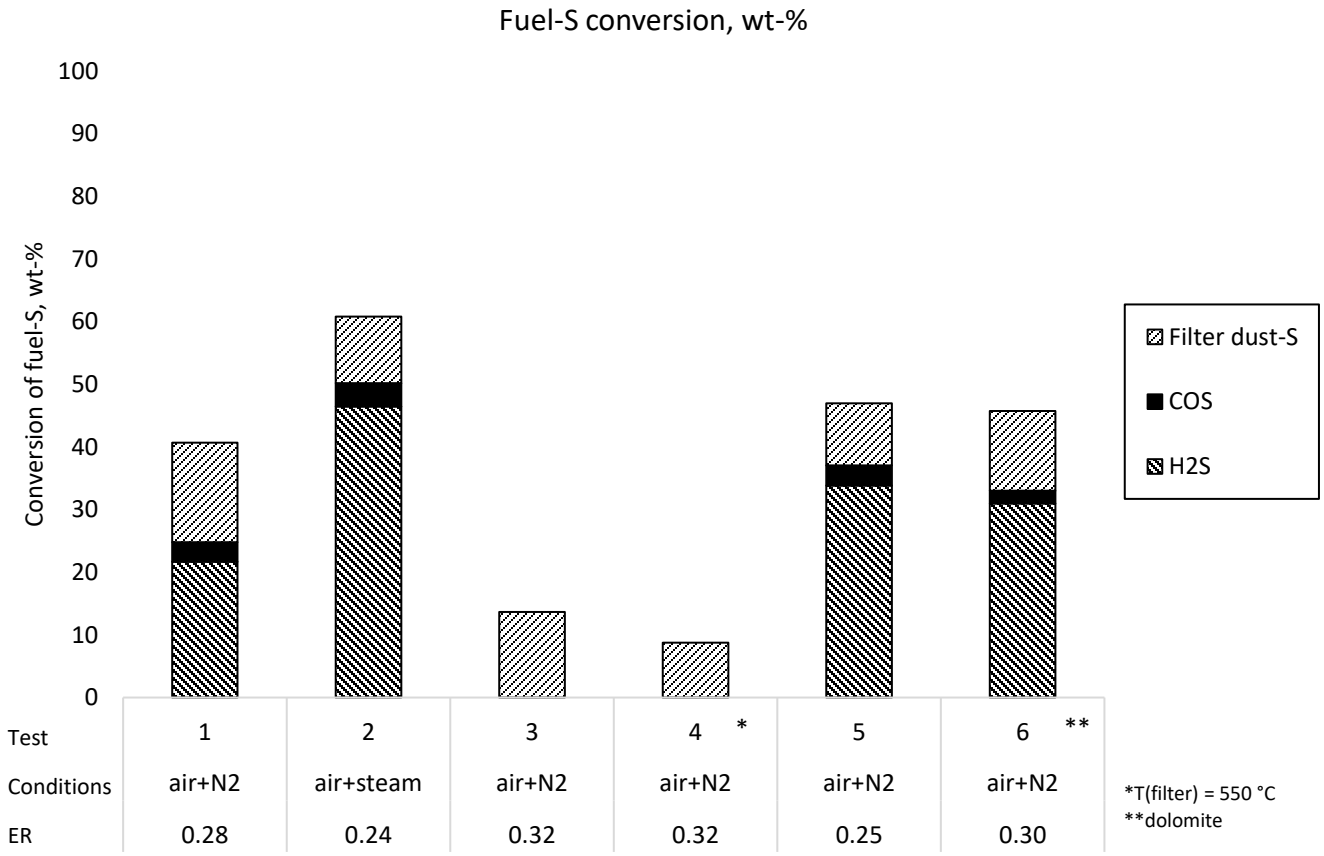

Figure 1.1. *Conversion of fuel-S (wt-%) into bottom ash-S, filter dust-S, COS and H_2S.*

Gaseous sulphur compounds were not measured in experiments 3 and 4. As expected, H_2S is the major sulphur species, and it is much higher than COS (8)(33)(90)(97)(98)(99).

The ER increase decreased the conversion into H_2S, while steam in the gasifying agent had the opposite effect, resulting in the highest H_2S concentration in the syngas (46.4 wt-% of the fuel-S ends up as H_2S) since more hydrogen was available for reaction.

About 3 wt-% of S in the fuel forms COS. This value did not seem to be affected by the ER. The results show that the formation of COS increased as steam is added to the gasification gas (3.7 wt-% in test 2), while it decreased when dolomite is used as bed material (2.0 wt-% in test 6) (100).

No sulphur was found retained in bottom ash in experiments 3 and 4, the only ones that analysed bottom-ash content. This may be related to the fact that fuel-S is generally converted at low temperatures during devolatilization stages (33). The increase in the filter temperature from 450°C to 550°C (test 4) decreased fuel-S conversion into filter dust-S, probably due to the lower capture of components-S in the filter.

The fuel-S conversion was not 100%, which is related to the S-containing species that were not measured, the filter ash that was not recovered and due to the sulphur retention in the reactor material and piping (65). Some additional S species may be formed, such as thiophene, and its derivates. However, their concentrations are very low and, thus, they are not included here (99). Extended information about the behaviour of sulphur compounds is available (65).

4.3.5. Conversion of fuel-Cl

Figure 4.7 shows the fuel-Cl conversion into bottom ash-Cl, filter dust-Cl and HCl.

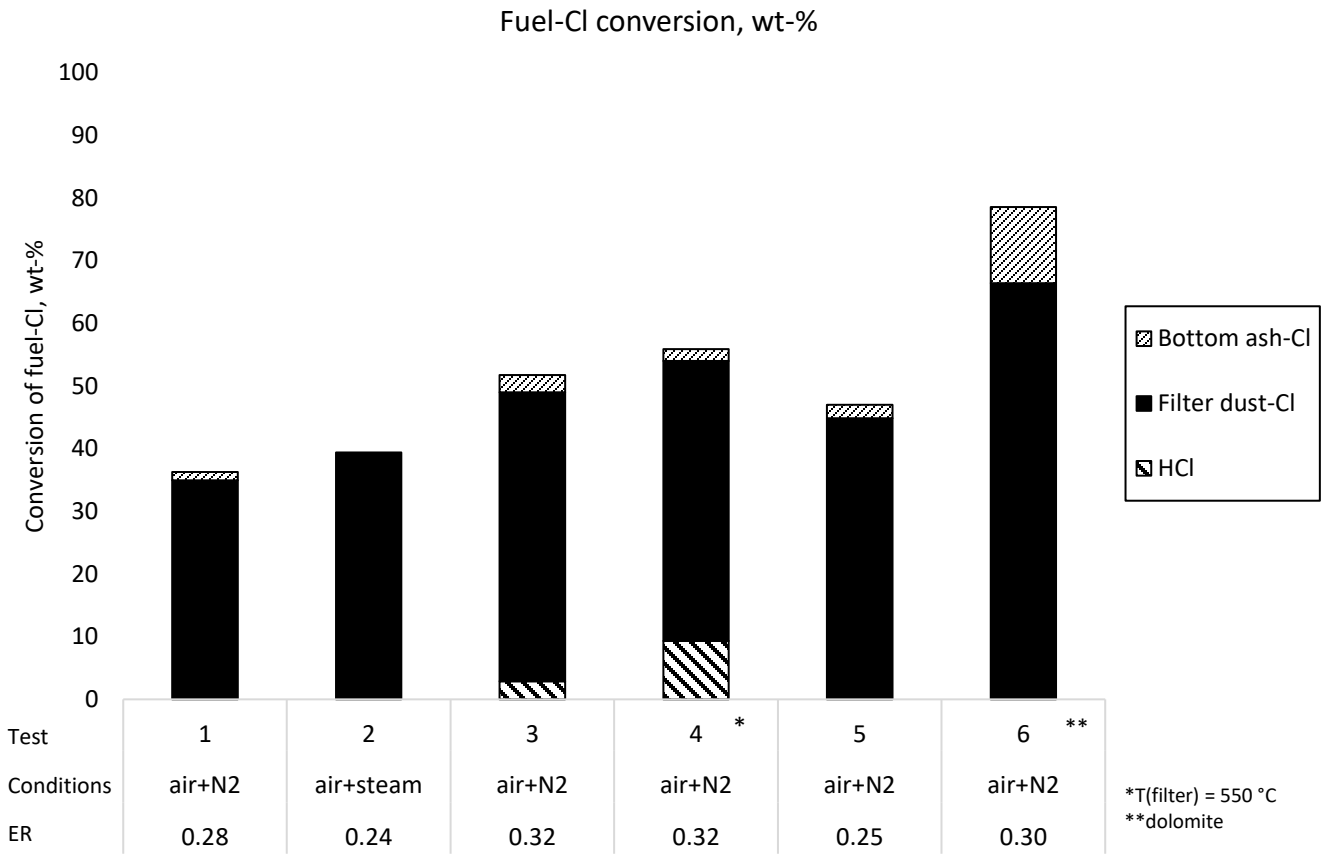

Figure 4.7. *Conversion of fuel-Cl (wt-%) into bottom ash-Cl, filter dust-Cl and HCl.*

HCl was measured only in experiments 3 and 4. In all experiments, most of fuel-Cl was converted into filter dust-Cl. During gasification, fuel-Cl is mostly released to the gas phase as HCl (some may also react with Na or K) forming NaCl or KCl (7). Afterwards, HCl can be retained in the filter (19)(24).

For instance, in experiment 4, where filter temperature is higher (550°C), more chlorine is found as HCl than in test 3 (filter temperature 450°C). Moreover, bottom ash-Cl and filter dust-Cl were highest in test 6 since dolomite retains Cl at solid phase ($CaCl_2$). The fuel-Cl conversion did not reach 100% in any experiment, which can be explained by the loss of filter ash material and mostly because of Cl's retention in the reactor walls and pipelines (65)(4). Extended information about the behaviour of chlorine compounds is available (65).

4.3.6. Conversion of trace elements

Table 4.5 contains the filter's composition and bottom ashes collected at the end of the experiments. Filter ash was analysed twice for each experiment (3 and 4), so the associated error is provided.

Table 4.5. *Filter and bottom ashes composition for experiments 3 and 4.*

Sample type	**Filter ash**				**Bottom ash**	
Test run	**3**	**Error (+/-)**	**4**	**Error (+/-)**	**3**	**4**
Ultimate analysis, wt-% (dry basis)						
C*	6.0	0.3	4.9	0.4	0.1	< 0.1
H*	0.3	0.0	0.2	0.1	< 0.1	< 0.1
N*	0.1	0.0	0.1	0.0	< 0.1	< 0.1
O (calc. as difference)	0.1	0.0	0.8	0.1	0.0	0.0
S**	0.3	0.0	0.2	0.0	<0.02	<0.02
Cl***	4.9	0.3	4.4	0.4	0.037	0.026
Ash 815 °C	93.3	0.3	93.9	0.4	99.9	100.0
Trace elements concentration						
Minor elements, mg/kg dry sample [+]						
As	11	0	11	0.9	2.3	2.2
Cd	10	0	2.6	0.1	0.14	0.11
Co	70	3	82	8.5	6.8	6.5
Cr	460	0	400	25	150	76
Cu	1100	0	970	130	240	20
Hg	<0.02	-	<0.02	0	<0.02	<0.02
Mn	640	0	740	50	340	350
Mo	45	0.5	44	4	3.8	2.9
Ni	320	5	270	10	61	21
Pb	580	15	190	10	14	14
Sb	290	20	170	15	33	21
Sn	120	5	64	5.5	11	7.6
Sr	350	5	400	30	200	210
V	44	1	48	1	23	23
Zn	1400	150	1300	195	250	240
Rb	93	2	110	6	63	65
Major elements, g/kg dry sample [++]						
Ca	142.0	3.0	138.0	4.5	24.3	23.3
Mg	14.4	0.3	13.8	0.5	3.6	3.5
Na	25.1	0.7	24.3	1.0	18.8	18.9
K	24.8	0.3	25.1	0.5	20.2	20.2
P	4.0	0.2	3.9	0.3	0.4	0.4
Fe	20.4	1.0	21.1	0.8	13.2	12.8
Al	95.7	1.7	99.0	6.0	49.0	48.8
Si	118.0	3.5	119.0	2.5	154.0	156.0
Ti	12.1	0.4	13.2	1.0	2.7	2.7
Ba	2.4	0.1	2.4	0.2	0.7	0.7

**SFS-EN ISO 16948, **ASTM D 5016 (mod), ***SFS-EN ISO 10304-1, [+]SFS-EN ISO 17294-2, [++]SFS-EN ISO 11885*

The concentrations in trace elements were used to calculate the elements conversion presented in Figure 4.8 and 4.9 below.

Figure 4.8 shows the conversions to filter and bottom ashes calculated for experiments 3 and 4.

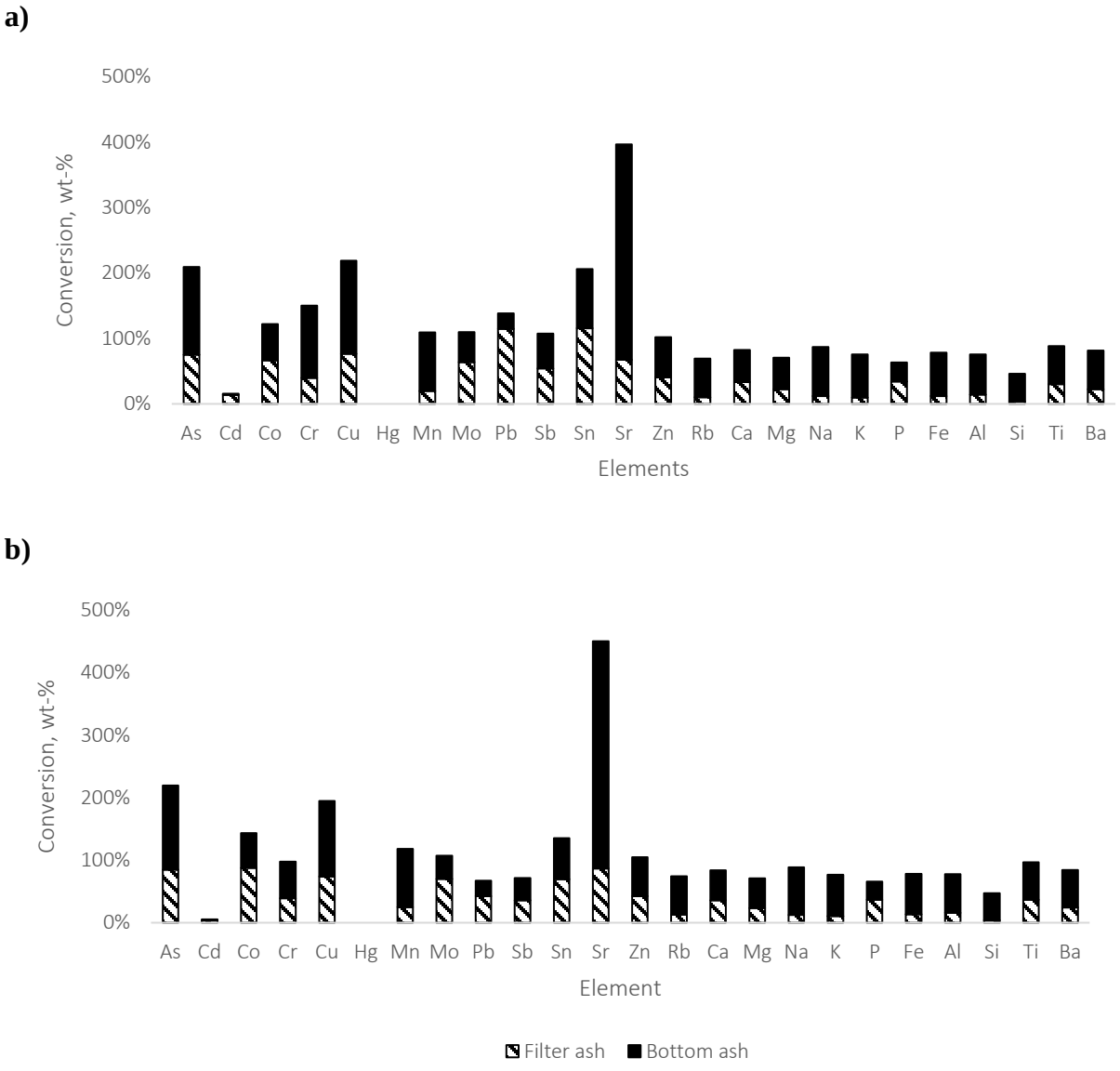

Figure 4.8. *Conversion of elements into filter ash and bottom ash for experiments varying the filter temperature a) T_{filter} 450°C (test 3) and b) T_{filter} 550°C (test 4).*

It was expected that the sum of the conversion is ≤100% for all elements. Nevertheless, it is possible to appreciate that for several elements (As, Co, Ni, Cu, Sn, Sr, and V) it greatly surpasses 100%. First, some elements (As and Sn) were not measured in the bed material, and some of them were below the detection limit of 0.01 wt% (V, Co, and Ni).

However, if measured with exact techniques, they could increase the conversion even in low quantity. Some elements also surpassed 100% for the conversion sum, but to a lower degree (Mn, Mo, Sn, Sb, and Pb). As the deviation is low, it may be related to the fuel heterogeneity, since it is a waste and, thus, its composition can vary from sample to sample.

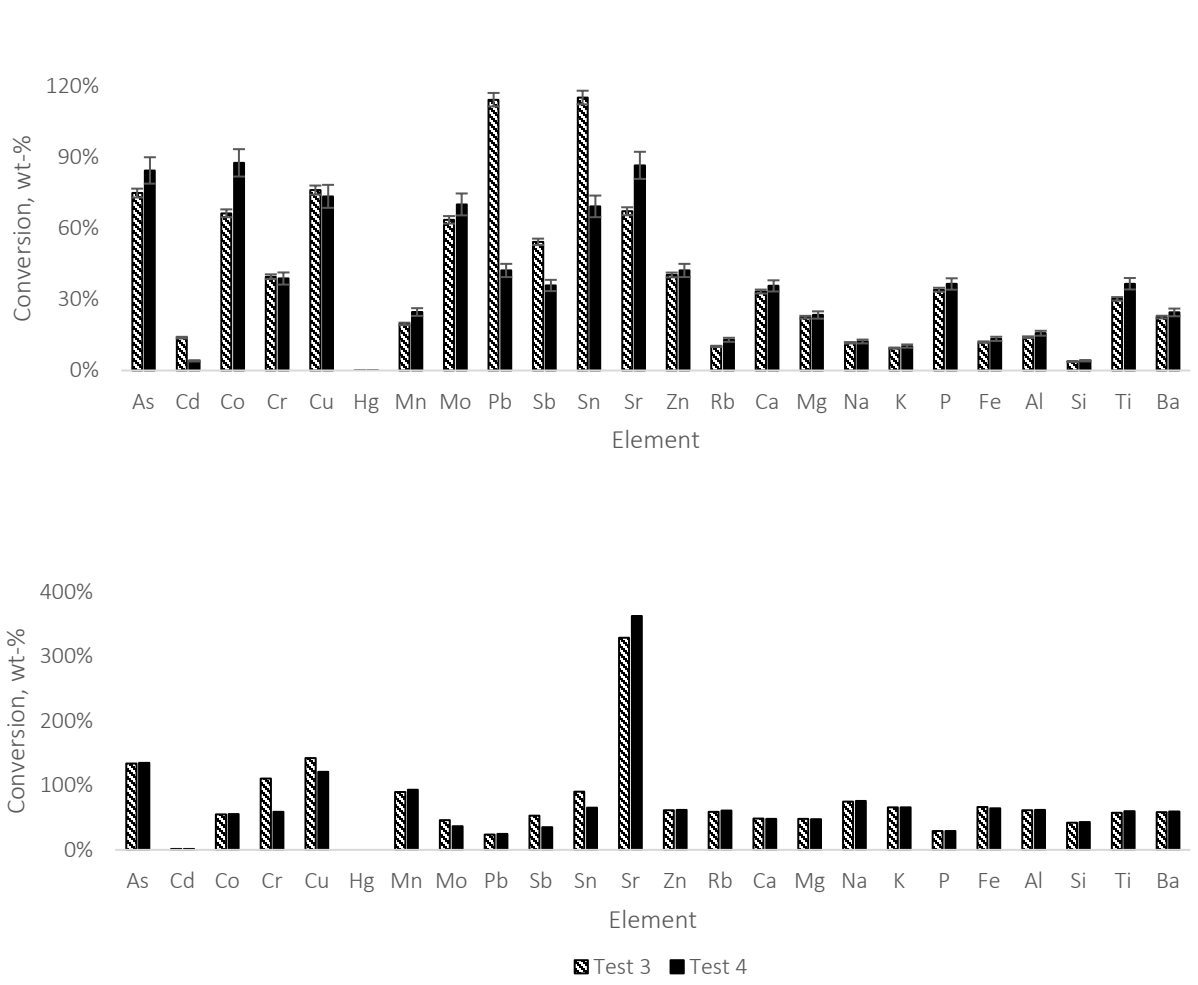

Figure 4.9. *Comparison of the conversion of trace elements for tests 3 and 4, comparing the conversion into* ***a)*** *the filter ashes and* ***b)*** *bottom ashes. The difference between experiments 3 and 4 lies on the filter temperature (T_{filter}(3)=450°C and T_{filter}(4)=550°C.*

Figure 4.9. contains the conversion of selected fuel elements into **(a)** filter ashes and **(b)** bottom ashes. In Figure 9a it was expected that the conversion of filter ashes elements would be higher in test 4 than in test 3 due to the lower filter temperature in test 4 (T_{filter}(4) = 550°C, T_{filter}(3) = 450°C) Therefore, it was expected that the increase in temperature of 100°C in test 4 would lower the elements retention in the filter. Nevertheless, the effect of filter ash temperature was minor, and for most elements (As, Co, Mn, Mo, Sr, V, Zn, Ca, Mg, P, Fe, Al, Ti, and Ba) the filter ash conversion was higher in experiments 4 (excluding only Cd, Pb, Sb and Sn). Experiments with different filter temperature,

increasing the temperature intervals are necessary to evaluate this effect on the retention of elements in the hot filter.

The release of volatile elements such as As, Cd, Hg, and Pb into filter ash is expected to be higher than bottom ash. This is because they are ultimately released to the reactor's gas phase and subsequently condense in the filter. Hg is exceptionally volatile (low condensation temperature) and was not captured in the hot filter (15). Cd was not found in the bottom ash, and a small fraction was converted to the filter ash. For Cd, the filter-ash conversion was higher in experiment 3 (lower filter temperature) than experiment 4, as expected (101). Pb conversion to filter ash was also higher than bottom ash conversion (102). Moreover, the filter-ash conversion of Pb was higher in experiment 3, as expected. Low-volatile elements, such as: Ca, Mg, Na, K, Fe, Al, Si, Ti and Ba were expected to be more concentrated in the bottom ash, which was observed in both experiments, 3 and 4.

The concentration of heavy metals on filter ash may enable using the bottom ash if they agree with the current legislation (103). Moreover, both filter and bottom ashes may serve as sources for valuable metals since they are concentrated in these streams. If this is not yet possible, the ash fraction has a lower volume than the original waste (RDF), reducing material fraction that needs to be landfilled (80).

4.3.7. Enrichment Factor

The calculated Enrichment Factor (EF) for the main trace elements in both bottom and filter ashes is presented in Table 4.6.

The EF of elements is usually higher for the filter ash than the bottom ash. This is because the trace elements concentration in the bottom ash is diluted in the bed material, in this case, sand. The only exception is Si since it is the primary element present in sand, the bed material used in these experiments.

EF for Hg was zero for both filter and bottom ashes, since it is extremely volatile and did not condense at the filter temperature (450°C and 550°C, for tests 3 and 4, respectively). Moreover, the EF for the bottom-ash elements, such as As, Cd and Pb, are low, consistent with their volatile behaviour (104). Co, Cr, Cu and Ni presented higher EF for the filter ashes. These trends are explained due to their

inherent volatility. Since they belong to Group 2 (trace element categorization based on their volatility behaviour (105)), they are partly volatile and are distributed between the bottom and the filter ashes. Ni's EF in filter ashes is high, which may be due to Ni's external source, for instance, from the reactor material's degradation.

Table 4.6. *Enrichment Factors for trace elements in filter and bottom ashes for experiments 3 and 4.*

	Filter ash		Bottom ash	
Test run	**3**	**4**	**3**	**4**
Minor elements				
As	1.09	0.92	0.23	0.18
Cd	0.17	0.17	0.00	0.01
Co	0.83	1.20	0.08	0.09
Cr	1.44	0.42	0.47	0.08
Cu	2.35	2.12	0.51	0.44
Hg	0.00	0.00	0.00	0.00
Mn	1.18	1.58	0.63	0.75
Mo	0.80	1.27	0.07	0.08
Ni	4.30	4.44	0.82	0.34
Pb	1.43	0.55	0.03	0.04
Sb	0.68	0.68	0.08	0.08
Sn	1.45	0.84	0.13	0.10
Sr	0.84	0.94	0.48	0.49
V	1.43	1.58	0.75	0.75
Zn	0.77	0.46	0.14	0.08
Rb	2.03	2.41	1.38	1.42
Major elements				
Ca	0.77	0.71	0.13	0.12
Mg	1.13	1.15	0.28	0.29
Na	0.94	0.86	0.71	0.67
K	1.37	1.36	1.12	1.09
P	0.94	0.83	0.09	0.08
Fe	1.60	1.76	1.03	1.07
Al	1.12	1.32	0.58	0.65
Si	1.29	1.42	1.68	1.86
Ti	0.57	0.58	0.13	0.12
Ba	1.03	1.10	0.31	0.34

As discussed previously, in Section 4.3.7, the filter temperature and the concentrations of trace elements on the filter ashes were not correlated. It was expected a higher EF in test 3 due to lower temperature (450°C), which was observed only for As, Cr, Cu, Pb, Sn, Zn, Ca, Na, K and P.

4.4. Conclusions

Six gasification tests were conducted at 850°C (bed and freeboard temperature), studying the effect of bed material (sand/dolomite), equivalence ratio (ER), fluidizing agent (air + N_2 /air + steam) and filter temperature. The characterization of the main inorganic species (N, S and Cl) and trace elements of the fuel into ash and gas streams was experimentally determined.

The distribution of trace elements into the filter and bottom ashes were analysed through the enrichment factor to assess the final disposal of the ash. The main results are summarized as follows:

The increase in the ER resulted in higher carbon and tar conversion and yields of CO and CO_2, while did not significantly affect the yield of H_2. Steam increased the yield of H_2 (test 2) and that of tar (for all tar groups). No catalytic effect of dolomite on reducing tars was observed. The dry gas heating value varied in the range of 4.0 – 5.3 MJ/kg, whereas the cold/hot gasification efficiency in the range of 64.4 – 71.0% and 81.4 – 85.8%, respectively.

The fuel-N was mainly converted into ammonia (≥ 40% of conversion), followed by HCN, filter dust-N and tar-N. The conversion into H_2S (≥ 20%) was the highest between the measured components-S, followed by filter dust-S, COS, and bottom ashes. The increase in the filter temperature decreased fuel-S conversion into filter dust-S. Most fuel-Cl was converted into filter dust-Cl due to release of Cl into HCl (the main gas compound containing the fuel-Cl), captured in the filter. The lack of balance closure of S and Cl was attributed to their retention in the reactor wall and pipelines (specially the S) and the feedstock heterogeneity.

Regarding the trace elements, the more volatile elements tended to be released to the gas phase and condensate on the filter, accumulating on the filter ash. Extremely volatile elements, such as Hg and Pb, did not condense on the filter but remained in the gas phase. From our experimental results, it was not possible to fully understand the effect of filter temperature on metal condensation on the filter, requiring further investigation.

Chapter 5

Conclusions

5.1. Aim and significance

In the current world situation, in which the circularity of materials and the reduction of the dependence on fossil fuels are critical to achieving the SDGs, using solid wastes as fuels are being extensively investigated. Gasification of solid wastes, such as RDF and DSS, in fluidized bed gasifiers are an attractive option for the thermochemical conversion of wastes. Nevertheless, the intrinsic heterogeneous nature of wastes, make it a challenge process to be implemented.

The aim of this work is to assess the performance of the gasification of solid wastes in fluidized bed focusing on their content in potential harmful elements. To achieve this goal, the literature was reviewed, and several selected experiments were conducted to analyse the sampling and measuring methods of contaminants both in solid and gaseous gasification process. In addition, devolatilization and continuous gasification tests were performed using DSS and RDF as fuels, which resulted in experimental data that enabled the studied of the partitioning of contaminants precursors, as well as other key parameters.

Thermodynamic studies were investigated to support the understanding of the conversion of solid wastes into contaminants using the software HSC.

A comparative study of the environmental impact of RDF gasification with landfilling was performed, based on data from own-dedicated continuous operation tests. A techno-economic assessment of gasification was also performed to investigate the economic feasibility of the gasification plant.

5.2. List of contributions

- Literature review of contaminants in literature, including elemental mass balances for inorganics, such as N, S and Cl, which are used as a basis for the explanation of inconsistencies found in the literature.

- Recommendations for proper measuring of these contaminants in research facilities that focus on the partitioning of elements that form contaminants.

- Selection of most suitable steel-based materials for waste-derived syngas containing Cl and S.

- Results of devolatilization experiments using DSS, wood pellets and RDF as fuels. Measurement of product streams, specifically N, S and Cl species in the gaseous phase and trace elements in the solid phase.

- Behaviour of minor elements during thermal conversion and estimation of their volatilization with temperature.

- Continuous gasification tests in a bench-scale FB gasifier, studying the effect of different parameters on the products. Focus on the contaminants precursors partitioning (N, S and Cl) as well as trace elements in the product solid material.

- Investigation of equilibrium simulations for biomass to understand the behaviour of selected elements during thermal conversion and proof of proposed methodologies to study the thermal conversion of biomass in equilibrium conditions.

- Comparative LCA study of RDF conversion to landfilling and techno-economic assessment of FB gasification of RDF.

5.3. Future work

The main efforts to build on this work should be focused on the further understanding of contaminants precursors and trace elements present in solid wastes.

The chemistry of the solid residue after the thermochemical conversion of solid wastes, specifically gasification. The understanding of how the chemistry of trace elements present in the fuel change would be very interesting to further investigate on thermodynamic simulations, what reactions happen in fuel conversion, the leachability of elements present in the ashes and its potential harm to the environment and, as a novel circular economy concept, the use of valuable elements from ashes into new materials.

Additional devolatilization experiments using an inert reactor material, such as quartz, would be crucial for the understanding of gaseous contaminants formation during gasification. Preliminary experiments using a quartz reactor were conducted during this thesis, however, they were not enough to trace elements and to be included here. Therefore, more tests in a similar facility would support the advancement of this research.

Moreover, the investigation of different types of solid wastes as fuels, or different RDFs would contribute to a more robust understanding and parametrization of syngas and solid residues composition. Modelling work using the extensive experimental data provided by this work is also encouraged.

Lastly, in terms of the LCA and the TEA, the comparison of other novel thermochemical conversion technologies, such as pyrolysis, gasification in different reactor types with FB gasification, using empirical data (i.e., all experiments in different facilities using the same fuel and measurement types) would be of interest for a fit-for-purpose and reliable comparison of these technologies in terms of their upscaling potential and future implementation.

Annex I

Thermodynamic study of the biomass thermochemical conversion process

AI.1. Summary

In this annex, the thermodynamic study of trace elements present in waste fuels during gasification conditions will be presented. The results from simulations carried out in the HSC Chemistry® (106) Software will be shown and discussed. The focus in understanding the behaviour of inorganics and trace elements during gasification conditions, by understanding their behaviour in equilibrium. The work presented in this chapter was executed in collaboration with a master's thesis, in which more examples of thermodynamic calculations using the HSC software can be found (107).

AI.2. Introduction

AI.2.1. Thermodynamic databases

The chemical equilibrium criterion is based on the second law of thermodynamics, and for a system at a specified temperature and pressure, it can be expressed as:

$$(dG)_{T,P} = 0 \qquad \text{(Eq. AI.1)}$$

Due to the large number of components that appear during the thermal conversion of fuels (C, H, O, N, S, Cl, and trace elements) it is desirable to use different software (based on Gibbs energy minimization) to calculate the composition in the chemical equilibrium.

Several thermodynamic databases are available for the calculation of the chemical equilibrium, being the most well known the following: FACTSAGE (108), HSC Chemistry (106), and the SGTE (Scientific Group Thermodata Europe) database (109), available through the software ChemSage

(110). All databases contain the same data for the gaseous compounds containing carbon, hydrogen, and oxygen, but they considerably differ on trace elements and condensing species.

HSC is the largest database, containing almost four thousand (4000) compounds, while FACTSAGE and SGTE contain only about two thousand and five hundred compounds (2500). Nevertheless, the databases may differ, for instance, the HSC database may lack some compounds that a smaller database contains.

A.I.3. Literature review

Inorganic and trace element composition during the thermal conversion of solid fuels has been the subject of several thermodynamic studies in recent years. A sampling of these works is shown in Table AI.1 below.

Table AI.1. *Literature review of the inorganics and trace elements during in thermodynamic simulations.*

Fuel	Studied elements	Software and database	System mode	Analysed parameters	Comments	Year	Reference
Carbon	As	HSC Chemistry® version 4.0	Gasification	Temperature	Considered the composition of a typical gasification syngas, including CO, CO_2, H_2, H_2O, HCl, H_2S and N_2	2003	*Díaz-Somoano* (111)
Biomass	S (H_2S, COS, CS_2, SO_2) and N (NH_3, HCN)	MATLAB	Pyrolysis, gasification and combustion	Atmosphere (equivalence ratio)	Solid fuel composition in the beginning, changing the equivalence ratio for a fixed pressure and temperature	2008	*Baratieri et al.* (112)
Municipal Solid Waste (MSW)	Na, K, Pb, Zn, As, Cr, Cd, Cl and S	Factsage 6.0 with a custom-selected database on the Scientific Group Thermodata Europe (SGTE)	Combustion	Six different waste (one by one), different waste together (two at a time) and temperature	Comaparison to experimental results show good agreement, but to fully comprehend the mechanisms at work, additional experimental laboratory and pilot-scale research under well-controlled test circumstances are required.	2010	*Becidan et al.* (113)
Solid recovered fuel (SRF)	• Inorganics: S (COS, H_2S), Cl (KCl, HCl) • Major trace elements: Al, Fe, K, Mg, Mn, Na, P, Si • Minor trace elements: As, Cd, Co, Cr, Cu, Hg, Ni, Pb, Ti, Tl, V, Zn	Software not specified. FACT database (Fact Sage 5.2.) was used for basic data, complemented with data from HSC Chemistry version 5.11; GFE database; SGTE pure substance database; and the Ivtanthermo for Windows for compounds not available in FACT database.	Fluidized bed gasification and product gas cooling	Temperature and different case scenarios considering different inputs	Focus of research on the behaviour of the following elements: As, Cd, Cr, Cu, Co, Hg, Mn, Ni, Pb, Sb, V and Zn	2012	*Konttinen et al.* (20)
Municipal Solid Waste (MSW)	Cu, Pb, Zn	Factage 7.2 software. FactPS, FToxid, FTsalt and HSCA databases.	Combustion	The authors also studied samples of ashes (20 bottom ashes and 17 fly ashes) using XRD, SEM-EDX and XPS techniques.	Oxygen Carrier Aided Combustion	2022	*Stanicic et al.* (114)

References: Konttinen et al. (20)*; Díaz-Somoano* (111)*; Baratieri et al.* (112)*; Stanicic et al.* (114)**;** *Becidan et al.* (113)

AI.4. Methodology

AI.4.1. Software HSC Chemistry

In this study, the database from the HSC Chemistry® *version 6.1* was selected to conduct the studies of thermochemical conversion of biomass. The HSC Chemistry® software allows the simulation of thermodynamic equilibriums of reactions and processes on a computer and can carry out conventional calculations quickly and easily. To do this, it uses a database in which enthalpy (H), entropy (S) and heat capacity (C) values are collected.

The program calculates the equilibrium composition of multicomponent mixtures in heterogeneous systems. As an input, the user needs to specify the chemical elements that make up the system (e.g.: C, H, O) and then determine the compounds that are in the starting compounds (e.g.: CO, H_2O...) and their quantities in mass or in moles. At this stage, it is also necessary to determine the initial temperature of these components, their physical state (solid, liquid, or gaseous) and in which phase of the system they will belong.

The software has predetermined the phases of the components, for example: sulphates, oxides, chlorides, gas, etc., and a component has the phase to which it is associated by default. As an example, there is the case of CO (gas), which is in the gas phase, while C (solid) is in the solid phase. However, the number of phases can be changed by the user and a simulation can be carried out with just one phase, even if the components of the phase belonged to a different phase at the beginning of the simulation.

The user must specify the potentially stable substances and phases that the software must consider during the equilibrium calculation. It is necessary to consider that the change of the species and of the phases considered in the equilibrium leads to a change in the results of the composition in the equilibrium.

This point is very important during the simulations, since the software offers for the calculation all the possible species found in its database and, therefore, it is up to the user to decide which components should or should not participate in the equilibrium calculation.

In addition, the software calculates equilibrium quantities under isothermal and isobaric conditions. The equilibrium composition is calculated using the GIBBs or SOLGASMIX solvers that use the Gibbs energy minimization method.

AI.4.2. Methodology used in literature

Konttinen et al. (20) conducted studies related to biomass gasification and recycled fuels for efficient power and heat production using the FACTSAGE software. The objective of his work was to develop and test thermodynamic models to analyse the behaviour of trace elements in the product gas.

Due to the number of elements that are present in fuels, the proposed method consisted in carrying out several simulation cases with FACTSAGE, progressively adding specific elements and analyzing the results. The steps performed are described as follows:

- Case 1: The main elements of the fuel and the trace elements are added, excluding the components of the ash (Ca, Mg, K, Na, Si, Al, Fe, P), in addition to the air fed into the gasifier.
- Case 2: The same elements are introduced as in first case, and also Na, K, Mg and P. Ca, Al and Si are excluded, because they were found to be of great importance for the calculation of chemical equilibrium. When they were introduced, the results presented solid compounds that are not kinetically realistic to be formed during the gasification process.
- Case 3: In this case, all the components presented in the ash and the bed material were included in the simulation.

The database used in the calculations had the following characteristics:

- Number of elements: 35
- Number of phases: 4 (1 gas + 3 liquids)
- Number of gaseous species: 200
- Number of solid species: 540

Kuramochi et al. (115) investigated the behaviour of HCl and H_2S released during the gasification of different fuels, analysing the influence of the composition of the feed due to the influence of some metals on the composition of the species mentioned (HCl, H_2S). The study of the behaviour of these

gases was predicted using the calculation of chemical equilibrium in a temperature range between 673 K and 1473 K.

The calculations were made with FACTSAGE using the Gibbs energy minimization method. However, the software presented a limiting number of the potential elements to be formed. Thus, a specific procedure was followed:

- Step 1: The elements were selected in order of greatest content and their elemental compositions were assigned until reaching the software limit.
- Step 2: The equilibrium calculations were performed and only species whose concentration were higher than 10^{-12} moles were considered.
- Step 3: Next, step 1 is carried out again, substituting the element with the lowest content that was considered in the initial calculation.
- Step 4: Follow again all the steps until the equilibrium calculations have been made for all the elements.

Figure A.1 below illustrates the scheme of the steps to follow in the proposed model:

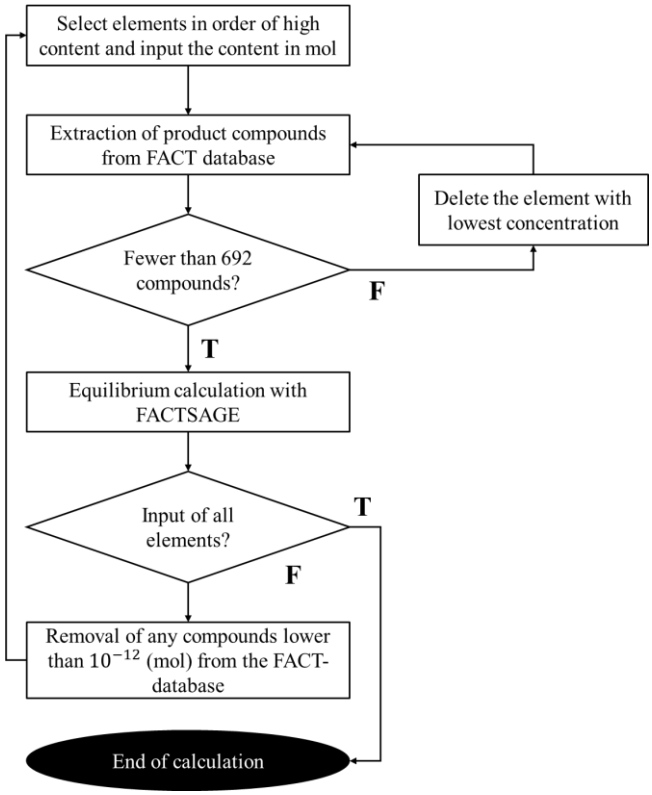

Figure A.1. *Diagram of the calculation procedure followed by Kuramochi et al.*

Regardless of the database used, although there are differences in the calculations, both methods presented by Konttinen et al. (116) and Kuramochi et al. (115) can be implemented.

The first method, proposed by Konttinen et al. (116) does not include Ca, Al, and Si in the simulations. This because when they are included, the results obtained are not kinetically possible in a real gasification experiment. This might be linked to the fact that including the bed material composition in the simulations, usually sand -which is very stable and does not react with the fuel and is in higher amount than the fuel – presents a high content of those elements, which would interfere in the simulation results. However, in this work, the author opted for including the bed material composition in the simulation, excluding only Ca, Al, and Si.

The second method, proposed by Kuramochi et al. (115), follows a more structured sequence. As a drawback, it can be highlighted that the calculations are performed without involving different minor elements simultaneously, since the ones with less concentration are excluded until the limiting number of potential compounds is reached, which is defined by the program. So, for instance, if two minor elements might react, and one of them is not included because of the software limitation, the study would not consider this potential compound.

Despite the weaknesses of the methods, satisfactory results can be obtained to understand the distribution of pollutants during gasification, which will be presented in the next section.

AI.5. Results and Discussion

AI.5.1. Thermodynamic analysis of the thermochemical conversion of biomass

In this section, a thermodynamic analysis of thermochemical conversion of biomass was performed. Baratieri et al. (112) proposed an equilibrium model (gas-solid) based on the minimization of the Gibbs free energy, to estimate the theoretical yield and the composition of the reaction products (gas of synthesis – syngas - and char) from the thermochemical conversion of biomass. In their work, the calculation of the chemical equilibrium was carried out the MATLAB (117), which determined the equilibrium composition by minimizing the Gibbs energy of an ideal mixture. The proposed algorithm calculated the composition for a specific temperature and pressure. With the aim of comparing studying the thermochemical conversion of biomass and exploring similarities and differences with

the work conducted by Baratieri, simulations were carried out using the HSC Chemistry® 6.1 software using the same fuel composition and conditions from their work.

AI.5.1.1. Fuel composition

One hundred kilograms (100kg) of fuel was used as a calculation basis. No bed material was considered in this simulation, as well as the composition of trace elements to limit the number of components and simplify the study. Tables A.2 shows the composition of the biomass used and the operating conditions.

Table AI.2. *Fuel composition*

Element	Content (wt.%)
C	**57.2**
H	**3.3**
O	**16.2**
N	**0.7**
S	**0.2**
Moisture	**9.0**
Ash	**13.4**

AI.5.1.2. Operating conditions

Table AI.3 below present the conditions considered for the study of the thermochemical conversion of biomass.

Table AI.3. *Conditions considered in the study of the thermochemical conversion of biomass*

Temperature (K)	1100
Pressure (kPa)	155
ER	0 - 1

The study was performed containing different amounts of oxygen, varying from zero (ER = 0) up to the amount necessary for complete combustion (ER = 1).

AI.5.1.3. Compounds considered in the equilibrium

Table AI.4 shows the species considered in the simulation conducted in the HSC Chemistry software, as well as the components considered by Baratieri et al. (112).

Table A.4. *Compounds considered at the equilibrium for the study of the thermochemical conversion of biomass. The first column* ***A)*** *shows the species considered by Baratieri et al., while the second column* ***B)*** *shows the species included in this work.*

Compounds	A) Baratieri et al.	B) HSC Chemistry
C	C(g), CO, CO_2	**C(g), CO, CO_2**
H	H, H_2, O, O_2, OH, H_2O, HO_2, H_2O_2, HCO	**H, H_2, O, O_2, OH, H_2O, HO_2, H_2O_2, HCO**
N	N, N_2, NH, NH_2, NH_3, NO, NO_2, N_2O, HNO, CN H_2CN, HCNN, HCNO HOCN, HNCO, NCO	**N, N_2, NH, NH_2, NH_3, NO, NO_2, N_2O, HNO, CN H_2CN, HOCN, HNCO, NCO**
S	S, SO_2, SO_3, H_2S, COS, CS_2	**S, SO_2, SO_3, H_2S, COS, CS_2**
Hydrocarbons	CH, CH_2, CH_3, CH_4, C_2H, C_2H_2, C_2H_3, C_2H_4, C_2H_5 C_2H_6, C_3H_7,C_3H_8, C_6H_6, $C_{10}H_8$, $C_{12}H_{10}$	**CH, CH_2, CH_3, CH_4, C_2H, C_2H_2, C_2H_3, C_2H_4, C_2H_5 C_2H_6, C_3H_7,C_3H_8, C_6H_6, $C_{10}H_8$, $C_{12}H_{10}$**
Other organics	CH_2O, CH_2OH, CH_3O, CH_3OH HCCO, CH_2CO, HCCOH, CH_2CHO, CH_3CHO	**CH_2O, CH_2OH, CH_3O, CH_3OH**
Solid Carbon	**C(s)**	**C(s)**

Most of the compounds considered by Baratieri et al. are included in the HSC simulation, with exception of some compounds in the sections of "*N*" and "*other organics*", highlighted in Table A.4.

A5.1.4. Results and comparison

The focus was on the evaluation of the gaseous species formed that contain S and N, since they are considered as pollutants. Their content on the final syngas may affect its use and determine the downstream cleaning processes that the syngas must go through. Figure A.2 below shows the comparison between the results obtained in this study and the ones obtained by Baratieri et al. (112).

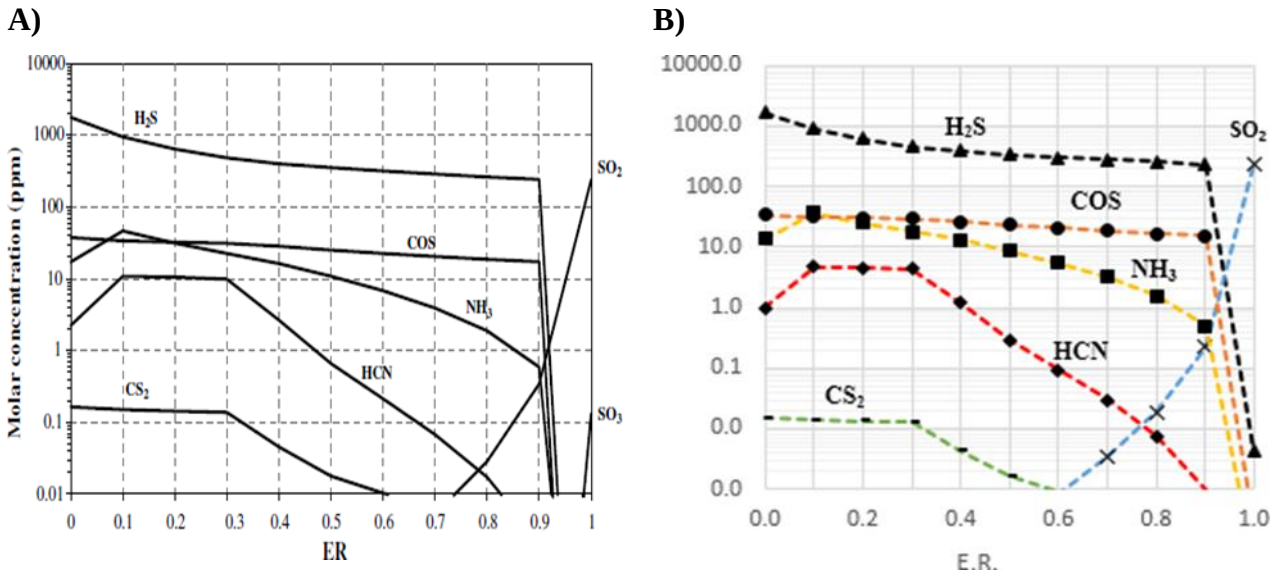

***Figure A.2**. Comparison of the results obtained **A)** by Baratieri et al. and **B)** in this work.*

The simulation was conducted in the temperature and pressure indicated previously in Table A.3, with the evolution of the Equivalence Ratio (ER). The results obtained in this study (Figure 5.2 B) will be discussed below.

As expected, in a reducing environment, S is decomposed mainly into H_2S. COS is also one of the main S-products, even though its concentration is much lower than H_2S (more than ten times). When the ER increases close to one (1), which shows an oxidizing environment, sulphur oxide is found (SO_2 in this work and SO_2 and SO_3 at Baratieri et al.'s work). Additionally, a very low amount of CS_2 appears in the results for ERs up to 0.6.

In the case of the N-compounds, at a reducing environment, NH_3 and HCN are the main products, being the concentration of NH_3 approximately ten times higher than the concentration of HCN. Each concentration increases from ER zero to 0.1 at a similar rate. Then the concentration of NH_3 slowly decreases from ER 0.1 to 0.9, to decrease at a high rate from 0.9 to 1. The concentration of HCN is the same from ER 0.1 to 0.3 and then decreases from ER 0.3 to 0.9.

Both results are very similar among them. Differences might be related to the compounds considered in the equilibrium, which were shown previously in Table A.3

AI.5.2. Thermodynamic analysis of the distribution of Arsenic during gasification using carbon as fuel

In this section, the study of the distribution on heavy metals was studied during the gasification of carbon, with focus on the behaviour of Arsenic with the temperature.

Díaz et al. (111) studied the behaviour of trace elements during the gasification of Carbon, using the software HSC Chemistry® version 4.0 - the same software used in this work, but in an older version. The analysis was made by calculating the equilibrium composition for each trace element separately, considering the major gaseous species (CO, CO_2, N_2, H_2, H_2S, HCl).

AI.5.2.1. Composition considered in the equilibrium

Tables AI.5 shows the composition used by Díaz et al. (111) as gasification atmosphere.

Table A.5. *Composition of the gaseous mix, simulating a gasification atmosphere, used by Díaz et al.*

Component	Content (kmol/l)
CO	**$2{,}57 \times 10^{-5}$**
CO_2	**$1{,}47 \times 10^{-6}$**
H_2	**$8{,}39 \times 10^{-6}$**
H_2O	**$1{,}79 \times 10^{-6}$**
HCl	**$4{,}02 \times 10^{-7}$**
H_2S	**$2{,}01 \times 10^{-8}$**
N_2	**$6{,}88 \times 10^{-6}$**

Differently from the work developed in the previous *Section A.3.1*, instead of using as an input for the simulation the fuel composition, in this case, the gasification atmosphere for the major gases was used.

AI.5.2.2. Operating conditions

The behaviour of Arsenic was studied for a temperature range of 200 - 1200 °C and at 25atm.

AI.5.2.3. Compounds considered in the equilibrium

Arsenic was considered in the form of FeAsS as an input for the equilibrium calculations, both by Díaz et al. and in this work. The compound in which Arsenic will be found in the fuel depends on the

type of carbon, and it can interfere with the simulation results. Understanding and determining in which compound a specific element is found in the fuel is an important step for thermodynamic calculations.

AI.5.1.4. Results and comparison

In the following Figure AI.3 the results obtained in our work (A) and by Díaz et. al (B) are presented.

A) **B)**

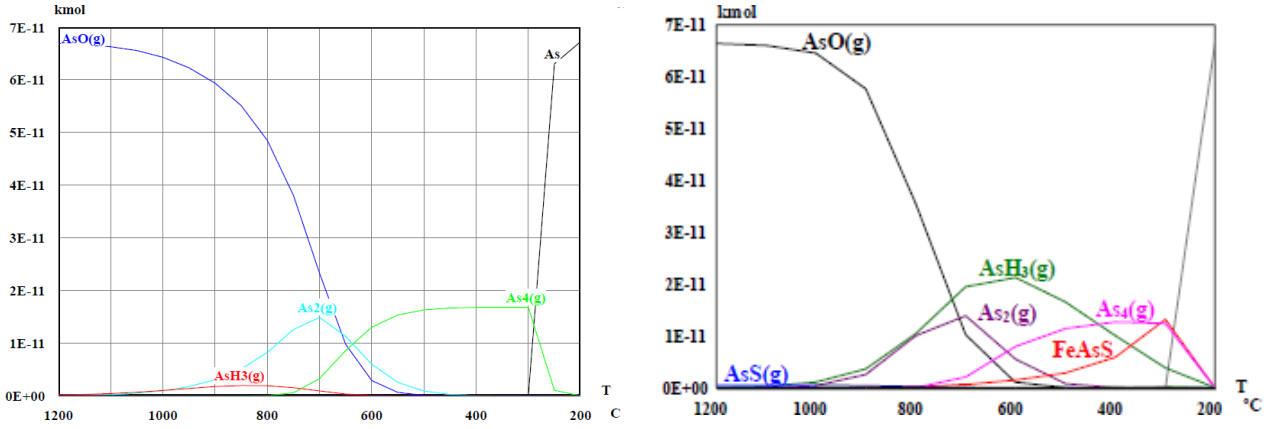

Figure AI.3. *Thermodynamics equilibrium diagram for FeAsS at 25atm at a gasification atmosphere varying with temperature.* ***A)*** *Results obtained in this work using HSC version 6.1 and* ***B)*** *results obtained from Díaz et al. using HSC version 4.1.*

By analysing the figures, the effect of temperature in the equilibrium composition can be observed. At usual gasification temperatures (950 – 800 °C), the main arsenic compound would be gaseous AsO for both results (A and B).

For results found in this work (A), The arsenic gaseous species would be majority from 300 – 1200 °C. Arsenic in solid state would be observed from 200 to 300 °C. Díaz et al. (B), however, found that the solid specie FeAsS – which was entered as an input in both simulations, A and B – was found from 200 – 800 °C.

Moreover, in this work (A) the species AsS(g) and FeAsS were not found. However, in general, the results obtained are similar among them. Since this is an equilibrium study and, thus, theoretical, it is not possible to determine which result is closer to the reality than the other.

The differences among the results when comparing A and B can be related to the database used. The software used was the same in both works, but the versions and, consequently the databases were not. Díaz et al. used the version 4.0 and thus the database 4, while here the version used was the 6.1, using the correspondent database.

However, in general, the results obtained are similar among them. Since this is an equilibrium study and, thus, theoretical, it is not possible to determine which result is closer to the reality than the other.

Furthermore, in Díaz et al. work (111), the list of components considered in the equilibrium was not described, as it was in the work presented in the last section. Therefore, it is not possible to compare which compounds were included in both works, which may affect the results obtained as explained in section 5.2.

In order to obtain the results presented in Figure 5.3B, species unlikely to appear in the equilibrium were eliminated, i.e., some species with As and others such as $FeCl_3$, or other chlorine components that may significantly affect the results obtained.

This is one of the most crucial steps of this type of work since knowledge about the fuel chemistry is required. Such expertise is very complex and goes beyond the scope of this thesis, that is focused on the optimization of gasification parameters, such as ER, temperature, and pressure for the successful gasification of waste derived fuels, while understanding how the above-mentioned parameters affect minor elements and pollutants. precursors.

AI.6. Conclusions

Equilibrium simulations support the understanding of what can be expected during a chemical reaction if equilibrium is achieved. Thermodynamic tools, such as the one used here, HSC Chemistry ® are extremely useful, since it allows the fast calculation of equilibrium compositions considering different parameters and an extensive database of potential components formed. To be able to excel in the use of such tools, it is important to have a reliable methodology when incorporating multiple elements in the simulation. The methodologies gathered in this chapter were used in other works and proved to be feasible and to work properly.

In this thesis, in which the gasification of waste derived fuels in a fluidized bed reactor, in which the residence time is short, this type of simulation can give hints of what could be expected, but to guarantee those species will be found in the products.

Moreover, in the case of waste fuels, determining the chemical format in which a specific element is found, can be even more complex. Since this type of fuels are not homogeneous, nor standardized.

In order to be able to conduct robust and reliable thermodynamic simulations to determine the composition of trace elements during the gasification of waste fuels is very challenging. During the study conducted for this thesis, several equilibrium simulations using HSC Chemistry were conducted and not included in this thesis. They followed the methodologies and approaches discussed by the researchers reviewed in this chapter and used the composition of our fuels (i.e., RDF and DSS). However, as it was not possible to compare our results with other peer-reviewed works and secure their reliability, ultimately, they were not included in this chapter and used only as a learning process of how this type of simulations work.

To move forward in this direction and to obtain meaningful results, it would be beneficial to have a chemical analysis of the fuel and the gasification solid residues to understand not only its elemental composition, but also in which component the elements are, i.e., by means of X-Ray Diffraction (XRD). This way, the selection of components that will be present in the equilibrium would be more assertive and the simulation results provided could be more meaningful and reliable. Although the deep understanding of the chemistry of fuels and solid residues are not in the scope of this thesis, which is focused on chemical processes, this type of analysis are recommended for future research

Annex II

Life Cycle Assessment of the Gasification of Refuse-Derived Fuel in Fluidized Bed to produce electricity – comparison to conventional landfilling

AII.1. Introduction

Our society is shifting from a linear to a circular economy while energy demand is constantly growing. Hence, energy recovery from waste presents itself as an attractive option. Several types of waste have been investigated, and new technologies have arisen to enable their conversion to energy. There are various routes for waste biomass-to-energy conversion, and each one presents advantages and disadvantages. Technology selection is typically made based on target waste and the required energy type, for instance, electricity, heat, or transportation fuels.

The Environmental Life Cycle Assessment (E-LCA) enables the measurement of the environmental impact of a specific technology, translating the process data – emissions, electricity, and heat requirements, etc. – into indicators that allow the comparison between several options for a production process or waste management. There are several studies that evaluate the environmental impact of the thermochemical use of wastes to generate energy (118)(119)(120)(121). However, few studies have experimental data to make a realistic assessment of a specific thermochemical technology and to compare it with other technologies also using real data (122).

Currently, the Social Life Cycle Assessment (S-LCA), which is a method that can be used to assess the social and sociological aspects of products, has been gaining more attention as an important and complementary study to the E-LCA (123)(124)(125).

Together with the E-LCA and Life Cycle Cost (LCC), the S-LCA takes part in the three pillars of sustainability, a crucial concept for achieving a circular and low-carbon economy. The Life Cycle Sustainability Assessment (LCSA) is an integrated assessment technology that integrates the

environmental, economic and social aspects and offers a holistic view of processes and products (126)(127)(128). Even though this analysis is not in the scope of this thesis, it is worth mentioning its importance since the valorisation of waste as fuels are crucial for achieving the Sustainable Development Goals (SDG), and studies are emerging (129).

In this chapter, the Life Cycle Assessment (LCA) of the gasification of Refuse-Derived Fuel was conducted using the experimental results presented in Chapter 4. Then, it was compared with landfilling of the MSW that originated the RDF. Finally, a brief economic assessment of the gasification technologies was also conducted to evaluate the feasibility of this option for the processing of solid wastes.

AII.2. Materials and methods

AII.2.1. Process and system description

The data used in this study is available in Chapter 4. In addition, the fuel composition is available in Table 4.1. In order to compare results obtained for the gasification of RDF (Case 1), the LCA of landfilling of waste (Case 0) was also conducted.

For Case 0, data were obtained from the literature. For Case 1, the gasification of RDF, the results from Test #1 were used as a baseline to make the LCA. The concentrations for Cl in the output gas were taken from Test #4 since Cl was not measured in the first experiment (only species containing N and S). Since the experimental tests conducted in Chapter 4 do not include the burning of syngas, to complete the study of the gasification process, the product syngas was considered to be burned to produce electricity, and the ashes were considered to be landfilled. More details are given below.

AII.2.1.1. Case 0: Direct landfilling of MSW

In Case 0, it was considered that the MSW that originated the RDF was landfilled and directly transported to a landfill.

AII.2.1.2. Case 1: Fluidized Bed Gasification of RDF pellets to produce electricity

The pelletizing process of Municipal Solid Waste (MSW) is conducted to produce Refuse Derived Fuel (RDF) pellets. Then, the RDF is fed to a bubbling fluidized bed (FB) reactor operating at 850 °C, atmospheric pressure and using silica sand as bed material. Sub stochiometric air is added to the bottom of the FB reactor, assuming an Equivalence Ratio (ER) of 0.25. ER is the amount of oxygen added (kg) divided by the stoichiometric oxygen needed for complete combustion (kg).

Gasification generates two major products: syngas and ashes (bottom and flying ashes). The gaseous stream, syngas, leaves the reactor and passes through a cyclone for flying ashes recovery and then through a hot filtration process. Up until this part of the process, experimental data from own conducted tests were used (Chapter 4). Therefore, the process description here follow the same one in Chapter 4. From this point of the process forward, selected steps were included to the conversion of syngas into electricity.

Afterwards, syngas is cooled to condense tars, and then it passes through a wet gas cleaning process to eliminate corrosive species. Then, the clean syngas is combusted in an internal combustion engine (ICE) to produce electricity (130). Gasification bottom and flying ashes exit the reactor periodically and are stored until their transportation to a landfill. The chemicals used during the process are also stored in the gasification facility until proper disposal.

Figure AII.1 below shows both cases considered in this study.

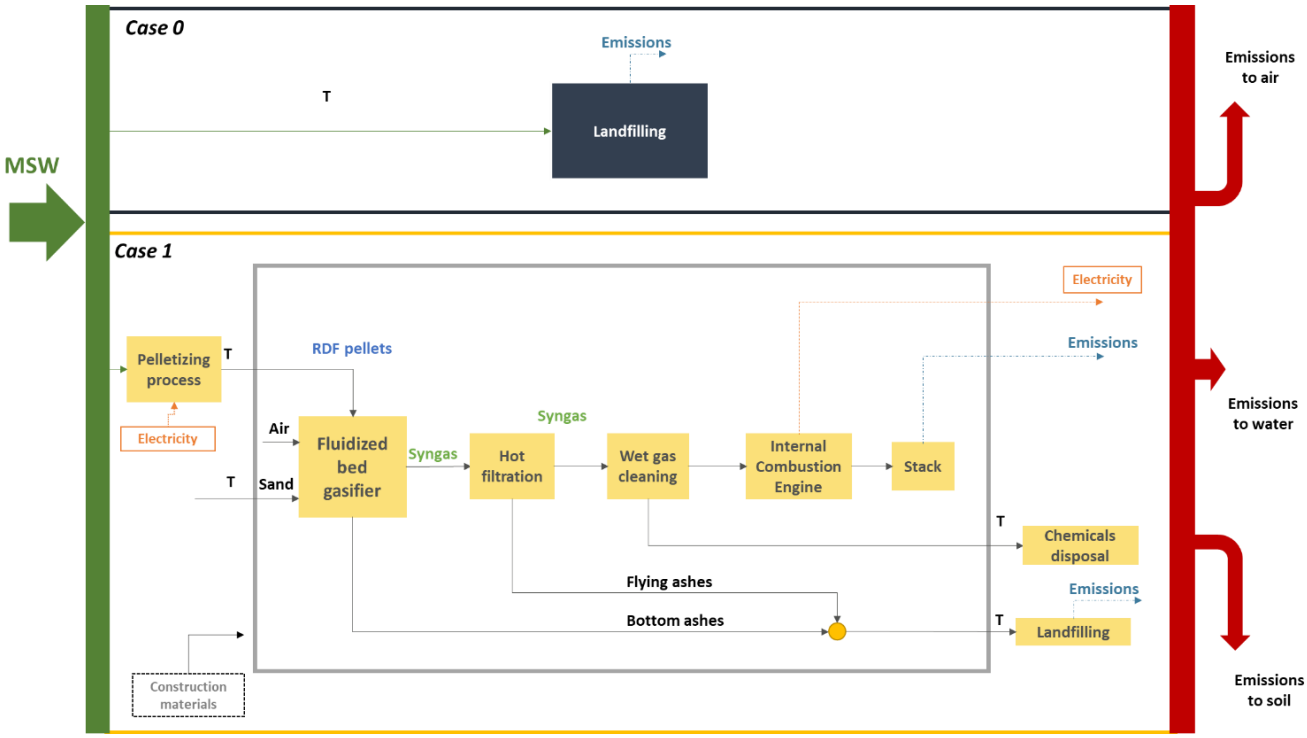

Figure AII.1. *Schematic diagram of the case of study of the gasification of Case 0: landfilling of MSW and Case 1: gasification of RDF pellets in fluidized bed to produce electricity.*

AII.2.3. Environmental Life Cycle Assessment (E-LCA)

LCA is defined as a framework used to analyse the environmental impacts of a product, process, or system throughout its life (131). It is comprised by four steps: goal and scope definition, inventory analysis, impact assessment and interpretation, which are described below.

AII.2.3.1. Goal and scope

The goal and scope of this study is to determine the resources consumption and environmental impact of RDF gasification in fluidized bed and compare it to the landfilling of MSW (common practice in Spain).

The functional unit was defined as 1000 kg (1t) of RDF (See composition at Table 4.1). The environmental assessment presented in this study was performed using a cradle-to-grave LCA approach. The system boundary contains building materials production, the transportation of the RDF

to the gasification facilities, ashes transportation, consumed electricity and fuels, chemicals production, electricity, and emissions. Figure AII.1 contains the major unit process of LCA for this case of study.

AII.2.3.2. Life Cycle Inventory Analysis

The LCI plays a key role in an LCA as the basis for the subsequent LCIA, sensitivity analysis, and economic analysis. LCIs associated with the treatment of 1000 kg of RDF for both cases – landfilling and fluidized bed gasification were compiled.

Data was obtained from own dedicated experimental tests (fluidized bed gasification tests) and literature, as described in the previous sections. The Ecoinvent Database was also used for the LCI (132).

An avoided burden approach was used in which displaced products provided a corresponding environmental benefit and allocation methods were avoided.

The following assumptions were made in the Life-Cycle Inventory Analysis:

Transportation:

- The distance from the RDF to the thermochemical facility was supposed to be 50 km, while the distance from ashes to landfilling and chemicals disposal were assumed as 50 km. Distances were limited to avoid transportation emissions.
- The flying and bottom ashes were assumed to be stored and then transported together to a landfill.
- The diesel consumption of the trucks was considered to be 0.4 L/km.
- The total truck capacity was considered to be 23.5 tons.
- The direct emission of diesel into CO2 was estimated as 2.68 kg of CO_2 equivalent / L of consumed diesel.
- Diesel was considered to be a fraction of 30% of crude.
- Crude density was estimated at 0.85 kg/L.

Other assumptions were made for the Life Cycle Inventory Analysis:

- All the above-mentioned transportations were assumed to be done by trucks using diesel as the fuel. The return distance of empty trunks was also accounted.
- The electricity used in the processes is assumed to be produced from the mix of electricity in Spain. In 2021, the average emissions of Spain were estimated to be 170 g of CO_2 equivalent / kWh. *System expansion** was used to account for the electricity produced from gasification.
- 1 ton of MSW is equivalent to 1 ton of RDF. The volume reduction of MSW to RDF was of seventy percent (70%).
- 100 m^2 was considered as the land occupied in both cases. Natural land occupation was not considered, just agricultural and urban land occupation, by supposing that a land that was already previously occupied was used in both cases.
- The content of fuel characterized as fixed carbon was considered to not be released to the atmosphere in the landfilling scenario (Case 0). The remaining carbon was considered to be released as CH_4 (61 %v) and CO_2 (39 %v), following data found in literature (133).
- 0.006 kg of N / kg of N-fuel was considered to be released as N_2O in the landfilling case, also using literature data (134).
- The consumption of energy (electricity) for the pelletizing process of MSW was considered to be 185 kWh / ton of MSW, following literature data (135).
- Using data from Chapter 4 of content of Hg and Cd in the ashes, it was considered that 90% of the Cd and all Hg went to the air phase, so it was considered for the elemental mass balances here.
- The remaining of Cd (10%) and the rest of minor elements were considered to be fully concentrated in the ashes and then to be split equally between soil and water phases after disposal. Then associated errors were calculated, by supposing that the elements would be placed totally in the soil or in the water, since leachability data of these elements in the fuel and ashes are not available. This is further detailed and discussed in the results section.
- Benzene was considered as the chemical representative of all tars produced in Case 1.
- The amount of bed material was estimated per the usual proportion of bed material and fuel and the residence time of the bed material in the reactor.

** Note: In system expansion, co-products are considered alternatives to other products on the market. Thus, in this case, the electricity produced avoided the impact of the electricity produced in Spain (The Spanish energy mix in 2021 was considered to do so).*

The energy, materials, and emissions inventory to deal with 1 ton of RDF for gasification is presented in Table AII.1 below:

Table AII.1. *Energy, materials, and emissions inventory to process 1 ton of MSW / RDF as received.*

LIFE CYCLE INVENTORY			
Item	**Unit**	**Case 0** ***Landfilling***	**Case 3** ***FB Gasification***
Energy consumed			
Electricity (total)	kWh	0	-1914.8
Diesel	L	4.9	8.8
Raw Materials - Fuel			
MSW / RDF (ar)	kg	1000	1000
Bed material, sand	kg	-	2000
Raw Materials - Building Materials			
Concrete	kg	0	3.17
Steel	kg	0	1.01
Aluminium	kg	0	0.01
Iron	kg	0	0.01
Gravel	kg	0	113.88
Direct Gas Emission			
CO_2 fossil	kg	13	23.5
CO_2 biogenic	kg	678.9	1512.3
CO_2 total	Kg	691.9	1535.8
CH_4	kg	388.1	-
SO_X	kg	-	4.10E-01
NO_X	kg	-	1.11E+01
NH_3	kg	-	-
N_2O	kg	9.00E-02	-
Cd	kg	-	3.00E-03
Hg	kg	-	2.00E-03
Direct Solid Emission (to soil and / or water)			
As	kg	9.59E-04	9.59E-04
Ba	kg	1.10E+00	1.10E+00
Cd	kg	3.26E-03	3.26E-04
Cl	kg	6.71E+00	6.71E+00
Co	kg	6.81E-03	6.81E-03
Cr	kg	5.61E-02	5.61E-02
Cu	kg	4.12E-02	4.12E-02
Hg	kg	2.11E-03	0.00E+00
Mn	kg	4.51E-02	4.51E-02
Mo	kg	4.12E-03	4.12E-03
Ni	kg	6.04E-03	6.04E-03
P	kg	7.82E+00	7.82E+00
Pb	kg	3.36E-02	3.36E-02
Sb	kg	3.02E-02	3.02E-02
V	kg	2.78E-03	2.78E-03
Zn	kg	2.06E-01	2.06E-01
Benzene	kg	0	2.14E-02
Solid Products			
Flying ash	kg	0	3.7
Bottom ash	kg	0	140
Energy produced			
Syngas	kWh	0	3500

AII.2.3.3. Life Cycle Impact Assessment

The ReCiPe methodology was used to conduct the Life-Cycle Impact Assessment, using the hierarchic point of view. In this methodology, four damage (endpoint) categories are considered: ecosystem quality, human health, resources conservation and climate change.

Seventeen impact (midpoint) categories are considered, for instance: agricultural land occupation (ALO), climate change (ECC), freshwater ecotoxicity (FET), freshwater eutrophication (FE), marine ecotoxicity (MET), natural land transformation (NLT), terrestrial acidification (TA), terrestrial ecotoxicity (TET), urban land occupation (ULO), human health climate change (HCC), human toxicity (HT), ionizing radiation (OR), ozone depletion (OD), particulate matter formation (PMF), photochemical oxidant formation (POF), fossil depletion (FD) and metal depletion (MD). The last two categories, FD and MD are related to resources, while the first nine ones are related to ecosystem quality. The remaining midpoints belong to human health (136)(137).

AII.2.3.4. Results interpretation

From the LCA, a comparison between the impacts of all cases is performed. Interpretation of LCA results gives insights for pros and cons of each alternative considered in this study. It also evidences which aspects from the process mostly contribute to the life cycle environmental impacts.

AII.2.4. Techno-Economic Assessment

The techno-economic analysis aims to determine the economic performance of the gasification process. For that, capital cost, operational costs, fuels and electricity costs and revenues from electricity was considered. An avoidance tip for CO_2 was included and further analysed in sensitivity analysis.

For the simplification of the calculations, the following assumptions were made:

- Electricity prices were based on the Spanish market. For electric power delivered to the grid, it was set initially as € 0.06 kWh^{-1}.

- CO_2 avoidance/emission cost was assumed as € 16 / ton of avoided CO_2 as a baseline. (138)
- The gate fee for MSW was assumed to be zero as a baseline.
- The Capital Costs (C_C) of thermochemical plants were taken from literature and are summarized at Table AII.2 below. Capital Costs were updated to the plant throughput of 5 MWe. Operational Costs (C_{OC}) were also taken from literature and are detailed at Table AII.2. (130)
- At the end life of the plant, there are expenses in the plant decommissioning, but the selling of some parts of the plant may generate incomes. Thus, the decommissioning costs in this work was assumed to be zero.

The following Table AII.2 shows the reference used for the calculation of capital costs (C_c) and operational costs (C_{oc}) for a gasification plant of 35MWe of capacity.

Table AII.2. *Reference for Capital Costs (C_C) and O&M costs of the gasification plant for a plant of 35MWe of capacity* (130).

Reference	Facility	Fuel (dry)	Year	Correspondence	Currency	Capital Costs	O&M
Aracil et al., 2018 (122)	Fluidized Bed Gasification (with ICE*)	MSW	2015	Euro/ton	Euro	332	58

** ICE: Internal Combustion Engine*

The Capital Costs were updated the plant capacity considered in this work of 5 MWe using the following Equation 6.1:

$$C_2 = C_1 \left(\frac{S_2}{S_1}\right)^n \quad \text{(Eq. AII.1)}$$

Where C_2 is the Capital Cost (C_C) of the plant with capacity S_2 and C_1 is the C_C of the plant with capacity of S_1. The exponent n is taken as 0.6 due to the chemical nature of this process (139).

The total associated value (π) for the gasification technology proposed in this study, in €/ton of MSW processed and is calculated using the following equation:

$$\pi = E + G + CO_2 - Transport - C_c - C_{oc} \quad \text{(Eq. AII.2)}$$

Where π is the value (positive or negative) associated with the processing of 1 ton of MSW (€ / ton of MSW). *E* is the value of the energy (i.e., electricity) created in the process, *G* is the gate fee obtained from any tipping or disposal fees received for the RDF; CO_2 is the revenue of the avoided CO_2. *Transport* is the transportation cost for both the feedstock and the products (i.e., ashes).

AII.3 Results and discussions

AII.3.1 Comparative LCA results

Figure AII.2 below shows the calculated midpoints for the two cases studied here in total points, considering the 1000kg of RDF treated in each case.

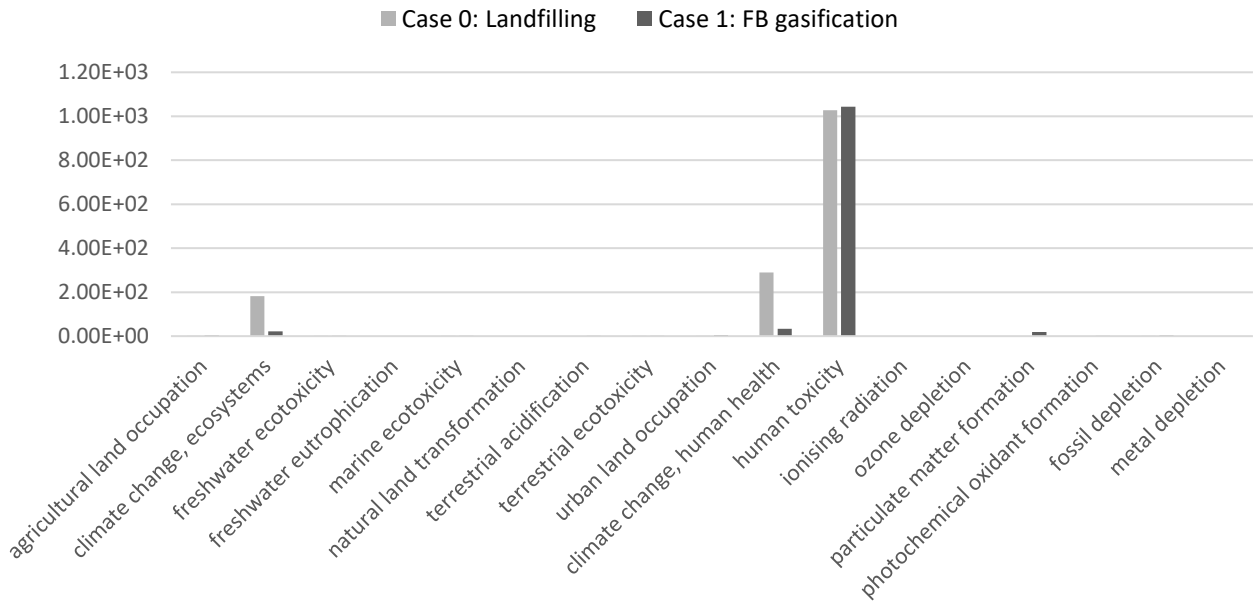

Figure AII.2. *Midpoints for Cases 0 and 1 studied.*

From Figure AII.2, it is possible to observe that the impact of landfilling is higher than the impact of FB gasification for most midpoints. The highest midpoint in all categories is *human toxicity*, which is linked to the impact of selected elements that are part of the RDF.

Table AII.2 below shows the LCIA end points for the different cases and the different end categories in points per kg of RDF.

Table AII.2. *LCIA end points and total points for the different cases studied*

Case	Ecosystem quality (pts / kg)	Human health (pts / kg)	Resources conservation (pts / kg)	Climate change (pts / kg)	Total (pts / kg)
0: Landfilling	1.84E-01	1.32E+00	1.80E-03	4.72E-01	1.97E+00
1: FB gasification	3.06E-02	1.10E+00	3.24E-03	5.48E-02	6.83E-01

Figure AII.3 shows the percentage in the total impact of each case studied, for the four end categories: ecosystem quality, human health, resources conservation and climate change.

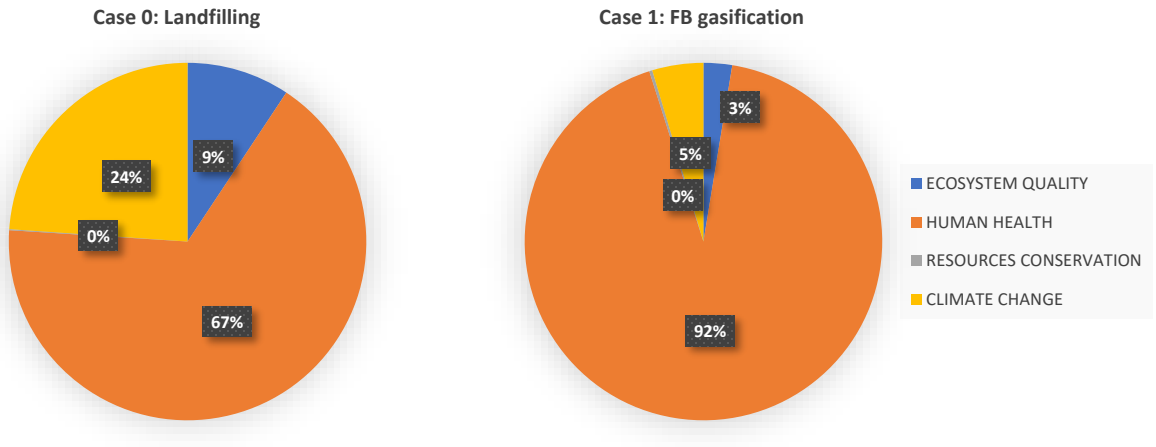

Figure AII.3. *Percentage in the total impact of each case for the four end categories: ecosystem quality, human health, resources conservation and climate change.*

From Table AII.2 and Figure AII.3 it is possible to observe that human health is the highest category, among the endpoints, followed by climate change, ecosystem quality and resources conservation, for both cases studied.

The impact of the human health endpoint is mostly linked to the content of certain elements present in the RDF due to the midpoint category “human toxicity”, accounting for the following elements: As, Ba, Cd, Co, Cr, Cu, Hg, Mn, Mo, Ni, Pb, Sb, V and Zn.

For both cases studied, it was considered that those elements were in the soil. Only Cd and Hg for Case 1 (FB gasification) were considered to be partially emitted to the gas phase, since they were not

fully recovered in the bottom and flying ashes from the mass balances from Chapter 4. Nevertheless, sensitivity analyses to investigate the partitioning of these elements to the soil and water were performed, since data from the leachability of these elements both in RDF and in the ashes are not available. This will be discussed below, from Figure 6.4 analysis.

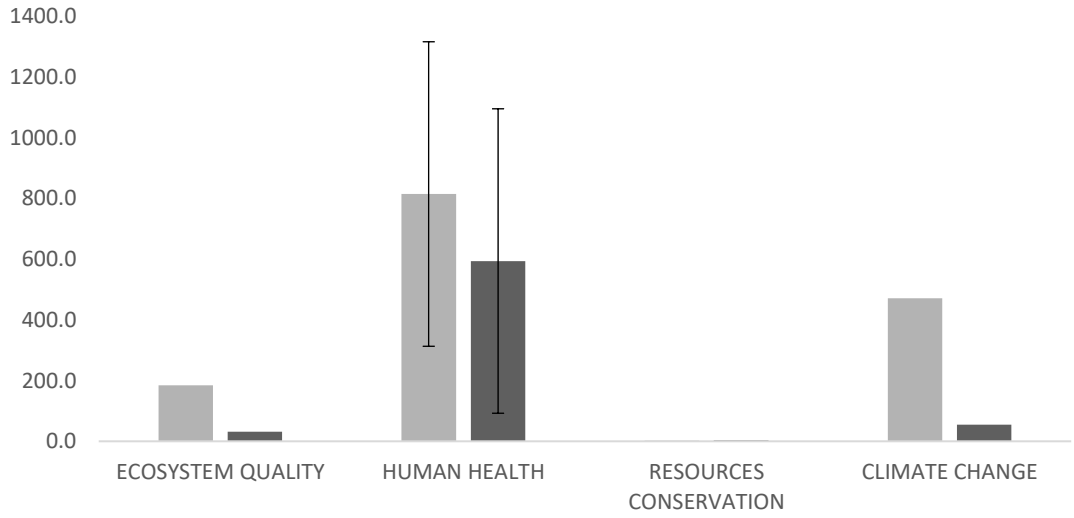

Figure AII.4. *Comparison between the total impact in points of Case 0: landfilling (orange) and Case 1: FB gasification (blue) in the endpoint categories: ecosystem quality, human health, resources conservation and climate change.*

The error bar in the human health category is associated with the uncertainty of the fate of the above-mentioned metals after their disposal. If they are considered to go totally to the water, they cause a lower impact (lower points of the error bars), and if they are considered to go entirely to the soil, they cause a higher impact (higher points of the error bars). The values shown in the bars were calculated considering that 50% of an element went to the soil, while the other 50% went to the water. Moreover, it is important to note that for both cases, and for all elements included, the "unspecified" categories for both soil and water were selected to calculate the midpoints, since the types of soil and water (i.e., agricultural, urban, etc.) were not defined in this study.

The fate of an element after the disposal of MSW (Case 0) or ashes (Case 1) is linked to the leachability of the element in water. After the thermochemical conversion the leachability of an element i may change and, for instance, if it increases, it may cause a lower impact, since the associated impact for water is lower than for the soil. Nevertheless, as this was not measured in this study, the sensibility

analysis presented showed the range of impact an element can cause, depending on if they will be maintained in the soil or will be released to the water.

If somehow it would be possible to stabilize the ashes so they do not enter in contact with the soil or water, the human health impact would severely decrease. This can be done more easily than stabilizing the MSW, since the amount of ashes is much lower, about 15% of the mass of RDF.

Moreover, currently, the lack of metals can bring the idea of mining landfills to recover elements. This could be specially interesting for the ashes, since elements get concentrated there. If the process to recover those metals from the wastes were with few steps and the chemical form in which the elements were found - they may change after thermochemical conversion – were useful to society, they could cause a positive impact instead by replacing conventional mining processes. Nevertheless, these thoughts are given just as potential new solutions and ways of decreasing the environmental impact of solid wastes, since they will not be studied here in depth.

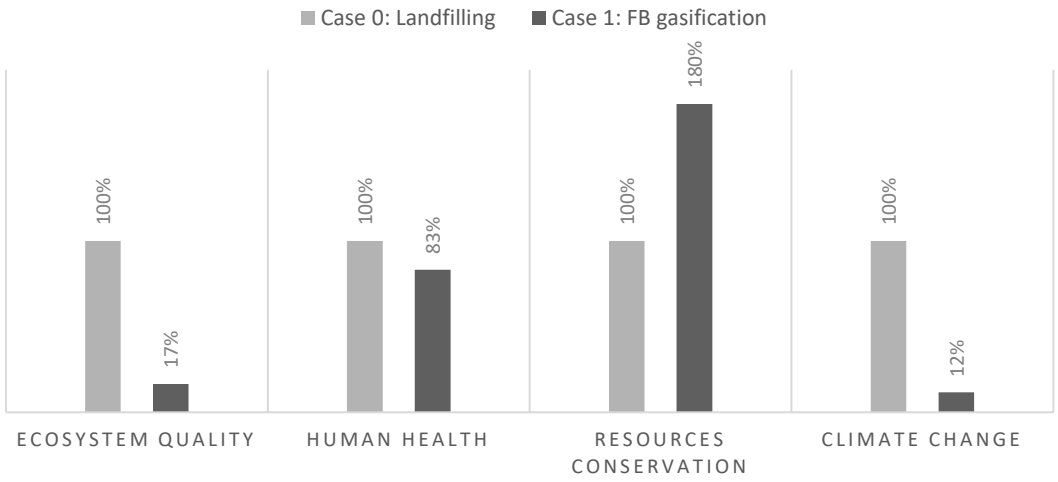

Figure AII.5. *Comparison between the impact of Case 0: landfilling (orange) and Case 1: FB gasification (blue) in the endpoint categories: ecosystem quality, human health, resources conservation and climate change. In this chart, the impact of landfilling represents 100% for each category and FB gasification is compared to that, also in percentage.*

From Figure AII.5 it is possible to observe that the impact of landfilling is higher for almost all categories. FB gasification only surpass landfilling in the resources conservation category. Nevertheless, from Figures AII.3 and AII.4, it is noted that resources conservation is the least impactful category for both cases, less than one percent (1%) of the total impact.

Figures AII.6 below shows the contribution of factors in the midpoints and endpoints for Case 1: FB gasification.

a)

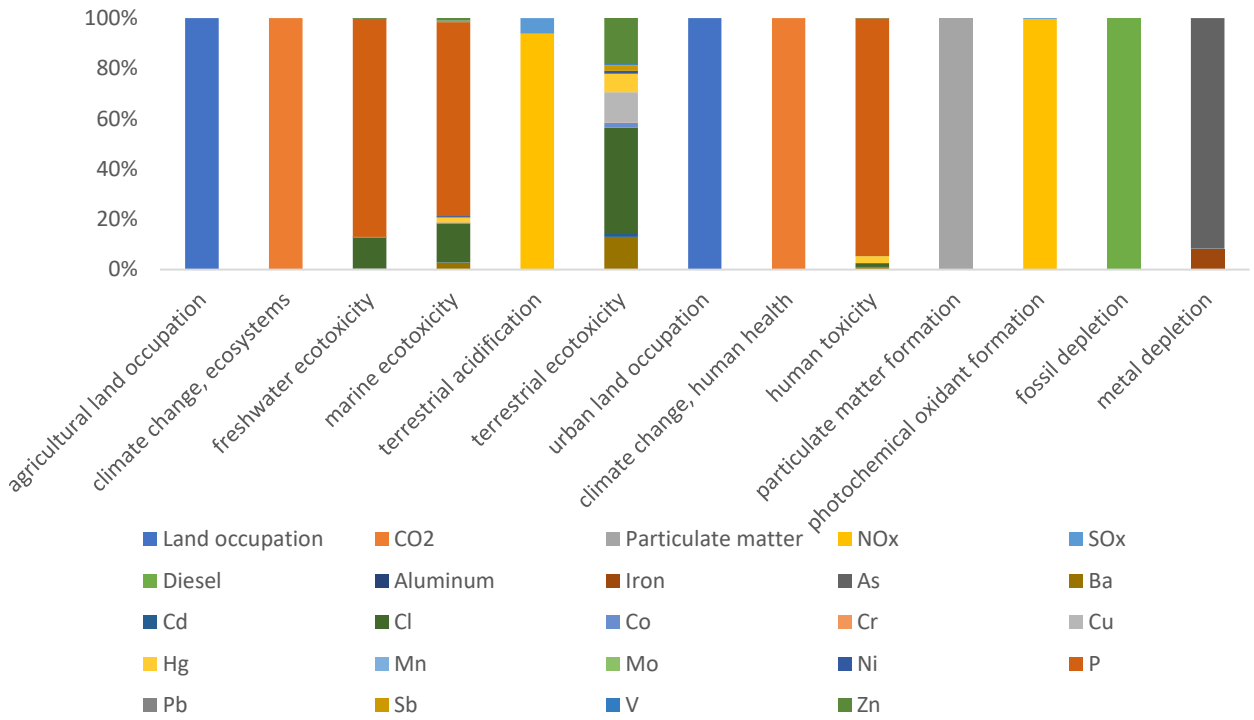

b)

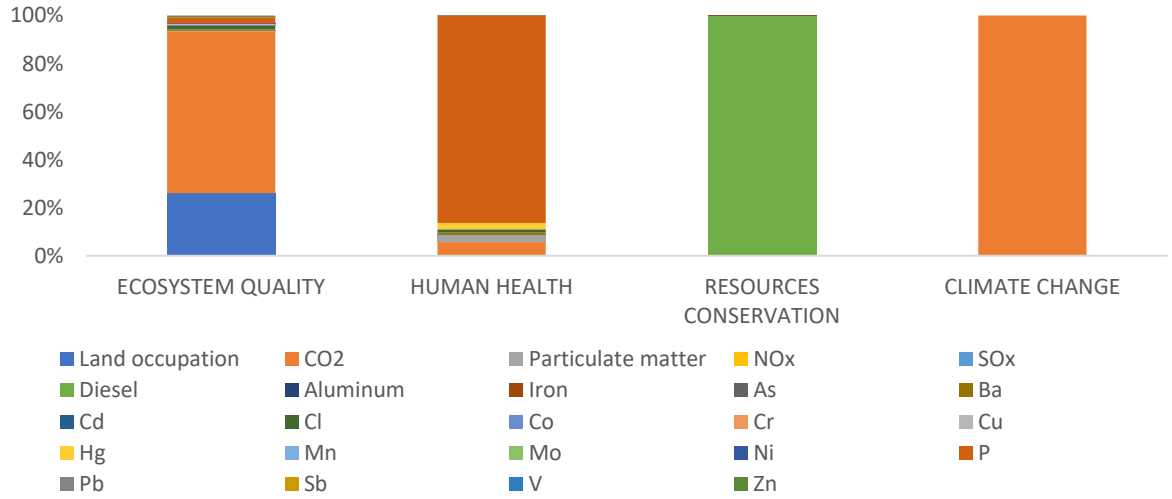

Figure AII.6. ***a)*** *Contribution of factors in the midpoint environmental categories for Case 1: FB gasification and,* ***b)*** *Breakdown analysis for the absolute life cycle impact on ecosystem quality, human health, resources conservation and climate change for Case 1: FB gasification.*

From the analysis of both Figures AII.6 *a* and *b*, it is possible to observe that while CO_2 is the main contributor to the *climate change* endpoint, the use of diesel for the transportation - of the fuel, bed material and ashes - is the main factor that contributes to the impact in the *resources conservation* endpoint.

For the *ecosystem quality* endpoint, the main factor is the release of CO_2, followed by land occupation. The factors that contribute in a minor extent to this category are the release of P, Cl, and some metals, such as Hg, Zn and Co.

Finally, for the *human health* endpoint the main contributor is the release of P, followed by the release of CO_2, particulate matter, Hg, Cl and Cd.

As this thesis addressed several times the presence of minor contaminants in solid wastes, it is valid to highlight that the contribution of heavy metals to the environment is not as big as other factors, such as the release of CO_2, or P. Some heavy metals, such as Hg and Cd did impact significantly to the total environmental impact of the process, but as their content in the fuel is small, the total impact is proportional.

5.3.2 TEA results

The Techno-Economic Assessment (TEA) was performed by considering three main scenarios: the worst-case scenario, the average case, and the best-case scenario. They will be described in Table AII.3 as follows:

Table AII.3. *Parameters considered in the analysis of the worst, average and best cases scenarios in the estimation of costs of the gasification plant.*

Scenario ***Unity***	**Capital (Cc) & Operational Cost (Coc)** ***MWe***	**Transport (T)** ***km***	**Electricity (E)** ***€ / MWh***	**Gate fee (G)** ***€ / ton of MSW***	**CO_2** ***€/ton of CO_2***
Worst	50	100	0	- 50	0
Average	5	50	0.05	0	+ 16
Best	1	0	0.15	+ 50	+50

The worst-case scenario means the one in which the costs are the highest and the revenues the lowest or even inexistent. The best-case scenario considers exactly the opposite of this, the costs are the lowest and the revenues the highest.

It is known that the higher the plant size, more profitable a gasification plant can be (130). Nevertheless, in this work, the higher the plant size, the higher the associated capital and operational costs, so the smaller plant was considered as the "best case scenario". Results are presented in Figure AII.7 below:

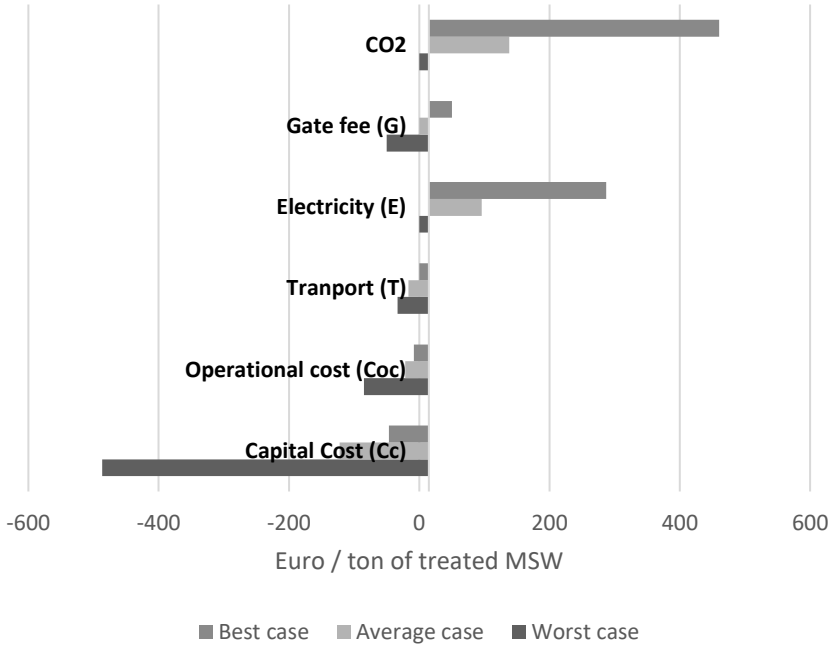

Figure AII.7. *Estimation of costs and revenues for the worst-case, average-case, and best-case scenarios in Euros per ton of processed MSW in a gasification plant.*

From Figure AII.7 it is possible to observe that the main contributors to the revenues of the gasification plant are electricity and CO_2. Gate fee can contribute as well to the revenues, but its impact even in the best-case scenario is much lower than the other streams of income mentioned.

In the costs, transportation ranges from 0 km (treatment onsite) to 100 km of distance of the MSW collection to the treatment plant. The impact of transport on costs is lower than the operational costs and the capital costs, which is the highest cost associated to a gasification plant. Capital costs can decrease if gasification plant were widely implemented. However, a medium to a lower size implicates in less investment and therefore associated less risk with the investment.

Figure AII.8 below shows the sum of the costs and revenues for each scenario evaluated:

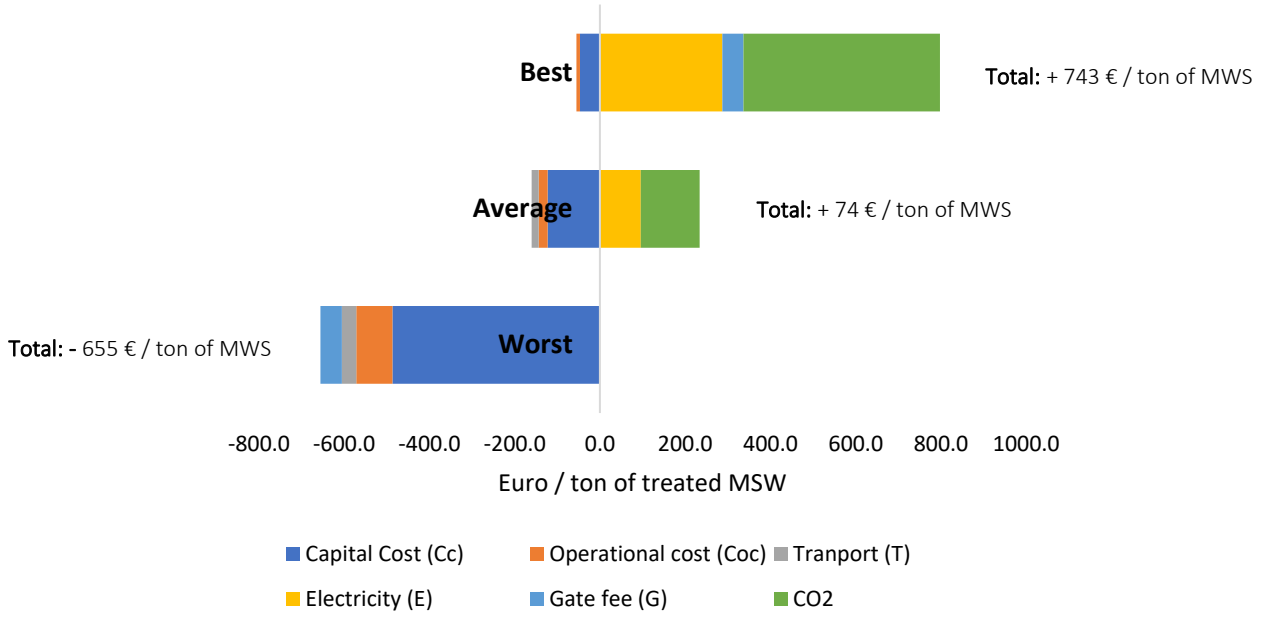

Figure AII.8. *Estimation of costs and revenues for the worst-case, average-case, and best-case scenarios in Euros per ton of processed MSW in a gasification plant.*

In the average scenario, a FB gasification plant of 5 MWe is considered, with no gate fee, an electricity selling price of 0.05 € / MWh and a CO_2 selling price of 16 € / ton of CO_2. The result is an income of 74 € / ton of treated MSW, which means that even in an average scenario, the process would be profitable.

In order for the π value (Eq. AII.2) to be zero, which means that the plant revenues would cover its costs, if the CO_2 selling price is zero, the minimum electricity selling price would be 0.08 € / MWh. Currently, the energy selling price is 0.15 € / MWh. Therefore, it is safe to say that a plant of this size would be profitable in the current economic situation (140).

Moreover, in a more optimistic scenario, in which avoided CO_2 equivalents is sold, the gasification plant would be even more profitable (see average and best-case scenarios). (138) It is known from IPCC and the current European regulation that the carbon market is a reality and carbon price will increase in the future. This makes those scenarios even more achievable (141)(142).

Nevertheless, in order to guarantee that a company can be certified in terms of carbon avoidance, a whole process needs to be implemented, which can cause some costs, which are not contemplated in this study.

AII.4 Conclusions

The study performed in this chapter highlighted the potential environmental benefits of the FB gasification technology could provide compared to the conventional landfilling of MSW through the LCA. The results of this study points that the environmental impact of FB gasification of RDF is much lower than waste landfilling, which is a common practice in many countries, including Spain. To summarize, this is mainly linked to the fact that when using waste that would be otherwise landfilled – which when decomposed emits CO_2 – as fuel to generate electricity, it is potentially decreasing the electricity generation from other sources, such as fossil fuels, while reducing the waste volumes to be managed among other economic potential benefits.

The sensitivity analysis in the case of the fate of minor elements after the MSW and ashes disposal were interesting to see the extent of their impact on the environment in the different endpoints considered here. Unfortunately, due to the content in heavy metals and the EU law, the RDF ashes cannot be used, for instance, as soil amendment, even if they present a high concentration of phosphorous, which is beneficial for the soil.

Three scenarios were proposed for the economic analysis, from the worst to the best-case scenario. Results shown that in the current scenario the gasification plant is feasible, but they highlighted an important reminder that there is a lot of uncertainty and variability associated with economic parameters for this technology, in which politic decisions can severely interfere on, such as the carbon market price, or even world crisis, such as the impact of the Ukraine war on the electricity price in Europe.

As a final comment, other thermochemical technologies that are considered novel and interesting for the conversion of RDF were not included in this study, since the prioritization of empirical data obtained along with the experiments performed in this thesis (Chapter 4) was made in order to obtain more reliable LCA results.

Nomenclature

Text Abbreviations

ALO: agricultural land occupation

BIGCC: Biomass Integrated Gasification Combined Cycle

CRM: Critical Raw Materials

DSS: Dried Sewage Sludge

ECC: climate change

EDD: European Dirty Dozen

E-LCA: Environmental Life Cycle Assessment

ER: Equivalence ratio

FD: fossil depletion

FE: freshwater eutrophication

FET: freshwater ecotoxicity

FTIR: Fourier-Transform Infrared Spectroscopy

HCC: human health climate change

HM: Heavy Metal

HT: human toxicity

IC: Ion Chromatography

ICP-MS: Inductively coupled plasma mass spectrometry

ID: Internal Diameter

LCA: Life Cycle Assessment

LCC: Life Cycle Cost

LCSA: Life Cycle Sustainability Assessment

MD: metal depletion

MET: marine ecotoxicity

NLT: natural land transformation

OD: ozone depletion

ODS: Objetivos de Desarrollo Sostenible

OR: ionizing radiation

PMF: particulate matter formation

POF: photochemical oxidant formation

RDF: Refused-Derived Fuel

SEM-EDX: Scanning Electron Microscopy with Energy Dispersive X-ray Spectroscopy

S-LCA: Environmental Life Cycle Assessment

SRF: Solid Recovered Fuel

TA: terrestrial acidification

TET: terrestrial ecotoxicity

ULO: urban land occupation

UV: Ultraviolet

VTT: VTT Research Centre in Finland Ltd

XPS: X-ray Photoelectron Spectroscopy

XRD: X-ray Diffraction

Abbreviations used in equations and tables

ar: as received

Ash: is the amount of ash (g)

BM: is the total amount of bed material added in the reactor (g)

BM_i: is the total amount of the element i entering the reactor in the bed material (g)

C_1: is the C_C of the plant with capacity of S_1

C_2: is the Capital Cost (C_C) of the plant with capacity S_2

$Cash_i$: is the concentration of element i in the ash (g/g)

CBM_i: is the concentration of the element i in the bottom ash (g/g)

Cc: Capital cost, € / ton of processes solid waste

CF_i: is the concentration of the element i in the fuel (g/g)

CO_2: is the revenue of the avoided CO_2, € / ton of processes solid waste

Coc: Operational cost, € / ton of processes solid waste

Conversion: is calculated by the amount of ash (filter/bottom), the concentration of the element *i* in the referred ash, divided by the total amount of element *i* that entered the reactor, %

daf: dry and ash free

E: electricity, € / ton of processes solid waste

E_i: is the amount of the element i entering the reactor (g)

FB: fluidized bed

F_i: is the total amount of the element i entering the reactor in the fuel (g)

G: gate fee, € / ton of processes solid waste

h: is the experiment time (h)

ND: Not detected

NM: Not measured

m_i^f: the mass of the element *i* in the fuel.

m_i^p: the mass of the element *i* in the phase (p) of interest (p: g, gas; s, solid)

ODT: own dedicated tests

Q: is the fuel feeding rate (g/h)

Ratio: is the ratio between the mass of the solid residue and the initial fuel mass

T: is the temperature in degree Celsius

Transport: is the transportation cost for both the feedstock and the products disposal, € / ton of processes solid waste

u_{mf}: minimum fluidization velocity (m/s)

V_i: volatility of an element *i* (%)

wt: weight

π: associated value for the technology, € / ton of processes solid waste

References

1. Thermelis NJ, Kim YH, Brady MH. Energy recovery from New York City municipal solid wastes. Waste Manag Res. 2002;20(3):223–33.

2. Arena U. Process and technological aspects of municipal solid waste gasification. A review. Elsevier. 2012;

3. Lopez G, Artetxe M, Amutio M, Alvarez J, Bilbao J, Olazar M. Recent advances in the gasification of waste plastics. A critical overview. Renew Sustain Energy Rev. 2018;82(July 2017):576–96.

4. Van Paasen, S.V.B; Cieplik, M.K; Phokawat NP. Gasification of Non-woody Biomass. Economic and Technical Perspectives of Chlorine and Sulphur Removal from Product Gas. osti.gov. 2006;54.

5. Malkow T. Novel and innovative pyrolysis and gasification technologies for energy efficient and environmentally sound MSW disposal. Waste Manag. 2004;24(1):53–79.

6. Bosmans A, Vanderreydt I, Geysen D, Helsen L. The crucial role of Waste-to-Energy technologies in enhanced landfill mining: A technology review. J Clean Prod. 2013;55:10–23.

7. Daouk E, Sani R, Pham Minh D, Nzihou A. Thermo-conversion of Solid Recovered Fuels under inert and oxidative atmospheres: Gas composition and chlorine distribution. Fuel. 2018;225(July 2017):54–61.

8. Valin S, Ravel S, Pons de Vincent P, Thiery S, Miller H. Fluidized bed air gasification of solid recovered fuel and woody biomass: Influence of experimental conditions on product gas and pollutant release. Fuel. 2019;242(January):664–72.

9. Jiang Y, Ameh A, Lei M, Duan L, Longhurst P. Solid–gaseous phase transformation of elemental contaminants during the gasification of biomass. Sci Total Environ. 2016;563–564:724–30.

10. Zevenhoven R, Pia K. Chapter 3: Sulphur. Control Pollut flue gases fuel gases [Internet].

2004;1–24. Available from: http://users.abo.fi/rzevenho/gasbook.html

11. Schweitzer D, Gredinger A, Schmid M, Waizmann G, Beirow M, Spörl R, et al. Steam gasification of wood pellets, sewage sludge and manure: Gasification performance and concentration of impurities. Biomass and Bioenergy. 2018;111:308–19.

12. Zevenhoven K. Chapter 4 Nitrogen. 2001;

13. Zevenhoven, Kilpinen. Chapter 7 Halogens, dioxins/furans. 2001;1–28.

14. Ferreira De Almeida V, Gómez-Barea A, Nilsson S, Tuomi S. Distribution of Inorganics and Trace Elements during Waste Gasification in a Bench-Scale Fluidized Bed. Energy and Fuels. 2021;35(19):15802–16.

15. Ronda A, Gómez-Barea A, Haro P, de Almeida VF, Salinero J. Elements partitioning during thermal conversion of sewage sludge. Fuel Process Technol. 2019 Apr 1;186:156–66.

16. Phyllis2 - Database for the physico-chemical composition of (treated) lignocellulosic biomass, micro- and macroalgae, various feedstocks for biogas production and biochar [Internet]. [cited 2022 Dec 13]. Available from: https://phyllis.nl/

17. Ryu C, Sharifi VN, Swithenbank J. Waste pyrolysis and generation of storable char. Int J Energy Res. 2007 Feb;31(2):177–91.

18. Pandey DS, Kwapinska M, Gómez-Barea A, Horvat A, Fryda LE, Rabou LPLM, et al. Poultry Litter Gasification in a Fluidized Bed Reactor: Effects of Gasifying Agent and Limestone Addition. Energy and Fuels. 2016;30(4):3085–96.

19. Arena U, Di Gregorio F. Fluidized bed gasification of industrial solid recovered fuels. Waste Manag. 2016;50:86–92.

20. Konttinen J, Backman R, Hupa M, Moilanen A, Kurkela E. Trace element behavior in the fluidized bed gasification of solid recovered fuels - A thermodynamic study. Fuel. 2013;106:621–31.

21. Zevenhoven R, Kilpinen P. Chapter 8 Trace elements, alkali metals 8.1. 2001;1–30.

22. Peng H, Forsberg K. Progress on the Recovery of Critical Raw Materials. Jom. 2022;74(5):1932–3.

23. Knudsen JN, Jensen PA, Lin W, Frandsen FJ, Dam-Johansen K. Sulfur Transformations during Thermal Conversion of Herbaceous Biomass. Energy & Fuels. 2004 May;18(3):810–9.

24. Ma W, Hoffmann G, Schirmer M, Chen G, Rotter VS. Chlorine characterization and thermal behavior in MSW and RDF. J Hazard Mater. 2010;178(1–3):489–98.

25. Reed GP, Paterson NP, Zhuo Y, Dugwell DR, Kandiyoti R. Trace Element Distribution in Sewage Sludge Gasification: Source and Temperature Effects. Energy & Fuels. 2005 Jan;19(1):298–304.

26. Campoy M, Gómez-Barea A, Ollero P, Nilsson S. Gasification of wastes in a pilot fluidized bed gasifier. Fuel Process Technol. 2014;121:63–9.

27. Chan WP, Veksha A, Lei J, Oh W Da, Dou X, Giannis A, et al. A hot syngas purification system integrated with downdraft gasification of municipal solid waste. Appl Energy. 2019;237(January):227–40.

28. Hervy M, Remy D, Dufour A, Mauviel G. Air-blown gasification of Solid Recovered Fuels (SRFs) in lab-scale bubbling fluidized-bed: Influence of the operating conditions and of the SRF composition. Energy Convers Manag. 2019;181(September 2018):584–92.

29. Bridgwater A V. The technical and economic feasibility of biomass gasification for power generation. Vol. 74, Fuel. Elsevier; 1995. p. 631–53.

30. Broer KM, Johnston PA, Haag A, Brown RC. Resolving inconsistencies in measurements of hydrogen cyanide in syngas. Fuel. 2015;140:97–101.

31. Ståhlberg P, Lappi M, Kurkela E a, Simell P a. Sampling of contaminants from product gases of biomass gasifiers. VTT Tiedotteita – Meddelanden – Research Notes. 1998. p. 1–95.

32. Arena U, Di Gregorio F. Erratum: Gasification of a solid recovered fuel in a pilot scale fluidized bed reactor (Fuel 117 (2013) (528-536)). Vol. 120, Fuel. 2014. p. 243.

33. Berrueco C, Recari J, Abelló S, Farriol X, Montané D. Experimental Investigation of Solid

Recovered Fuel (SRF) Gasification: Effect of Temperature and Equivalence Ratio on Process Performance and Release of Minor Contaminants. Energy & Fuels. 2015 Nov;29(11):7419–27.

34. Recari J, Berrueco C, Abelló S, Montané D, Farriol X. Gasification of two solid recovered fuels (SRFs) in a lab-scale fluidized bed reactor: Influence of experimental conditions on process performance and release of HCl, H 2 S, HCN and NH 3. Fuel Process Technol. 2016;142:107–14.

35. Recari J, Berrueco C, Puy N, Alier S, Bartrolí J, Farriol X. Torrefaction of a solid recovered fuel (SRF) to improve the fuel properties for gasification processes. Appl Energy. 2017;203:177–88.

36. Recari J, Berrueco C, Abelló S, Montané D, Farriol X. Effect of Bed Material on Oxygen/Steam Gasification of Two Solid Recovered Fuels (SRFs) in a Bench-Scale Fluidized-Bed Reactor. Energy & Fuels. 2017 Aug;31(8):8445–53.

37. Porbatzki D, Stemmler M, Müller M. Release of inorganic trace elements during gasification of wood, straw, and miscanthus. Biomass and Bioenergy. 2011;35(SUPPL. 1).

38. Bläsing M, Hasir NBA, Müller M. Release of Inorganic Elements from Gasification and Co-Gasification of Coal with Miscanthus, Straw, and Wood at High Temperature. Energy & Fuels. 2015 Nov;29(11):7386–94.

39. Materazzi M, Lettieri P, Mazzei L, Taylor R, Fuel CC-, 2015 U. Fate and behavior of inorganic constituents of RDF in a two stage fluid bed-plasma gasification plant. Fuel. 2015;150:473–85.

40. de Jong W, Ünal Ö, Andries J, Hein KR., Spliethoff H. Biomass and fossil fuel conversion by pressurised fluidised bed gasification using hot gas ceramic filters as gas cleaning. Biomass and Bioenergy. 2003 Jul;25(1):59–83.

41. Zevenhoven R, Kilpinen P. Control of Pollutants in Flue Gases and Fuel Gases. 2001;

42. Jönsson B, Lu Q, Chandrasekaran D, Berglund R, Rave F. Oxidation and Creep Limited Lifetime of Kanthal APMT®, a Dispersion Strengthened FeCrAlMo Alloy Designed for Strength and Oxidation Resistance at High Temperatures. Oxid Met. 2013 Feb;79(1–2):29–39.

43. Norton GA, Brown RC. Wet Chemical Method for Determining Levels of Ammonia in Syngas from a Biomass Gasifier. Energy & Fuels. 2005 Mar;19(2):618–24.

44. Nilsson S, Gómez-Barea A, Fuentes-Cano D, Haro P, Pinna-Hernández G. Gasification of Olive Tree Pruning in Fluidized Bed: Experiments in a Laboratory-Scale Plant and Scale-up to Industrial Operation. Energy & Fuels. 2017 Jan;31(1):542–54.

45. Laramie W. Materials of Gasification. 2005.

46. Elliott P. Choose materials for high-temperature environments. Chem Eng Prog. 2001;

47. Gómez-Barea A, Leckner B. Modeling of biomass gasification in fluidized bed. Prog Energy Combust Sci. 2010;36(4):444–509.

48. Gomez-Barea A, Nilsson S, Barrero FV, Campoy M. Devolatilization of wood and wastes in fluidized bed. Fuel Process Technol. 2010;91(11):1624–33.

49. Malsegna B, Di Giuliano A, Gallucci K. Experimental study of absorbent hygiene product devolatilization in a bubbling fluidized bed. Energies. 2021;14(9).

50. Iannello S, Foscolo PU, Materazzi M. Investigation of single particle devolatilization in fluidized bed reactors by X-ray imaging techniques. Chem Eng J [Internet]. 2022;431(P1):133807. Available from: https://doi.org/10.1016/j.cej.2021.133807

51. Tokmurzin D, Nam JY, Lee TR, Park SJ, Nam H, Yoon SJ, et al. High temperature flash pyrolysis characteristics of waste plastics (SRF) in a bubbling fluidized bed: Effect of temperature and pelletizing. Fuel [Internet]. 2022;326(May):125022. Available from: https://doi.org/10.1016/j.fuel.2022.125022

52. Troiano M, Cammarota A, Tregambi C, Chirone R, Salatino P, Solimene R. Fluidized bed combustion of solid lignin-rich residues from bioethanol production. Powder Technol [Internet]. 2020;371:170–9. Available from: https://doi.org/10.1016/j.powtec.2020.05.070

53. Nikku M, Deb A, Sermyagina E, Puro L. Reactivity characterization of municipal solid waste and biomass. Fuel [Internet]. 2019;254(February):115690. Available from: https://doi.org/10.1016/j.fuel.2019.115690

54. Menares T, Herrera J, Romero R, Osorio P, Arteaga-Pérez LE. Waste tires pyrolysis kinetics and reaction mechanisms explained by TGA and Py-GC/MS under kinetically-controlled regime. Waste Manag [Internet]. 2020;102:21–9. Available from: https://doi.org/10.1016/j.wasman.2019.10.027

55. Chen J, Sun Y, Zhang Z. Evolution of trace elements and polluting gases toward clean co-combustion of coal and sewage sludge. Fuel [Internet]. 2020;280(June):118685. Available from: https://doi.org/10.1016/j.fuel.2020.118685

56. Lasek JA, Głód K, Słowik K. The co-combustion of torrefied municipal solid waste and coal in bubbling fluidised bed combustor under atmospheric and elevated pressure. Renew Energy. 2021;179:828–41.

57. Czech T, Marchewicz A, Sobczyk AT, Krupa A, Jaworek A, Śliwiński, et al. Heavy metals partitioning in fly ashes between various stages of electrostatic precipitator after combustion of different types of coal. Process Saf Environ Prot. 2020;133:18–31.

58. Soria-Verdugo A, Kauppinen J, Soini T, García-Gutiérrez LM, Pikkarainen T. Pollutant emissions released during sewage sludge combustion in a bubbling fluidized bed reactor. Waste Manag [Internet]. 2020;105:27–38. Available from: https://doi.org/10.1016/j.wasman.2020.01.036

59. Cheng Y, Oleszek S, Shiota K, Oshita K, Takaoka M. Comparison of sewage sludge mono-incinerators: Mass balance and distribution of heavy metals in step grate and fluidized bed incinerators. Waste Manag [Internet]. 2020;105:575–85. Available from: https://doi.org/10.1016/j.wasman.2020.02.044

60. Kluska J, Turzyński T, Ochnio M, Kardaś D. Characteristics of ash formation in the process of combustion of pelletised leather tannery waste and hardwood pellets. Renew Energy. 2020;149:1246–53.

61. Šyc M, Pohořelý M, Jeremiáš M, Vosecký M, Kameníková P, Skoblia S, et al. Behavior of heavy metals in steam fluidized bed gasification of contaminated biomass. Energy and Fuels. 2011;25(5):2284–91.

62. Valin S, Ravel S, Vincent PP De, Thiery S, Miller H. Fluidized bed air gasi fi cation of solid recovered fuel and woody biomass : In fl uence of experimental conditions on product gas and pollutant release. 2019;242(January):664–72.

63. Pandey D, Katsaros G, Tassou S. Air-steam gasification of poultry litter in a bubbling fluidised bed reactor. 2020;(September).

64. Ruiz M, Schnitzer A, Arnoux P, Mauviel G. Gasification of N-rich fibreboard in an air-blown fluidized bed reactor : A study on the fate of tars , NH 3 and HCN during oxidative mild Hot Gas Filtration. Fuel [Internet]. 2021;303(June):121317. Available from: https://doi.org/10.1016/j.fuel.2021.121317

65. de Almeida VF, Gómez-Barea A, Arroyo-Caire J, Pardo I. On the Measurement of the Main Inorganic Contaminants Derived from Cl, S and N in Simulated Waste-Derived Syngas. Waste and Biomass Valorization [Internet]. 2020;(0123456789). Available from: https://doi.org/10.1007/s12649-019-00879-4

66. Yi K, Liu H, Wang J, Lu G, Jin M, Hu H, et al. The adsorption and transformation of SO 2 , H 2 S and NH 3 by using sludge gasification ash: Effects of Fenton oxidation and CaO pre-conditioning. Chem Eng J. 2019;360(September 2018):1498–508.

67. Jeremiáš M, Pohořelý M, Bode P, Skoblia S, Beňo Z, Svoboda K. Ammonia yield from gasification of biomass and coal in fluidized bed reactor. Fuel. 2014;117(PARTB):917–25.

68. Nilsson S, Gómez-Barea A, Pardo-Arias I, Suárez-Almeida M, De Almeida VF. Comparison of Six Different Biomass Residues in a Pilot-Scale Fluidized Bed Gasifier. Energy and Fuels. 2019;33(11):10978–88.

69. de Almeida VF, Ronda A, Arroyo-Caire, J. Suárez-Almeida M, Pardo I, Fuentes-Cano, D., Haro P, et al. Heavy metals partitioning during thermal devolatilization of solid wastes in a fluidized bed reactor. In: Conference W, editor. Praga; 2018.

70. Vassilev S V., Vassileva CG, Baxter D. Trace element concentrations and associations in some biomass ashes. Fuel. 2014;129:292–313.

71. Poho M, Jeremi M, Voseck M, Kameníkov P, Skoblia S, Svoboda K, et al. Behavior of Heavy

Metals in Steam Fluidized Bed Gasification of Contaminated Biomass a. 2011;2284–91.

72. Arena U, Di F. Gasification of a solid recovered fuel in a pilot scale fluidized bed reactor. FUEL [Internet]. 2014;117:528–36. Available from: http://dx.doi.org/10.1016/j.fuel.2013.09.044

73. Channiwala SA, Parikh PP. A unified correlation for estimating HHV of solid, liquid and gaseous fuels. Fuel. 2002;81(8):1051–63.

74. SFS. Water quality. Application of inductively coupled plasma mass spectrometry (ICP-MS). Part 2: Determination of selected elements including uranium isotopes (ISO 17294-2:2016). 2016.

75. Water quality. Determination of selected elements by inductively coupled plasma optical emission spectrometry (ICP-OES) (ISO 11885:2007). 2007.

76. Wen CY, Yu YH. A generalized method for predicting the minimum fluidization velocity. AIChE J [Internet]. 1966 May 1 [cited 2021 Aug 5];12(3):610–2. Available from: https://aiche.onlinelibrary.wiley.com/doi/full/10.1002/aic.690120343

77. Anonym. Pall Dia-Schumalith filter elements – datasheet. 2014.

78. Tuomi S, Kurkela E, Simell P, Reinikainen M. Behaviour of tars on the filter in high temperature filtration of biomass-based gasification gas. Fuel [Internet]. 2015;139:220–31. Available from: http://dx.doi.org/10.1016/j.fuel.2014.08.051

79. Biomass gasification – tar and particles in product gases – sampling and analysis. TC BT/TF 143 WI CSC 03002.4. Technical Specification. 2004.

80. Vonk G, Piriou B, Wolbert D, Cammarano C, Vaïtilingom G. Analysis of pollutants in the product gas of a pilot scale downdraft gasifier fed with wood, or mixtures of wood and waste materials. Biomass and Bioenergy. 2019;125(April):139–50.

81. Pudasainee D, Paur HR, Fleck S, Seifert H. Trace metals emission in syngas from biomass gasification. Fuel Process Technol. 2014;120:54–60.

82. Gómez-barea A, Leckner B. Estimation of gas composition and char conversion in a fluidized bed biomass gasifier. 2013;107:419–31.

83. Timmer KJ, Brown RC. Transformation of char carbon during bubbling fluidized bed gasification of biomass. Fuel. 2019;242(September 2018):837–45.

84. Sebastiani A, Macrì D, Gallucci K, Materazzi M. Steam - oxygen gasification of refuse derived fuel in fluidized beds: Modelling and pilot plant testing. Fuel Process Technol. 2021;216(October 2020):106783.

85. Nilsson S, Gómez-Barea A, Fuentes-Cano D, Haro P, Pinna-Hernández G. Gasification of olive tree pruning in fluidized bed: Experiments in a laboratory-scale plant and scale-up to industrial operation. Energy and Fuels. 2017;31(1):542–54.

86. Asadullah M, Miyazawa T, Ito SI, Kunimori K, Koyama S, Tomishige K. A comparison of Rh/CeO2/SiO2 catalysts with steam reforming catalysts, dolomite and inert materials as bed materials in low throughput fluidized bed gasification systems. Biomass and Bioenergy. 2004;26(3):269–79.

87. Kurkela E, Kurkela M, Hiltunen I. The effects of wood particle size and different process variables on the performance of steam-oxygen blown circulating fluidized-bed gasifier. Environ Prog Sustain Energy. 2014 Oct;33(3):681–7.

88. Hansson KM, Samuelsson J, Tullin C, Åmand LE. Formation of HNCO, HCN, and NH3 from the pyrolysis of bark and nitrogen-containing model compounds. Combust Flame. 2004;137(3):265–77.

89. Vriesman P, Heginuz E, Sjöström K. Biomass gasification in a laboratory-scale AFBG: influence of the location of the feeding point on the fuel-N conversion. Fuel. 2000;79(11):1371–8.

90. Tchapda AH, Pisupati S V. A review of thermal co-conversion of coal and biomass/waste. Energies. 2014;7(3):1098–148.

91. Amure O, Hanson S, Cloke M, Patrick JW. The formation of ammonia in air-blown gasification: Does char-derived NO act as a precursor? Fuel. 2003;82(15–17):2139–43.

92. Wójtowicz MA, Bassilakis R, Serio MA. Ammonia and hydrogen cyanide release during coal pyrolysis at low heating rates. ACS Div Fuel Chem Prepr. 2001;46(1):133–7.

93. Becidan M, Skreiberg Ø, Hustad JE. NO x and N 2 O precursors (NH 3 and HCN) in pyrolysis of biomass residues. Energy and Fuels. 2007;21(2):1173–80.

94. Schäfer S, Bonn B. Hydrolysis of HCN as an important step in nitrogen oxide formation in fluidised combustion. Part II: Heterogeneous reactions involving limestone. Fuel. 2002;81(13):1641–6.

95. Shimizu T, Ishizu K, Kobayashi S, Kimura S, Shimizu T, Inagaki M. Hydrolysis and Oxidation of HCN over Limestone under Fluidized Bed Combustion Conditions. Energy and Fuels. 1993;7(5):645–7.

96. Leppälahti J, Kurkela E. Behaviour of nitrogen compounds and tars in fluidized bed air gasification of peat. Fuel. 1991;70(4):491–7.

97. Pinto F, André RN, Carolino C, Miranda M, Abelha P, Direito D, et al. Gasification improvement of a poor quality solid recovered fuel (SRF). Effect of using natural minerals and biomass wastes blends. Fuel. 2014;117(PARTB):1034–44.

98. Jazbec M, Sendt K, Haynes BS. Kinetic and thermodynamic analysis of the fate of sulphur compounds in gasification products. Fuel. 2004;83(16):2133–8.

99. Kaufman Rechulski MD, Schildhauer TJ, Biollaz SMA, Ludwig C. Sulfur containing organic compounds in the raw producer gas of wood and grass gasification. Fuel. 2014;128:330–9.

100. Hepola J, Kurkela E, Ståhlberg P, Lappi M. Sulphur removal by calcium-based sorbents in fluidized bed gasification. ASHRAE; 1991. p. 267–76.

101. Zhou X, Liu W, Zhang P, Wu W. Study on Heavy Metals Conversion Characteristics During Refused Derived Fuel Gasification Process. Procedia Environ Sci. 2016;31:514–9.

102. Adefeso IB, Ikhu-Omoregbe D, Isa YM. Assessment of heavy metals in RDF for thermochemical conversion. E3S Web Conf. 2020;158:1–8.

103. Commission E. Council Directive on the Protection of the. 1986;(June):1–10.

104. Perry S, Perry RH, Green DW, Maloney JO. Perry's chemical engineers' handbook. Vol. 38, Choice Reviews Online. 2000. 38-0966-38–0966 p.

105. Bunt JR, Waanders FB. Trace element behaviour in the Sasol-Lurgi MK IV FBDB gasifier. Part 1 - The volatile elements: Hg, As, Se, Cd and Pb. Fuel. 2008;87(12):2374–87.

106. HSC Chemistry, Software for Process simulation, Reactions Equations, Heat and Material Balances, Heat Loss Calculator, Equilibrium Calculations, Electrochemical Cell Equilibriums, Eh-pH Diagrams – Pourbaix diagram, Tpp Diagrams – Stability diagrams, Miner.

107. Jesús M, Acosta G, Gómez Barea A. Estudio termodinámico para predecir especies contaminantes durante la conversión termoquímica de residuos sólidos combustibles.

108. FactSage.com.

109. SGTE Solution Database - SGTE - Scientific Group Thermodata Europe.

110. ChemSage Modules - GTT-Technologies.

111. Díaz-Somoano M, Martínez-Tarazona MR. Trace element evaporation during coal gasification based on a thermodynamic equilibrium calculation approach. Fuel. 2003;82(2):137–45.

112. Baratieri M, Baggio P, Fiori L, Grigiante M. Biomass as an energy source: Thermodynamic constraints on the performance of the conversion process. Bioresour Technol. 2008 Oct;99(15):7063–73.

113. Becidan M, Sørum L, Lindberg D. Impact of municipal solid waste (MSW) quality on the behavior of alkali metals and trace elements during combustion: A thermodynamic equilibrium analysis. Energy and Fuels. 2010;24(6):3446–55.

114. Stanicic I, Backman R, Cao Y, Mattisson T, Rydén M, Aronsson J. Fate of trace elements in Oxygen Carrier Aided Combustion (OCAC) of municipal solid waste Citation for the original published paper (version of record): Fate of trace elements in Oxygen Carrier Aided Combustion (OCAC) of municipal solid waste. Fuel. 2022;

115. Kuramochi H, Wu W, Kawamoto K. Prediction of the behaviors of H2S and HCl during gasification of selected residual biomass fuels by equilibrium calculation. Fuel. 2005 Mar;84(4):377–87.

116. Konttinen J, Backman R, Hupa M, Moilanen A, Kurkela E. Trace element behavior in the

fluidized bed gasification of solid recovered fuels – A thermodynamic study. Fuel. 2013 Apr;106:621–31.

117. MATLAB - MathWorks - MATLAB & Simulink.

118. Chidikofan G, Benoist A, Sawadogo M, Volle G, Valette J, Coulibaly Y, et al. Assessment of Environmental Impacts of Tar Releases from a Biomass Gasifier Power Plant for Decentralized Electricity Generation. Energy Procedia [Internet]. 2017;118:158–63. Available from: http://dx.doi.org/10.1016/j.egypro.2017.07.034

119. Ardolino F, Lodato C, Astrup TF, Arena U. Energy recovery from plastic and biomass waste by means of fluidized bed gasification: A life cycle inventory model. Energy [Internet]. 2018;165:299–314. Available from: https://doi.org/10.1016/j.energy.2018.09.158

120. Tang Y, Dong J, Li G, Zheng Y, Chi Y, Nzihou A, et al. Environmental and exergetic life cycle assessment of incineration- and gasification-based waste to energy systems in China. Energy [Internet]. 2020;205:118002. Available from: https://doi.org/10.1016/j.energy.2020.118002

121. Marques TE, Santiago YC, Renó MLG, Maya DMY, Sphaier LA, Shi Y, et al. Environmental and energetic evaluation of refuse-derived fuel gasification for electricity generation. Processes. 2021;9(12):1–17.

122. Dong J, Tang Y, Nzihou A, Chi Y, Weiss-Hortala E, Ni M, et al. Comparison of waste-to-energy technologies of gasification and incineration using life cycle assessment: Case studies in Finland, France and China. J Clean Prod [Internet]. 2018;203:287–300. Available from: https://doi.org/10.1016/j.jclepro.2018.08.139

123. Social Life Cycle Assessment (S-LCA) - Life Cycle Initiative [Internet]. [cited 2022 Aug 10]. Available from: https://www.lifecycleinitiative.org/starting-life-cycle-thinking/life-cycle-approaches/social-lca/

124. Sala S, Vasta A, Mancini L, Dewulf J, Rosembaum E. Social Life Cycle Assessment - State of the art and challenges for supporting product policies. JRC Technical Reports. Italy; 2015.

125. Husgafvel R, Pajunen N, Päällysaho M, Paavola IL, Inkinen V, Heiskanen K, et al. Social metrics in the process industry: Background, theory and development work. Int J Sustain Eng.

2014;7(2):171–82.

126. Larsen VG, Tollin N, Sattrup PA, Birkved M, Holmboe T. What are the challenges in assessing circular economy for the built environment? A literature review on integrating LCA, LCC and S-LCA in life cycle sustainability assessment, LCSA. J Build Eng. 2022;50(January):104203.

127. Sala S, Ciuffo B, Nijkamp P. A systemic framework for sustainability assessment. Ecol Econ [Internet]. 2015;119:314–25. Available from: http://dx.doi.org/10.1016/j.ecolecon.2015.09.015

128. Sala S. Triple bottom line, sustainability and sustainability assessment, an overview [Internet]. Biofuels for a More Sustainable Future. Elsevier Inc.; 2020. 47–72 p. Available from: http://dx.doi.org/10.1016/B978-0-12-815581-3.00003-8

129. Olabi AG, Obaideen K, Elsaid K, Wilberforce T, Sayed ET, Maghrabie HM, et al. Assessment of the pre-combustion carbon capture contribution into sustainable development goals SDGs using novel indicators. Renew Sustain Energy Rev. 2022;153(October 2021):111710.

130. Aracil C, Haro P, Fuentes-Cano D, Gómez-Barea A. Implementation of waste-to-energy options in landfill-dominated countries: Economic evaluation and GHG impact. Waste Manag. 2018;76:443–56.

131. Rebitzer G, Ekvall T, Frischknecht R, Hunkeler D, Norris G, Rydberg T, et al. Life cycle assessment Part 1: Framework, goal and scope definition, inventory analysis, and applications. Environ Int. 2004;30(5):701–20.

132. ecoinvent – ecoinvent [Internet]. [cited 2022 Aug 10]. Available from: https://ecoinvent.org/

133. Atabi F, Ali Ehyaei M, Ahmadi MH. Calculation of CH4 and CO2 Emission Rate in Kahrizak Landfill Site with Land GEM Mathematical Model. 2014;e006.

134. Tian H, Xu R, Canadell JG, Thompson RL, Winiwarter W, Suntharalingam P, et al. A comprehensive quantification of global nitrous oxide sources and sinks. Nature [Internet]. 2020;586(7828):248–56. Available from: http://dx.doi.org/10.1038/s41586-020-2780-0

135. Wilson JM, McKinney LJ, Theerarattananoon K, Ballard TC, Wang D, Staggenborg SA, et al.

Energy and cost for pelleting and transportation of select cellulosic biomass feedstocks for ethanol production. Appl Eng Agric. 2014;30(1):77–85.

136. Goedkoop M, Heijungs R, Huijbregts M, Schryver A De, Struijs J, Zelm R Van. ReCiPe 2008. Potentials [Internet]. 2009;1–44. Available from: http://www.pre-sustainability.com/download/misc/ReCiPe_main_report_final_27-02-2009_web.pdf

137. Huijbregts MAJ, Steinmann ZJN, Elshout PMF, Stam G, Verones F, Vieira M, et al. ReCiPe2016: a harmonised life cycle impact assessment method at midpoint and endpoint level. Int J Life Cycle Assess [Internet]. 2017;22(2):138–47. Available from: http://dx.doi.org/10.1007/s11367-016-1246-y

138. Stanton EA, Fisher J. Carbon Dioxide Price. 2015;

139. Towler G, Sinnott RAY. Chemical engineering design: principles, practice and economics of plant and process design. Chemical Engineering Design. 2013. i.

140. Batlle C, Schittekatte T, Knittel CR. Power price crisis in the EU 2.0+: Desperate times call for desperate measures. SSRN Electron J. 2022;2–28.

141. Basse Mama H, Mandaroux R. Do investors care about carbon emissions under the European Environmental Policy? Bus Strateg Environ. 2022;31(1):268–83.

142. Koytsoumpa EI, Magiri – Skouloudi D, Karellas S, Kakaras E. Bioenergy with carbon capture and utilization: A review on the potential deployment towards a European circular bioeconomy. Renew Sustain Energy Rev [Internet]. 2021;152(February):111641. Available from: https://doi.org/10.1016/j.rser.2021.111641